2013-05-07

Weak Scattering of Scalar and Electromagnetic Random Fields

Zhisong Tong
University of Miami, tongzhisong@hotmail.com

UNIVERSITY OF MIAMI

WEAK SCATTERING OF SCALAR AND ELECTROMAGNETIC RANDOM FIELDS

By

Zhisong Tong

A DISSERTATION

Submitted to the Faculty
of the University of Miami
in partial fulfillment of the requirements for
the degree of Doctor of Philosophy

Coral Gables, Florida

May 2013

UNIVERSITY OF MIAMI

A dissertation submitted in partial fulfillment of
the requirements for the degree of
Doctor of Philosophy

WEAK SCATTERING OF SCALAR AND ELECTROMAGNETIC RANDOM FIELDS

Zhisong Tong

Approved:

_____ Olga Korotkova, Ph.D. Associate Professor of Physics	_____ M. Brian Blake, Ph.D. Dean of the Graduate School
_____ Howard Gordon, Ph.D. Professor of Physics	_____ Kenneth Voss, Ph.D. Professor of Physics

_____
Greg Gbur, Ph.D.
Associate Professor of Physics
University of North Carolina at Charlotte

TONG, ZHISONG (Ph.D., Physics)
Weak Scattering of Scalar and Electromagnetic Random Fields (May 2013)

Abstract of a dissertation at the University of Miami.

Dissertation supervised by Professor Olga Korotkova.
No. of pages in text. (106)

This dissertation encompasses several studies relating to the theory of weak potential scattering of scalar and electromagnetic random, wide-sense statistically stationary fields from various types of deterministic or random linear media. The proposed theory is largely based on the first Born approximation for potential scattering and on the angular spectrum representation of fields.

The main focus of the scalar counterpart of the theory is made on calculation of the second-order statistics of scattered light fields in cases when the scattering medium consists of several types of discrete particles with deterministic or random potentials. It is shown that the knowledge of the correlation properties for the particles of the same and different types, described with the newly introduced pair-scattering matrix, is crucial for determining the spectral and coherence states of the scattered radiation. The approach based on the pair-scattering matrix is then used for solving an inverse problem of determining the location of an "alien" particle within the scattering collection of "normal" particles, from several measurements of the spectral density of scattered light. Weak scalar scattering of light from a particulate medium in the presence of optical turbulence existing between the scattering centers is then approached using the combination of the Born's theory for treating the light interaction with discrete particles and the Rytov's theory for light propagation in extended turbulent medium. It is demonstrated how the

statistics of scattered radiation depend on scattering potentials of particles and the power spectra of the refractive index fluctuations of turbulence. This theory is of utmost importance for applications involving atmospheric and oceanic light transmission.

The second part of the dissertation includes the theoretical procedure developed for predicting the second-order statistics of the electromagnetic random fields, such as polarization and linear momentum, scattered from static media. The spatial distribution of these properties of scattered fields is shown to be substantially dependent on the correlation and polarization properties of incident fields and on the statistics of the refractive index distribution within the scatterers. Further, an example is considered which illustrates the usefulness of the electromagnetic scattering theory of random fields in the case when the scattering medium is a thin bio-tissue layer with the prescribed power spectrum of the refractive index fluctuations. The polarization state of the scattered light is shown to be influenced by correlation and polarization states of the illumination as well as by the particle size distribution of the tissue slice.

To my wife *Jing Lei* and my son *Eric Ruihan Tong*

ACKNOWLEDGMENT

I want to express my deepest gratitude to my wife Jing Lei who sacrificed a lot during the preparation of this thesis when she has to take the responsibility to take care of our new baby even if she was so weak right after the baby's birth. Without her strong support and great dedication this work could never been finished so smoothly and I could never spend a lot of time and energy on it. She is a person with strong will and very important to me.

I want to thank my supervisor Dr. Olga Korotkova who provided many constructive suggestions for the structure and writing of this thesis. And I also want to thank all the committee members Dr. Kenneth Voss, Dr. Howard Gordon and Dr. Greg Gbur for the valuable modifications of this thesis.

One special acknowledgement is given to Dr. Van Vliet who is my scholarly mentor and beneficial friend in my life. I also acknowledge Dr. Rafael Nepomechie for his support during the writing of this thesis.

Moreover, I would like to express gratitude to all the faculty, staff and students who provided me great help and strong support during the preparation of this thesis, especially, to Hong Qi.

In addition, I am indebted to my parents Xianming Tong and Yaofen Wu for their endless help and wise guidance throughout my life.

Table of Contents

List of Figures

List of Tables

Chapter 1

Introduction

The recently formulated unified theory of coherence and polarization of light has made it possible to predict the changes in spectrum, coherence and polarization of light beams on interaction with deterministic and random linear media, and allowed in-depth theoretical examination of the various phenomena of light accompanying light propagation, scattering and imaging by natural media and man-made optical systems. Employing this theory as the main theoretical foundation, we have studied the propagation of light through free space [1-2], laser resonators [3], active bistatic LIDAR system [4], negative-phase materials [5-6] and atmospheric turbulence [7-8]; explored the properties of light scattered from collections of particles [9-13], $\delta-$correlated media [14-15] and biological tissues [16]; and investigated the imaging of light by an isoplanatic two-lens imaging system [17] and ghost imaging system [18].

In this thesis, the focus is made on developing the theories of scalar and electromagnetic scattering of light from deterministic and random media. The text is divided into three chapters. In Chapter 1, we review the classic weak potential scattering theory and the angular spectrum representation of waves, a commonly used mathematical tool needed for efficient light description. In Chapter 2 we first introduce the pair-structure matrix describing the relations among multiple kinds of particles in a scattering collection, and then use it for introducing a new technique for tracing the position of an alien object embedded in a random particulate medium. At the end of this chapter we

develop the method for predicting the interaction of optical fields with turbulent medium containing particles. Chapter 3 deals with generalization of the classic scalar, weak scattering theory of random fields to the electromagnetic case. Such extension allows evaluating polarization and momentum of scattered light. The electromagnetic theory of scattering is then applied to the situation when a random beam with arbitrary states of coherence and polarization is scattered from a thin bio-tissue slice with prescribed power spectrum of refractive index distribution. The state of polarization of the resulting field is shown to have strong dependence on the properties of incident light and statistics of the tissue.

1.1 Description and models of random fields

We begin by introducing the major quantities of the theory of coherence and polarization of light which we will be using throughout the thesis for characterization of illumination and scattered fields. The cross-spectral density function of a scalar field U is defined as a correlation function [19]

$$W(\mathbf{r}_1, \mathbf{r}_2, \omega) = \left\langle U^*(\mathbf{r}_1, \omega) U(\mathbf{r}_2, \omega) \right\rangle, \tag{1.1}$$

where angular brackets stand for the ensemble average of monochromatic realizations, r_1 and r_2 are two position vectors and ω is the angular frequency. From the cross-spectral density function the expressions for the spectral density

$$S(\boldsymbol{r}, \omega) = W(\boldsymbol{r}, \boldsymbol{r}, \omega), \tag{1.2}$$

and the spectral degree of coherence

$$\mu(\boldsymbol{r}_1,\boldsymbol{r}_2,\omega)=\frac{W(\boldsymbol{r}_1,\boldsymbol{r}_2,\omega)}{\sqrt{W(\boldsymbol{r}_1,\boldsymbol{r}_1,\omega)}\sqrt{W(\boldsymbol{r}_2,\boldsymbol{r}_2,\omega)}}, \tag{1.3}$$

follow.

The basic analytic model for a random beam is the Gaussian Schell-model model for which the cross-spectral density function at the source plane $z=0$ has form [20]

$$W^{(0)}(\boldsymbol{\rho}_1,\boldsymbol{\rho}_2,\omega)=A^2\exp\left[-\frac{\boldsymbol{\rho}_1^2+\boldsymbol{\rho}_2^2}{4\sigma^2}\right]\exp\left[-\frac{(\boldsymbol{\rho}_1-\boldsymbol{\rho}_2)^2}{2\delta^2}\right], \tag{1.4}$$

where A is the amplitude, σ is the r.m.s. width of the spectral density and δ is the r.m.s. width of the degree of coherence. Limits $\delta\to 0$ and $\delta\to\infty$ correspond to incoherent and coherent beams, respectively.

When the beam is electromagnetic it can be described by the cross-spectral density matrix

$$W_{\alpha\beta}(r_1,r_2,\omega)=\left\langle E_\alpha^*(\mathbf{r}_1,\omega)E_\beta(\mathbf{r}_2,\omega)\right\rangle,\ (\alpha,\beta=x,y) \tag{1.5}$$

where E_x and E_y are the mutually orthogonal components of the electric field transverse to the direction of propagation. In this case, the spectral density and spectral degree of coherence are defined by the expressions

$$S(\boldsymbol{r},\omega)=Tr\boldsymbol{W}(\boldsymbol{r},\boldsymbol{r},\omega), \tag{1.6}$$

and

$$\eta(\boldsymbol{r}_1,\boldsymbol{r}_2,\omega)=\frac{Tr\boldsymbol{W}(\boldsymbol{r}_1,\boldsymbol{r}_2,\omega)}{\sqrt{Tr\boldsymbol{W}(\boldsymbol{r}_1,\boldsymbol{r}_1,\omega)}\sqrt{Tr\boldsymbol{W}(\boldsymbol{r}_2,\boldsymbol{r}_2,\omega)}}, \tag{1.7}$$

where Tr represents trace of the matrix. One more quantity that we should deal with in the vector-field treatment and can not be accounted for in the scalar-field treatment is the spectral degree of polarization

$$P(\boldsymbol{r},\omega)=\sqrt{1-\frac{4Det\boldsymbol{W}(\boldsymbol{r},\omega)}{\left[Tr\boldsymbol{W}(\boldsymbol{r},\omega)\right]^2}}, \tag{1.8}$$

where Det denotes the determinant of the matrix.

The electromagnetic extension of the Gaussian Schell-model beam has the form

$$W_{\alpha\beta}^{(0)}(\boldsymbol{\rho}_1,\boldsymbol{\rho}_2,\omega)=A_\alpha A_\beta B_{\alpha\beta}\exp\left[-\frac{\boldsymbol{\rho}_1^2+\boldsymbol{\rho}_2^2}{4\sigma^2}\right]\exp\left[-\frac{(\boldsymbol{\rho}_1-\boldsymbol{\rho}_2)^2}{2\delta_{\alpha\beta}^2}\right],\ (\alpha,\beta=x,y), \tag{1.9}$$

where σ is the r.m.s width of the spectral density, δ_{xx}, δ_{yy}, δ_{xy} are the r.m.s. widths of auto-correlation functions of the x component of the field, of the y component of the field and of the mutual correlation function of x and y field components, respectively, B_{xy} is the complex correlation coefficient between x and y components of the electric field. Parameters A_α, $B_{\alpha\beta}$, σ and $\delta_{\alpha\beta}$ are independent of position and, in our analysis, of frequency.

1.2 Classic Weak Scattering Theory

Let us consider a monochromatic scalar field $U(\boldsymbol{r},\omega)$, incident on a linear, isotropic, nonmagnetic medium occupying a finite domain V. Assuming that there are no sources in V, we begin our analysis of the weak scattering theory with the scalar equation [19]

$$\nabla^2 U(\boldsymbol{r},\omega)+k^2 n^2(\boldsymbol{r},\omega)U(\boldsymbol{r},\omega)=0, \tag{1.10}$$

where $k=\omega/c$ and $n(\boldsymbol{r},\omega)=\sqrt{\varepsilon(\boldsymbol{r},\omega)}$ denotes the refractive index of the medium with $\varepsilon(\boldsymbol{r},\omega)$ being the dielectric 'constant'. Equation (1.10) has a similar form as the Helmholtz equation and may be called the Helmholtz equation in medium. It is valid under the assumption that $\varepsilon(\boldsymbol{r})$ varies slowly with position [19].

We now rewrite Eq. (1.10) in the form

$$\nabla^2 U(\boldsymbol{r},\omega)+k^2 U(\boldsymbol{r},\omega)=-4\pi F(\boldsymbol{r},\omega)U(\boldsymbol{r},\omega), \tag{1.11}$$

where

$$F(\boldsymbol{r},\omega)=\begin{cases}\dfrac{1}{4\pi}k^2[n^2(\boldsymbol{r},\omega)-1], & \boldsymbol{r}\in V\\ 0, & \boldsymbol{r}\notin V\end{cases} \tag{1.12}$$

is called the scattering potential of the medium.

Let us now express $U(\boldsymbol{r},\omega)$ as a sum of the incident field $U^{(i)}(\boldsymbol{r},\omega)$ and the scattered field $U^{(s)}(\boldsymbol{r},\omega)$, i.e.

$$U(\boldsymbol{r},\omega)=U^{(i)}(\boldsymbol{r},\omega)+U^{(s)}(\boldsymbol{r},\omega). \tag{1.13}$$

Since the incident field satisfies the Helmholtz equation in free space, i.e., the source generating the field is outside the medium volume V, it may be excluded from consideration. Then for $U^{(i)}(\boldsymbol{r},\omega)$ and $U^{(s)}(\boldsymbol{r},\omega)$ we obtain the equations

$$(\nabla^2 + k^2)U^{(i)}(\boldsymbol{r},\omega) = 0\,, \tag{1.14}$$

and

$$(\nabla^2 + k^2)U^{(s)}(\boldsymbol{r},\omega) = -4\pi F(\boldsymbol{r},\omega)U(\boldsymbol{r},\omega)\,, \tag{1.15}$$

the latter being an inhomogeneous Helmholtz equation. With the Sommerfeld radiation condition, the solution to Eq. (1.15) is the convolution

$$U^{(s)}(\boldsymbol{r},\omega) = (G * FU)(\boldsymbol{r},\omega) = \int_V G(\boldsymbol{r}-\boldsymbol{r}',\omega)F(\boldsymbol{r}',\omega)U(\boldsymbol{r}',\omega)d^3r'\,, \tag{1.16}$$

where $G(\boldsymbol{r}-\boldsymbol{r}',\omega)$ is the Green's function of the Helmholtz operator, i.e., the solution to the equation

$$(\nabla^2 + k^2)G(\boldsymbol{r}-\boldsymbol{r}',\omega) = -4\pi\delta^{(3)}(\boldsymbol{r}-\boldsymbol{r}')\,, \tag{1.17}$$

where $\delta^{(3)}(\boldsymbol{r}-\boldsymbol{r}')$ is the three-dimensional Dirac delta function. We now choose $G(\boldsymbol{r}-\boldsymbol{r}',\omega)$ to be the outgoing free-space Green's function of the Helmholtz operator:

$$G(\boldsymbol{r}-\boldsymbol{r}',\omega) = \frac{\exp(ik\left|\boldsymbol{r}-\boldsymbol{r}'\right|)}{\left|\boldsymbol{r}-\boldsymbol{r}'\right|}\,. \tag{1.18}$$

On using Eq. (1.16) in Eq. (1.13) we see that the total field could be determined from the equation

$$U(\boldsymbol{r},\omega) = U^{(i)}(\boldsymbol{r},\omega) + \int_V G(\boldsymbol{r}-\boldsymbol{r}',\omega)F(\boldsymbol{r}',\omega)U(\boldsymbol{r}',\omega)d^3r', \tag{1.19}$$

which is called the integral equation of potential scattering. In most cases of practical interest, Eq. (1.19) is impossible to handle due to the existence of $U(\boldsymbol{r},\omega)$ under the integral sign. However, it appears to be possible to obtain analytical solution of Eq. (1.19) under the first-order Born approximation in situations when the scattering is weak, for instance when the refractive index in the scattering medium is close to unity. Then throughout the scatterer we can assume that

$$\left|U^{(s)}(\boldsymbol{r},\omega)\right| \ll \left|U^{(i)}(\boldsymbol{r},\omega)\right|. \tag{1.20}$$

Under such approximation, known as the first-order Born approximation, the integral equation of potential scattering (1.19) becomes

$$U(\boldsymbol{r},\omega) = U^{(i)}(\boldsymbol{r},\omega) + \int_V G(\boldsymbol{r}-\boldsymbol{r}',\omega)F(\boldsymbol{r}',\omega)U^{(i)}(\boldsymbol{r}',\omega)d^3r', \tag{1.21}$$

or

$$U^{(s)}(\boldsymbol{r},\omega) = \int_V G(\boldsymbol{r}-\boldsymbol{r}',\omega)F(\boldsymbol{r}',\omega)U^{(i)}(\boldsymbol{r}',\omega)d^3r'. \tag{1.22}$$

We now consider a more involved case when the light field incident onto a scatterer is not deterministic, but spatially partially coherent. In other words, the field fluctuations at different points are not longer statistically similar [21]. In such a case, the incident field can be characterized by the cross-spectral density function, i.e.,

$$W^{(i)}(\boldsymbol{r}_1,\boldsymbol{r}_2,\omega) = \left\langle U^{(i)*}(\boldsymbol{r}_1,\omega)U^{(i)}(\boldsymbol{r}_2,\omega)\right\rangle, \tag{1.23}$$

where angular brackets denote the average over the statistical ensemble of monochromatic realizations of the field. The cross-spectral density function is the major quantity in the unified theory of coherence and polarization of light [22]. Similarly, the scattered field may also be represented by an ensemble of monochromatic realizations of the field and its cross-spectral density function may be expressed in a similar manner, i.e. as

$$W^{(s)}(\boldsymbol{r}_1, \boldsymbol{r}_2, \omega) = \left\langle U^{(s)*}(\boldsymbol{r}_1, \omega) U^{(s)}(\boldsymbol{r}_2, \omega) \right\rangle. \tag{1.24}$$

Generally the scattering media may be of deterministic or random nature. In the case when the scatterer is deterministic, the scattering potential $F(\boldsymbol{r}, \omega)$ is a well-defined function of position. With the scattered field $U^{(s)}(\boldsymbol{r}, \omega)$ and the incident field $U^{(i)}(\boldsymbol{r}, \omega)$ being related by Eq. (1.22), the cross-spectral density function of the scattered field, under the accuracy of the first-order Born approximation then takes the form

$$W^{(s)}(\boldsymbol{r}_1, \boldsymbol{r}_2, \omega) = \int_V \int_V W^{(i)}(\boldsymbol{r}_1', \boldsymbol{r}_2', \omega) F^*(\boldsymbol{r}_1', \omega) F(\boldsymbol{r}_2', \omega)$$
$$\times G^*(\boldsymbol{r}_1 - \boldsymbol{r}_1', \omega) G(\boldsymbol{r}_2 - \boldsymbol{r}_2', \omega) d^3\boldsymbol{r}_1' d^3\boldsymbol{r}_2'. \tag{1.25}$$

Then due to the random nature of the incident field the scattered field also becomes random, although the scatterer is deterministic.

In the case when the scattering medium is random the scattering potential becomes a random variable. One realistic example of a random medium is the atmospheric turbulence in which the refractive index fluctuates randomly in space and in time due to the fluctuations in temperature and pressure. By averaging Eq. (1.25) over the ensemble

of realizations of the scattering medium we then obtain for the cross-spectral density function of the scattered field the expression

$$W^{(s)}(\boldsymbol{r}_1,\boldsymbol{r}_2,\omega)=\int_V\int_V W^{(i)}(\boldsymbol{r}_1',\boldsymbol{r}_2',\omega)C_F(\boldsymbol{r}_1',\boldsymbol{r}_2',\omega)$$

$$\times G^*(\boldsymbol{r}_1-\boldsymbol{r}_1',\omega)G(\boldsymbol{r}_2-\boldsymbol{r}_2',\omega)d^3\boldsymbol{r}_1'\,d^3\boldsymbol{r}_2', \tag{1.26}$$

where

$$C_F(\boldsymbol{r}_1',\boldsymbol{r}_2',\omega)=\left\langle F^*(\boldsymbol{r}_1',\omega)F(\boldsymbol{r}_2',\omega)\right\rangle_m, \tag{1.27}$$

is the correlation function of the scattering potential with $\langle ... \rangle_m$ being the average taken over different realizations of the scatterer. One notes that the other average in the integrand of Eq. (1.26) is taken over the ensemble of the incident field.

Let us consider a case where the incident field is a monochromatic plane wave. By approximating the Green's function in the far-field of the scatterers

$$G(|r\boldsymbol{s}-\boldsymbol{r}'|,\omega)\sim\frac{\exp(\mathrm{i}kr)}{r}\exp(-ik\boldsymbol{s}\cdot\boldsymbol{r}'), \tag{1.28}$$

it can be shown that the cross-spectral density function of the scattered wave reduces to the form

$$W^{(s)}(\boldsymbol{r}_1,\boldsymbol{r}_2,\omega)=\frac{1}{r^2}S^{(i)}(\omega)\widetilde{C}_F(-\boldsymbol{K}_1,\boldsymbol{K}_2,\omega), \tag{1.29}$$

where $S^{(i)}(\omega)$ is the spectral density of incident light and

$$\widetilde{C}_F(-\boldsymbol{K}_1,\boldsymbol{K}_2,\omega)=\int_V\int_V C_F(\boldsymbol{r}_1',\boldsymbol{r}_2',\omega)\exp[-i(\boldsymbol{K}_2\cdot\boldsymbol{r}_2'-\boldsymbol{K}_1\cdot\boldsymbol{r}_1')]d^3r_1'd^3r_2', \qquad (1.30)$$

is the six-dimensional Fourier transform of the correlation function $C_F(\boldsymbol{r}_1',\boldsymbol{r}_2',\omega)$ and $\boldsymbol{K}_i=k(\boldsymbol{s}_i-\boldsymbol{s}_0)\ \ (i=1,2)$ is known as the momentum transfer vector.

1.3 Angular spectrum representation of optical fields

An important mathematical tool for description of light fields is its angular spectrum representation, i.e. the representation by the superposition of differently tilted and differently weighted plane waves. Let us first consider a monochromatic scalar field $U(\boldsymbol{r},\omega)$ oscillating at angular frequency ω and propagating into the positive half-space $z>0$ to a point with position vector $\boldsymbol{r}=(\boldsymbol{\rho},z)$. In the form of the above representation, the field can be expressed as [23]

$$U(\boldsymbol{r},\omega)=\int a(\boldsymbol{s},\omega)\exp(ik\boldsymbol{s}\cdot\boldsymbol{r})d^2\boldsymbol{s}_\perp, \tag{1.31}$$

where $\boldsymbol{s}=\left(s_x,s_y,s_z\right)$ is a unit vector, $\boldsymbol{s}_\perp=\left(s_x,s_y,0\right)$ is its projection onto the source plane, and $a(\boldsymbol{s},\omega)$ is the amplitude of a plane wave which may be related to the field in the source plane $U^0(\boldsymbol{\rho}',\omega)\equiv U(\boldsymbol{\rho}=\boldsymbol{\rho}',z=0,\omega)$ by the expression

$$a(\boldsymbol{s},\omega)=\left(\frac{k}{2\pi}\right)^2\int U^0(\boldsymbol{\rho}',\omega)\exp(-ik\boldsymbol{s}\cdot\boldsymbol{\rho}')d^2\rho', \tag{1.32}$$

where $\boldsymbol{\rho}'=(x',y')$ is a point in the source plane.

In Eq. (1.31), the plane wave modes can be of two kinds. The modes for which $\left|\boldsymbol{s}_\perp\right|\le 1$ and

$$s_z=+\sqrt{1-\left|\boldsymbol{s}_\perp\right|^2}=+\sqrt{1-s_x^2-s_y^2} \tag{1.33}$$

are called the homogeneous (propagating) plane waves. The modes for which $|\boldsymbol{s}_\perp| > 1$ and hence

$$s_z = +i\sqrt{|\boldsymbol{s}_\perp|^2 - 1} = +i\sqrt{s_x^2 + s_y^2 - 1} \tag{1.34}$$

are known as evanescent waves. They decay exponentially in amplitude at distances on the order of a wavelength from the source plane. One sees that all high spatial frequency components of plane wave modes correspond to evanescent waves and therefore the information about them is lost during propagation. This explains the diffraction effects on imaging. In the far field of the source, the regime which will be of our major interest, only the homogeneous waves (low spatial frequency components) are of importance.

We now generalize Eq. (1.31) to electromagnetic case. Let us consider a two-dimensional electric vector-field $\boldsymbol{E}(\boldsymbol{r},\omega) = \left[E_x(\boldsymbol{r},\omega), E_y(\boldsymbol{r},\omega)\right]$ with E_x and E_y being two mutually orthogonal components transverse to direction of propagation z. If the field is radiated from the source plane, $z = 0$, into the positive half-space z > 0, then its plane-wave expansion may be written as

$$E_x(\boldsymbol{r},\omega) = \int a_x(\boldsymbol{s},\omega)\exp(ik\boldsymbol{s}\cdot\boldsymbol{r})d^2\boldsymbol{s}_\perp, \tag{1.35a}$$

$$E_y(\boldsymbol{r},\omega) = \int a_y(\boldsymbol{s},\omega)\exp(ik\boldsymbol{s}\cdot\boldsymbol{r})d^2\boldsymbol{s}_\perp, \tag{1.35b}$$

where

$$a_x(\boldsymbol{s},\omega) = \left(\frac{k}{2\pi}\right)^2 \int E_x^0(\boldsymbol{\rho}',\omega)\exp(-ik\boldsymbol{s}\cdot\boldsymbol{\rho}')d^2\rho', \tag{1.36a}$$

$$a_y(\boldsymbol{s},\omega)=\left(\frac{k}{2\pi}\right)^2\int E_y^0(\boldsymbol{\rho}',\omega)\exp(-ik\boldsymbol{s}\cdot\boldsymbol{\rho}')d^2\rho'. \tag{1.36b}$$

where $\boldsymbol{E}^0(\boldsymbol{\rho}',\omega)=\left[E_x^0(\boldsymbol{\rho}',\omega),E_y^0(\boldsymbol{\rho}',\omega)\right]$ is the field at the source plane. Now that $E_x(\boldsymbol{r},\omega)$ and $E_y(\boldsymbol{r},\omega)$ in Eq. (1.35) provide with the accurate form of the propagating field, let us show that we could verify Eq. (1.35) and Eq. (1.36) [or Eq. (1.31) and Eq. (1.32)] using a formula relating $\boldsymbol{E}(\boldsymbol{r},\omega)$ and $\boldsymbol{E}^0(\boldsymbol{r},\omega)$ directly. Indeed, instead of the two-dimensional field, we consider a three-dimensional field and further generalize the angular spectrum representation of plane wave from 2D to 3D. We again assume that an electromagnetic source $\boldsymbol{E}^{(0)}(\boldsymbol{\rho}',\omega)$ located in the plane $z=0$, radiates into the half-space $z>0$. Then the three Cartesian components of the electric field are given by the Luneberg's formulas:

$$E_x(\boldsymbol{r},\omega)=-\frac{1}{2\pi}\int E_x^{(0)}(\boldsymbol{\rho}',\omega)G_z(\boldsymbol{r},\boldsymbol{\rho}')d^2\boldsymbol{\rho}'\ , \tag{1.37a}$$

$$E_y(\boldsymbol{r},\omega)=-\frac{1}{2\pi}\int E_y^{(0)}(\boldsymbol{\rho}',\omega)G_z(\boldsymbol{r},\boldsymbol{\rho}')d^2\boldsymbol{\rho}', \tag{1.37b}$$

$$E_z(\boldsymbol{r},\omega)=\frac{1}{2\pi}\int[E_x^{(0)}(\boldsymbol{\rho}',\omega)G_x(\boldsymbol{r},\boldsymbol{\rho}')+E_y^{(0)}(\boldsymbol{\rho}',\omega)G_y(\boldsymbol{r},\boldsymbol{\rho}')]d^2\boldsymbol{\rho}', \tag{1.37c}$$

where $G_x(\boldsymbol{r},\boldsymbol{\rho}')$, $G_y(\boldsymbol{r},\boldsymbol{\rho}')$, $G_z(\boldsymbol{r},\boldsymbol{\rho}')$ are the partial derivatives of the outgoing free-space Green's function,

$$G(\boldsymbol{r},\boldsymbol{\rho}')=\frac{\exp(ik\left|\boldsymbol{r}-\boldsymbol{\rho}'\right|)}{\left|\boldsymbol{r}-\boldsymbol{\rho}'\right|}=\frac{ik}{2\pi}\int\frac{1}{s_z}\exp[ik\boldsymbol{s}\cdot(\boldsymbol{r}-\boldsymbol{\rho}')]d^2\boldsymbol{s}_\perp, \tag{1.38}$$

The last term of Eq. (1.38) is a form of the Weyl's representation of a diverging spherical wave (see Sec. 3.2.4 of [23]). Then, the three partial derivatives of $G(\boldsymbol{r},\boldsymbol{\rho}')$ can be expressed as

$$G_\alpha(\boldsymbol{r},\boldsymbol{\rho}') = -\frac{k^2}{2\pi}\int \frac{s_\alpha}{s_z}\exp[ik\boldsymbol{s}\cdot(\boldsymbol{r}-\boldsymbol{\rho}')]d^2\boldsymbol{s}_\perp,\ (\alpha = x,y,z)\,. \tag{1.39}$$

On substituting from Eq. (1.39) into Eq. (1.37), one obtains after interchanging the orders of integrals,

$$E_\alpha(\boldsymbol{r},\omega) = \int a_\alpha(\boldsymbol{s},\omega)\exp(ik\boldsymbol{s}\cdot\boldsymbol{r})d\boldsymbol{s}_\perp^2\,, \tag{1.40}$$

where

$$a_x(\boldsymbol{s},\omega) = \left(\frac{k}{2\pi}\right)^2\int E_x^{(0)}(\boldsymbol{\rho}',\omega)\exp[-ik\boldsymbol{s}\cdot\boldsymbol{\rho}']d^2\rho'\,, \tag{1.41a}$$

$$a_y(\boldsymbol{s},\omega) = \left(\frac{k}{2\pi}\right)^2\int E_y^{(0)}(\boldsymbol{\rho}',\omega)\exp[-ik\boldsymbol{s}\cdot\boldsymbol{\rho}']d^2\rho'\,, \tag{1.41b}$$

$$\begin{aligned} a_z(\boldsymbol{s},\omega) &= -\left(\frac{k}{2\pi}\right)^2\int\left[\frac{s_x}{s_z}E_x^{(0)}(\boldsymbol{\rho}',\omega)+\frac{s_y}{s_z}E_y^{(0)}(\boldsymbol{\rho}',\omega)\right]\exp[-ik\boldsymbol{s}\cdot\boldsymbol{\rho}']d^2\rho' \\ &= -\frac{1}{s_z}\Big[s_x a_x(\boldsymbol{s},\omega)+s_y a_y(\boldsymbol{s},\omega)\Big]\,. \end{aligned} \tag{1.41c}$$

One notes that the $x-$ and $y-$ components of the amplitude of the plane wave modes $a_x(\boldsymbol{s},\omega)$ and $a_y(\boldsymbol{s},\omega)$ have exactly the same form as in Eq. (1.36) while the $z-$ component $a_z(\boldsymbol{s},\omega)$ is expressed via the transverse components through the simple

transformation in Eq. (1.41c). Therefore Eq. (1.40) and Eq. (1.41) are the three-dimensional generalization from its one-dimensional form and exactly equivalent to Luneberg's formulas. While in the treatment involving beam-like (highly directional) fields, we need only $E_x(\boldsymbol{r},\omega)$ and $E_y(\boldsymbol{r},\omega)$ components of the electric field propagating from the planar source into the $+z$ half space, in studies of general fields we should consider all the three Cartesian components. Such situation arises in the analysis of near-fields or on scattering at high angles, for instance.

On taking the average over the ensemble of the light field for each component of the electric field vector $\boldsymbol{E}(\boldsymbol{r},\omega)$, we can form the 3x3 cross-spectral density matrix $\boldsymbol{W}(\boldsymbol{r}_1,\boldsymbol{r}_2,\omega)$ with components

$$W_{\alpha\beta}(\boldsymbol{r}_1,\boldsymbol{r}_2,\omega)=\left\langle E_\alpha^*(\boldsymbol{r}_1,\omega)E_\beta(\boldsymbol{r}_2,\omega)\right\rangle,\quad(\alpha,\beta=x,y,z). \tag{1.42}$$

On substituting from Eq. (1.40) into Eq. (1.42), we obtain the following expression for the cross-spectral density matrix of the field, in the form of angular-spectrum representation of plane waves propagating into the half-space $z>0$:

$$W_{\alpha\beta}(\boldsymbol{r}_1,\boldsymbol{r}_2,\omega)=\int\int A_{\alpha\beta}(\boldsymbol{s}_1,\boldsymbol{s}_2,\omega)\exp[ik(\boldsymbol{s}_2\cdot\boldsymbol{r}_2-\boldsymbol{s}_1^*\cdot\boldsymbol{r}_1)]ds_{1\perp}^2ds_{2\perp}^2. \tag{1.43}$$

Here $\alpha,\beta=x,y,z$, and $A_{\alpha\beta}(\boldsymbol{s}_1,\boldsymbol{s}_2,\omega)=\left\langle a_\alpha^*(\boldsymbol{s}_1,\omega)a_\beta(\boldsymbol{s}_2,\omega)\right\rangle$ is the angular correlation function between components of two plane-wave modes of the electric field

$$A_{\alpha\beta}(\boldsymbol{s}_1,\boldsymbol{s}_2,\omega)=\left(\frac{k}{2\pi}\right)^4\int\int W_{\alpha\beta}^{(0)}(\boldsymbol{\rho}_1',\boldsymbol{\rho}_2',\omega)\exp[-ik(\boldsymbol{s}_2\cdot\boldsymbol{\rho}_2'-\boldsymbol{s}_1\cdot\boldsymbol{\rho}_1')]d^2\boldsymbol{\rho}_1'd^2\boldsymbol{\rho}_2', \tag{1.44}$$

where only components $A_{xx}(\boldsymbol{s}_1, \boldsymbol{s}_2, \omega)$, $A_{xy}(\boldsymbol{s}_1, \boldsymbol{s}_2, \omega)$, $A_{yx}(\boldsymbol{s}_1, \boldsymbol{s}_2, \omega)$, $A_{yy}(\boldsymbol{s}_1, \boldsymbol{s}_2, \omega)$ contribute to the far field.

Chapter 2

Scalar Scattering Theory

2.1 Pair-structure Matrix of Random Collection of Particles.

In order to determine the statistical properties of light scattered from a collection of particles it is important to know various physical properties of the collection such as particle size, distribution of the refractive index, particles' absorptive properties, anisotropic features, etc. [24-25]. In the situation if the collection is random statistical properties governing individual particles and the collection as a whole should be specified. In a particular case when each individual particle has deterministic potential but the locations of particle centers are random the structure factor [26-27] and the pair-structure factor [28-29] are crucial quantities for the analysis of the second-order statistics of the scattered light. The structure factor [26] relates a single momentum-transfer vector, i.e. the scaled difference of incident and scattered directions, to the positions of the particles of the system. The pair-structure factor [28] relates two momentum-transfer vectors, taking into account two incident and two scattered directions, to correlations among the positions of the particles in the system. It was demonstrated that while for determination of the second-order statistical properties of scattered light at a single point in space, such as intensity and polarization, the structure factor provides sufficient

amount of information, the pair-structure factor is necessary for finding the correlation properties of scattered radiation, e.g. its degree of coherence.

However, in situations when a scattering collection contains particles of different types other quantities might play crucial part in determining the properties of scattered radiation. Even though in practice collections with different types of particles are commonly encountered, scattering of classic light from such collections has not yet been rigorously treated.

2.1.1 Light scattering from random collections of particles of two types

In this section we introduce a physical quantity, in the form of a matrix, for accounting of the correlations between particles belonging to different types, i.e. possessing different (deterministic) potentials. We show, in particular, that the off-diagonal elements of the new matrix, which relate to the joint correlations between different particle types, enter the formula for the degree of coherence of the scattered light and, hence, are of utmost importance for the scattering experiments in cases where interference effects cannot be neglected.

Let us begin by considering a monochromatic plane wave oscillating at angular frequency ω, and spatial position $\boldsymbol{r}'$, $U^{(i)}(\boldsymbol{r}',\omega)$, which propagates in a direction specified by a real unit vector $\boldsymbol{s}_0$ and is incident on a collection of particles. We may express the cross-spectral density function of the incident plane wave at a pair of points specified by the position vectors $\boldsymbol{r}_1'$ and $\boldsymbol{r}_2'$ as [20]

$$W^{(i)}(\boldsymbol{r}_1',\boldsymbol{r}_2',\omega)=\left\langle U^{(i)*}(\boldsymbol{r}_1',\omega)U^{(i)}(\boldsymbol{r}_2',\omega)\right\rangle \\ =S^{(i)}(\omega)\exp[ik\boldsymbol{s}_0\cdot(\boldsymbol{r}_2'-\boldsymbol{r}_1')], \tag{2.1}$$

where $S^{(i)}(\omega)$ is the spectral density of incident light and $k=\omega/c$ is the free-space wave number.

Before being involved with the general case let us first consider the situation when the scattering collection consists only of two different types. Let the particles have deterministic scattering potentials, but be randomly distributed in scattering volume V. In this case the scattering potential of the entire collection which in general is defined by Eq. (1.12) has the form

$$F(\boldsymbol{r}',\omega)=\sum_{m=1}^{M_1}f_1(\boldsymbol{r}'-\boldsymbol{r}_{1m},\omega)+\sum_{n=1}^{M_2}f_2(\boldsymbol{r}'-\boldsymbol{r}_{2n},\omega). \tag{2.2}$$

Here two different kinds of particles have scattering potentials $f_1(\boldsymbol{r}-\boldsymbol{r}_{1m},\omega)$ and $f_2(\boldsymbol{r}-\boldsymbol{r}_{2n},\omega)$ and are located at points with position vectors $\boldsymbol{r}_{1m}$ (i=1,…, M_1) and $\boldsymbol{r}_{2n}$ (j =1,… M_2), respectively. In such a case, the correlation function of the scattering potentials $C_F(\boldsymbol{r}_1',\boldsymbol{r}_2',\omega)$ defined in Eq. (1.27) reduces to the form

$$C_F(\boldsymbol{r}_1',\boldsymbol{r}_2',\omega)=\left\langle\sum_{m_1=1}^{M_1}\sum_{m_2=1}^{M_1}f_1^*(\boldsymbol{r}_1'-\boldsymbol{r}_{1m_1},\omega)f_1(\boldsymbol{r}_2'-\boldsymbol{r}_{1m_2},\omega)\right\rangle \tag{2.3a}$$

$$+\left\langle\sum_{m=1}^{M_1}\sum_{n=1}^{M_2}f_1^*(\boldsymbol{r}_1'-\boldsymbol{r}_{1m},\omega)f_2(\boldsymbol{r}_2'-\boldsymbol{r}_{2n},\omega)\right\rangle \tag{2.3b}$$

$$+\left\langle \sum_{n=1}^{M_2}\sum_{m=1}^{M_1} f_2^{\,*}(\boldsymbol{r}_1' - \boldsymbol{r}_{2n}, \omega) f_1(\boldsymbol{r}_2' - \boldsymbol{r}_{1m}, \omega) \right\rangle \tag{2.3c}$$

$$+\left\langle \sum_{n_1=1}^{M_2}\sum_{n_2=1}^{M_2} f_2^{\,*}(\boldsymbol{r}_1' - \boldsymbol{r}_{2n_1}, \omega) f_2(\boldsymbol{r}_2' - \boldsymbol{r}_{2n_2}, \omega) \right\rangle. \tag{2.3d}$$

Here Eqs. (2.3a) and (2.3d) denote the self-correlation functions of the scattering potentials of type 1 and type 2 particles, respectively, and Eqs. (2.3b) and (2.3c) represent their joint correlation functions. Self-correlation functions refer here to correlations between particles of one type and joint correlation functions refer to correlations between particles of two different types. On substituting from Eq. (2.3) into Eq. (1.30), and interchanging the orders of integrals and summations we find, after integration, that

$$\widetilde{C}_F(-\boldsymbol{K}_1, \boldsymbol{K}_2, \omega) = \widetilde{f}_1^{\,*}(\boldsymbol{K}_1, \omega)\widetilde{f}_1(\boldsymbol{K}_2, \omega) M_{11}(\boldsymbol{K}_1, \boldsymbol{K}_2, \omega) \tag{2.4a}$$

$$+\widetilde{f}_1^{\,*}(\boldsymbol{K}_1, \omega)\widetilde{f}_2(\boldsymbol{K}_2, \omega) M_{12}(\boldsymbol{K}_1, \boldsymbol{K}_2, \omega) \tag{2.4b}$$

$$+\widetilde{f}_2^{\,*}(\boldsymbol{K}_1, \omega)\widetilde{f}_1(\boldsymbol{K}_2, \omega) M_{21}(\boldsymbol{K}_1, \boldsymbol{K}_2, \omega) \tag{2.4c}$$

$$+\widetilde{f}_2^{\,*}(\boldsymbol{K}_1, \omega)\widetilde{f}_2(\boldsymbol{K}_2, \omega) M_{22}(\boldsymbol{K}_1, \boldsymbol{K}_2, \omega), \tag{2.4d}$$

where $\tilde{f}_1$ and $\tilde{f}_2$ are the Fourier transforms of the scattering potentials , i.e.

$$\widetilde{f}_i(\boldsymbol{K}, \omega) = \int_V f_i(\boldsymbol{r}', \omega) \exp(-i\boldsymbol{K}\cdot\boldsymbol{r}') \mathrm{d}^3 r' \qquad (i = 1, 2). \tag{2.5}$$

In Eq. (2.4) the quantities

$$M_{ij}(\boldsymbol{K}_1,\boldsymbol{K}_2,\omega)=\left\langle \sum_{m=1}^{M_i}\sum_{n=1}^{M_j}\exp[i(\boldsymbol{K}_1\cdot\boldsymbol{r}_{im}-\boldsymbol{K}_2\cdot\boldsymbol{r}_{jn})]\right\rangle \ (i,j=1,2), \tag{2.6}$$

have the following meaning: $M_{11}(\boldsymbol{K}_1,\boldsymbol{K}_2,\omega)$ and $M_{22}(\boldsymbol{K}_1,\boldsymbol{K}_2,\omega)$ are the pair-structure factors of type 1 and type 2 particle subcollections, as they were introduced in Ref. [28]; $M_{12}(\boldsymbol{K}_1,\boldsymbol{K}_2,\omega)$ and $M_{21}(\boldsymbol{K}_1,\boldsymbol{K}_2,\omega)$ are the joint pair-structure factors, which have not been introduced before. We note that in general $M_{12}(\boldsymbol{K}_1,\boldsymbol{K}_2,\omega)$ is not the complex conjugate of $M_{21}(\boldsymbol{K}_1,\boldsymbol{K}_2,\omega)$. Upon denoting $Q_i(\boldsymbol{K})=\sum_{m=1}^{M_i}\exp[-i\boldsymbol{K}\cdot\boldsymbol{r}_{im}]$ $(i=1,2)$, and on forming a vector $\boldsymbol{F}(\boldsymbol{K},\omega)=(\widetilde{f}_1(\boldsymbol{K},\omega),\widetilde{f}_2(\boldsymbol{K},\omega))^T$ (T standing for transposition) whose entries are the scattering potentials of two types, Eq. (2.4) may be expressed in a convenient matrix form as

$$\widetilde{C}_F(-\boldsymbol{K}_1,\boldsymbol{K}_2,\omega)=\boldsymbol{F}^{\dagger}(\boldsymbol{K}_1,\omega)\boldsymbol{M}^{(2)}(\boldsymbol{K}_1,\boldsymbol{K}_2,\omega)\boldsymbol{F}(\boldsymbol{K}_2,\omega), \tag{2.7}$$

where $\dagger=*T$ denotes the Hermitian operator and

$$\boldsymbol{M}^{(2)}(\boldsymbol{K}_1,\boldsymbol{K}_2,\omega)=\begin{pmatrix}\left\langle Q_1^{*}(\boldsymbol{K}_1,\omega)Q_1(\boldsymbol{K}_2,\omega)\right\rangle & \left\langle Q_1^{*}(\boldsymbol{K}_1,\omega)Q_2(\boldsymbol{K}_2,\omega)\right\rangle\\ \left\langle Q_2^{*}(\boldsymbol{K}_1,\omega)Q_1(\boldsymbol{K}_2,\omega)\right\rangle & \left\langle Q_2^{*}(\boldsymbol{K}_1,\omega)Q_2(\boldsymbol{K}_2,\omega)\right\rangle\end{pmatrix}. \tag{2.8}$$

2.1.2 Light scattering from random collections of particles of *L* types

We will now extend the preceding analysis to the case of scattering of light from collection consisting of particles of L different types. Under these circumstances the scattering potential $F(\mathbf{r}',\omega)$ has the form

$$F(\boldsymbol{r}',\omega)=\sum_{i=1}^{L}\sum_{m=1}^{M_i} f_i(\boldsymbol{r}'-\boldsymbol{r}_{im},\omega)\,, \tag{2.9}$$

where $\boldsymbol{r}_{im}$ is the location of a scattering center of a particle of type l, $f_i(\boldsymbol{r}'-\boldsymbol{r}_{im},\omega)$ is the scattering potential of the scatter of type i and M_i is the number of particles of type i. Then, Eq. (2.3) can be generalized to the form

$$C_F(\boldsymbol{r}_1',\boldsymbol{r}_2',\omega)=\sum_{i=1}^{L}\sum_{j=1}^{L}\sum_{m=1}^{M_i}\sum_{n=1}^{M_j}\left\langle f_i^*(\boldsymbol{r}'-\boldsymbol{r}_{im},\omega) f_j^*(\boldsymbol{r}'-\boldsymbol{r}_{jn},\omega)\right\rangle\,. \tag{2.10}$$

In a similar fashion as it was done for two particle types it can be shown that the Fourier transform of the correlation function of the collection of L different types has the form of the matrix product

$$\widetilde{C}_F(-\boldsymbol{K}_1,\boldsymbol{K}_2,\omega)=\boldsymbol{F}^{\dagger}(\boldsymbol{K}_1,\omega)\boldsymbol{M}^{(L)}(\boldsymbol{K}_1,\boldsymbol{K}_2,\omega)\boldsymbol{F}(\boldsymbol{K}_2,\omega)\,, \tag{2.11}$$

where $\boldsymbol{F}(\boldsymbol{K},\omega)=(\widetilde{f}_1(\boldsymbol{K},\omega),\widetilde{f}_2(\boldsymbol{K},\omega),...,\widetilde{f}_L(\boldsymbol{K},\omega))^T$ and

$\boldsymbol{M}^{(L)}(\boldsymbol{K}_1,\boldsymbol{K}_2,\omega)$

$$=\begin{pmatrix} \left\langle Q_1^*(\boldsymbol{K}_1,\omega)Q_1(\boldsymbol{K}_2,\omega)\right\rangle & \left\langle Q_1^*(\boldsymbol{K}_1,\omega)Q_2(\boldsymbol{K}_2,\omega)\right\rangle & ... & \left\langle Q_1^*(\boldsymbol{K}_1,\omega)Q_L(\boldsymbol{K}_2,\omega)\right\rangle \\ \left\langle Q_2^*(\boldsymbol{K}_1,\omega)Q_1(\boldsymbol{K}_2,\omega)\right\rangle & \left\langle Q_2^*(\boldsymbol{K}_1,\omega)Q_2(\boldsymbol{K}_2,\omega)\right\rangle & ... & \left\langle Q_2^*(\boldsymbol{K}_1,\omega)Q_L(\boldsymbol{K}_2,\omega)\right\rangle \\ ... & ... & ... & ... \\ \left\langle Q_L^*(\boldsymbol{K}_1,\omega)Q_1(\boldsymbol{K}_2,\omega)\right\rangle & \left\langle Q_L^*(\boldsymbol{K}_1,\omega)Q_2(\boldsymbol{K}_2,\omega)\right\rangle & ... & \left\langle Q_L^*(\boldsymbol{K}_1,\omega)Q_L(\boldsymbol{K}_2,\omega)\right\rangle \end{pmatrix}. \tag{2.12}$$

As above, the diagonal elements of this matrix are known as the pair-structure factors of each particle type and off-diagonal elements are the joint pair-structure factors for each pair of particle types. Diagonal and off-diagonal elements of this matrix can have

different values, in general. Hence the entire matrix $\boldsymbol{M}^{(L)}(\boldsymbol{K}_1, \boldsymbol{K}_2, \omega)$ contains all the information of the correlation properties of between particles within one type and across different types it may be natural to call it the *pair-structure matrix*.

2.1.3 Dependence of coherence state of scattered light on the pair-structure matrix

Within the validity of the first-order Born approximation, the cross-spectral density function of the scattered field at two points specified by position vectors $r\boldsymbol{s}_1$ and $r\boldsymbol{s}_2$ from a monochromatic plane wave is given by Eq. (1.29). After substituting from Eq. (2.11) into Eq. (1.29) one can obtain the formula for the cross-spectral density function of the field scattered from a collection of particles of L different types in the form

$$W^{(s)}(r\mathbf{s}_1, r\mathbf{s}_2, \omega) = \frac{1}{r^2} S^{(i)}(\omega) \boldsymbol{F}^{+}(\boldsymbol{K}_1, \omega) \boldsymbol{M}^{(L)}(\boldsymbol{K}_1, \boldsymbol{K}_2, \omega) \boldsymbol{F}(\boldsymbol{K}_2, \omega). \tag{2.13}$$

Hence the spectral degree of coherence defined by the Eq. (1.3) takes the form

$$\mu(r\boldsymbol{s}_1, r\boldsymbol{s}_2, \omega)$$

$$= \frac{\boldsymbol{F}^{\dagger}(\boldsymbol{K}_1, \omega) \boldsymbol{M}^{(L)}(\boldsymbol{K}_1, \boldsymbol{K}_2, \omega) \boldsymbol{F}(\boldsymbol{K}_2, \omega)}{\sqrt{\boldsymbol{F}^{\dagger}(\boldsymbol{K}_1, \omega) \boldsymbol{M}^{(L)}(\boldsymbol{K}_1, \boldsymbol{K}_1, \omega) \boldsymbol{F}(\boldsymbol{K}_1, \omega)} \sqrt{\boldsymbol{F}^{+}(\boldsymbol{K}_2, \omega) \boldsymbol{M}^{(L)}(\boldsymbol{K}_2, \boldsymbol{K}_2, \omega) \boldsymbol{F}(\boldsymbol{K}_2, \omega)}}.$$

(2.14)

Eq. (2.14) is the main result of this section which indicates the dependence of the state of coherence of scattered light on the correlation properties of the particles within one type and across different types.

In the special case when $M_{ii}^{(L)}(\boldsymbol{K},\boldsymbol{K},\omega) \approx M^{(L)}(\boldsymbol{K},\boldsymbol{K},\omega)$, which means that the particles of different types are similarly distributed in space, Eq. (2.14) reduces to a simpler form

$$\mu(r\boldsymbol{s}_1, r\boldsymbol{s}_2, \omega) = \frac{\sum_{i=1}^{L}\sum_{j=1}^{L} \tilde{f}_i^{*}(\boldsymbol{K}_1,\omega)\tilde{f}_j(\boldsymbol{K}_2,\omega) m_{ij}^{(L)}(\left|\boldsymbol{K}_1 - \boldsymbol{K}_2\right|,\omega)}{\left|\sum_{i=1}^{L}\sum_{j=1}^{L} \tilde{f}_i(\boldsymbol{K}_1,\omega)\tilde{f}_j(\boldsymbol{K}_2,\omega)\right|} \quad . \tag{2.15}$$

where

$$m_{ij}^{(L)}(\left|\boldsymbol{K}_1 - \boldsymbol{K}_2\right|,\omega) = \frac{M_{ij}^{(L)}(\boldsymbol{K}_1,\boldsymbol{K}_2,\omega)}{\sqrt{M_{ij}^{(L)}(\boldsymbol{K}_1,\boldsymbol{K}_1,\omega)}\sqrt{M_{ij}^{(L)}(\boldsymbol{K}_2,\boldsymbol{K}_2,\omega)}}, \tag{2.16}$$

where Eq. (2.16) is the degree of angular correlation of the collection of particles of different kinds (if $i \neq j$) or of same kind (if $i = j$), which is a generalization form from Eq. (10) in Ref. [28].

2.1.4 Example and concluding remarks

To see the dependence of the spectral degree of coherence on the pair-structure matrix, especially on the off-diagonal components denoting the correlation between different kinds of particles, we consider two classes of particles distributed randomly in a finite volume, which are assumed to be similarly distributed in space, so that Eq. (2.21) is valid in this situation. We also assume that $m_{ij}^{(2)}$ has the Gaussian distribution type, which is of the form

$$m_{ij}^{(2)}(|\boldsymbol{K}_1 - \boldsymbol{K}_2|, \omega) = \exp\left[-\frac{|\boldsymbol{K}_1 - \boldsymbol{K}_2|^2}{(k\delta_{ij})^2}\right], \tag{2.17}$$

where δ_{ij} characterizes the correlation strength between the collection of particles of different classes (if $i \neq j$) or of same class (if $i = j$). Suppose that each particle has a scattering potential of Gaussian distribution of the form $f_i(\mathbf{r}', \omega) = \exp\left[-\mathbf{r}'^2 / 2\sigma_i^2\right]$. The parameters are chosen as: $\lambda = 632.8nm$, $\sigma_1 = 0.15\lambda$, $\sigma_2 = 0.3\lambda$, $\delta_{11} = \delta_{22} = 1$. Fig. 2.1 shows the dependence of the spectral degree of coherence of the scattered field on the off-diagonal component of the pair-structure matrix $\boldsymbol{M}^{(2)}(\boldsymbol{K}_1, \boldsymbol{K}_2, \omega)$. Different correlation strengths between different kinds of particles influence the spectral degree of coherence substantially, as is seen from Fig. 2.1.

In summary, Eqs. (2.15)-(2.17) clearly show that the coherence properties of scattered light are intimately related to the various correlations between particles in the scattering collection, and, more importantly, to the possible non-zero correlations between particles pertinent to different types. Thus the introduced pair-scattering matrix may be employed in theoretical procedures and experiments involving scattering of light from complex collections of scatterers.

Among important applications of our theory is the development of novel sensing techniques in such natural environments as atmosphere and ocean where random particle distributions are commonly encountered.

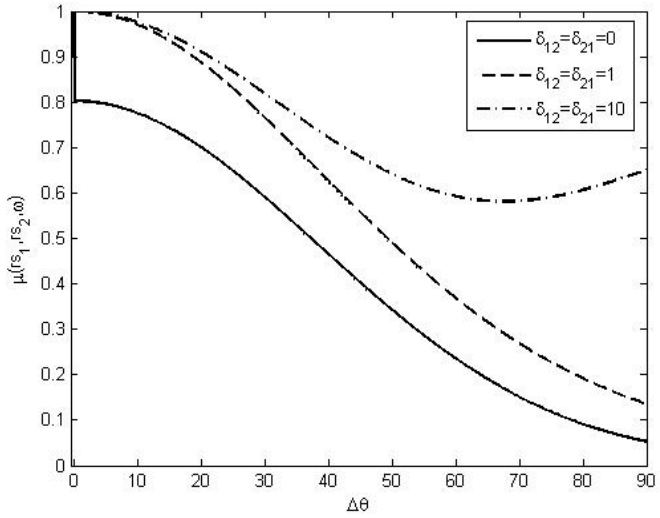

Fig. 2.1 Dependence of the spectral degree of coherence $\mu(r\boldsymbol{s}_1, r\boldsymbol{s}_2, \omega)$ on $\Delta\theta$, where $\boldsymbol{s} = (\sin\theta\cos\varphi, \sin\theta\sin\varphi, \cos\theta)$, $\boldsymbol{s}_0 = (0,0,1)$, $\varphi_1 = \varphi_2 = \pi/2$, $\theta_1 = 0$, $\Delta\theta = \theta_2 - \theta_1 = \theta_2$.

2.2 Method for tracing the position of an alien object embedded in random particulate medium

Due to its vast applications in remote sensing and medical diagnostics the subject of light scattering from particulate media is always of a vivid interest for both scientific and engineering communities. Recently important steps forward were made in understanding how the interaction of light with linear media with arbitrary correlation properties, whether of continuous or particulate nature occurs [30-32].

Scattering potential is one of the important concepts for description of the scattering media. Once the statistics of this quantity are known those of the refractive index can be easily found [20]. As was shown in [33-34] several inverse scattering problems can be solved providing with the statistics of the scattering potential. All these techniques, however, either deal with a single random scatterer or with a random collection consisting of the identical particles.

In this section we will be interested, based on the concept of pair-structure matrix introduced in Sec. 2.1, in solving an inverse problem that involves light scattering from a medium in which not necessarily identical particles are present. We first develop the general method for reconstruction of the correlation function of the scattering potential pertaining to particles of different types. Then we solve a specific problem of finding the position of a single deterministic particle, referred to below as an “alien particle” or “impurity”, in a random collection of other particles, referred to as “normal particles”. More specifically, by designing three scattering experiments, we first measure the pair-structure function of the original particulate media without the impurity. Then, after

embedding the alien particle within the collection at a certain position, we provide the technique for its tracing.

2.2.1 Scattering of light from particulate media

Suppose that a spatially coherent polychromatic plane wave propagating in a direction specified by a real unit vector $\boldsymbol{s}_0$ is incident onto a collection of particles occupying domain D. The incident light at position $\boldsymbol{r}'$ may be characterized by a statistical ensemble $\{U^{(i)}(\mathbf{r}', \mathbf{s}_0; \omega)\exp[-i\omega t]\}$ of realizations, all of the form

$$U^{(i)}(\boldsymbol{r}', \boldsymbol{s}_0; \omega) = a(\omega)\exp(ik\boldsymbol{s}_0 \cdot \boldsymbol{r}'), \tag{2.18}$$

where $a(\omega)$ is, in general, complex and $k = \omega / c$, with c being the light speed in vacuum. Then the cross-spectral density function of the incident field at a pair of points, specified by the position vectors $\boldsymbol{r}_1'$ and $\boldsymbol{r}_2'$ may be expressed in the form [20]

$$W^{(i)}(\boldsymbol{r}_1', \boldsymbol{r}_2', \boldsymbol{s}_0, \omega) = \left\langle U^{(i)*}(\boldsymbol{r}_1', \boldsymbol{s}_0, \omega) U^{(i)}(\boldsymbol{r}_2', \boldsymbol{s}_0, \omega) \right\rangle, \tag{2.19}$$

where the asterisk denotes the complex conjugate and the angular brackets denote the ensemble average. On substituting from Eq. (2.18) into Eq. (2.19), the cross-spectral density function of the incident field becomes

$$W^{(i)}(\boldsymbol{r}_1', \boldsymbol{r}_2', \boldsymbol{s}_0, \omega) = S^{(i)}(\omega)\exp[ik\boldsymbol{s}_0 \cdot (\boldsymbol{r}_2' - \boldsymbol{r}_1')], \tag{2.20}$$

with $S^{(i)}(\omega) = \left\langle a^*(\omega) a(\omega) \right\rangle$ being the spectral density of the incident light.

In what follows we will assume that the incident light and the medium are statistically independent and, hence, their ensemble averages can be separated. If the refractive index differs only slightly from unity the scattering is weak and can be analyzed within the accuracy of the first-Born approximation. Then, the scattered field at a point, specified by position vector $r\boldsymbol{s}$, $\boldsymbol{s}$ being the unit vector, obeys the law Eq. (1.22). The cross-spectral density function of the scattered field at two points specified by position vectors $r\boldsymbol{s}_1$ and $r\boldsymbol{s}_2$ is then defined by

$$W^{(s)}(r\boldsymbol{s}_1, r\boldsymbol{s}_2, \boldsymbol{s}_0, \omega) = \left\langle U^{(s)*}(r\boldsymbol{s}_1, \omega) U^{(s)}(r\boldsymbol{s}_2, \omega) \right\rangle. \tag{2.21}$$

To obtain the cross-spectral density function of the scattered field in the far zone we rewrite Eq. (1.29) as

$$W^{(s)}(r\boldsymbol{s}_1, r\boldsymbol{s}_2, \boldsymbol{s}_0, \omega) = \frac{1}{r^2} S^{(i)}(\omega) \widetilde{C}_F[-k(\boldsymbol{s}_1 - \boldsymbol{s}_0), k(\boldsymbol{s}_2 - \boldsymbol{s}_0), \omega], \tag{2.22}$$

where $\widetilde{C}_F[-\boldsymbol{K}_1, \boldsymbol{K}_2, \omega]$ is defined in Eq. (1.30) called the six-dimensional spatial Fourier transform of the correlation function $\mathrm{C}_F(\boldsymbol{r}_1', \boldsymbol{r}_2', \omega)$ of the scattering potential and

$$\boldsymbol{K}_1 = k(\boldsymbol{s}_1 - \boldsymbol{s}_0), \qquad \boldsymbol{K}_2 = k(\boldsymbol{s}_2 - \boldsymbol{s}_0). \tag{2.23}$$

Here $\boldsymbol{K}_1$ and $\boldsymbol{K}_2$ are analogous to the momentum transfer vector of quantum mechanical theory of potential scattering. They have absolute values $|\boldsymbol{K}_1| \le 2k = \frac{4\pi}{\lambda}$ and $|\boldsymbol{K}_2| \le 2k = \frac{4\pi}{\lambda}$.

We now consider a particulate scattering media composed of two different types of particles. We assume that the two types of particles are located at points with three-dimensional position vectors $\boldsymbol{r}_{1m}$ ($m=1,\ldots,M_1$) and $\boldsymbol{r}_{2n}$ ($n=1,\ldots M_2$), and have scattering potentials $f_1(\boldsymbol{r}',\omega)$ and $f_2(\boldsymbol{r}',\omega)$, respectively. The Fourier transforms of the scattering potentials then have the forms

$$\widetilde{f}_i(\boldsymbol{K},\omega)=\int_V f_i(\boldsymbol{r}',\omega)\exp(-i\boldsymbol{K}\cdot\boldsymbol{r}')\mathrm{d}^3r' \qquad (i=1,2). \tag{2.24}$$

Further, by setting $Q_i(\boldsymbol{K})=\sum_{m=1}^{M_i}\exp[-i\boldsymbol{K}\cdot\boldsymbol{r}_{im}]$ $(i=1,2)$, and forming a vector $\boldsymbol{F}(\boldsymbol{K},\omega)=(\widetilde{f}_1(\boldsymbol{K},\omega),\widetilde{f}_2(\boldsymbol{K},\omega))^T$, it is possible to obtain the cross-spectral density function of the far field scattered from a collection of particles of two different types. Namely, one has:

$$W^{(s)}(r\boldsymbol{s}_1,r\boldsymbol{s}_2,\boldsymbol{s}_0,\omega)=\frac{1}{r^2}S^{(i)}(\omega)\boldsymbol{F}^{+}(\boldsymbol{K}_1,\omega)\boldsymbol{M}^{(2)}(\boldsymbol{K}_1,\boldsymbol{K}_2,\omega)\boldsymbol{F}(\boldsymbol{K}_2,\omega), \tag{2.25}$$

where $\dagger=*T$ denotes the Hermitian operator and

$$\boldsymbol{M}^{(2)}(\boldsymbol{K}_1,\boldsymbol{K}_2,\omega)=\begin{pmatrix}\left\langle Q_1^{*}(\boldsymbol{K}_1,\omega)Q_1(\boldsymbol{K}_2,\omega)\right\rangle & \left\langle Q_1^{*}(\boldsymbol{K}_1,\omega)Q_2(\boldsymbol{K}_2,\omega)\right\rangle\\ \left\langle Q_2^{*}(\boldsymbol{K}_1,\omega)Q_1(\boldsymbol{K}_2,\omega)\right\rangle & \left\langle Q_2^{*}(\boldsymbol{K}_1,\omega)Q_2(\boldsymbol{K}_2,\omega)\right\rangle\end{pmatrix}, \tag{2.26}$$

which is defined in Eq. (2.12). Since the cross-spectral density function $W^{(s)}(r\boldsymbol{s}_1,r\boldsymbol{s}_2,\boldsymbol{s}_0,\omega)$ is proportional to the degree of coherence, it can be measured from interference experiments [33]. Then, the Fourier transform of the correlation function of the scattering potential of the scatterer can be obtained experimentally [29, 33] as

$$\widetilde{C}_F(-\boldsymbol{K}_1,\boldsymbol{K}_2,\omega)=\boldsymbol{F}^{\dagger}(\boldsymbol{K}_1,\omega)\boldsymbol{M}^{(2)}(\boldsymbol{K}_1,\boldsymbol{K}_2,\omega)\boldsymbol{F}(\boldsymbol{K}_2,\omega)=r^2\frac{W^{(s)}(r\boldsymbol{s}_1,r\boldsymbol{s}_2,\boldsymbol{s}_0,\omega)}{S^{(i)}(\omega)}. \quad (2.27)$$

2.2.2 Inverse problem of tracing an impurity in the random collection of particles

On the basis of the theory described in Section 2.2.1, we will now develop a novel technique for tracing the position of an alien particle embedded in the collection of normal particles. We assume that the impurity consists of just one deterministic particle with scattering potential $f_0(\boldsymbol{r}',\omega)$ located at a point, specified by position vector $\boldsymbol{r}_0$, and that the normal particles with scattering potentials $f_1(\boldsymbol{r}',\omega)$ are located at $\boldsymbol{r}_{1m}$ $(m=1,...,M)$. As the first step, we obtain from an experiment the Fourier transform of the correlation function of the scattering potential of the original collection, i.e. the collection consisting only of normal particles, as

$$\widetilde{C}_F^{(0)}(-\boldsymbol{K},\boldsymbol{K})=\widetilde{f}_1^{*}(\boldsymbol{K})\widetilde{f}_1(\boldsymbol{K})\left\langle Q_1^{*}(\boldsymbol{K})Q_1(\boldsymbol{K})\right\rangle, \quad (2.28)$$

where we set $\boldsymbol{K}_1=\boldsymbol{K}_2=\boldsymbol{K}$, i.e., $\boldsymbol{s}_1=\boldsymbol{s}_2=\boldsymbol{s}$ and omit the dependence of ω for simplicity.

In the next step, we make two reference samples which consist of the original collection of normal particles and a known deterministic alien particle with scattering potential $f_2(\boldsymbol{r}',\omega)$. Suppose, for the first sample we have the known "test particle" located at the origin point O, and for the second sample we have the known "test particle" located at a known position $\boldsymbol{r}_2$. Thus we assume that at this step the alien particle has the known positions, which are not influenced by the original particulate media. From the

experiment, we can determine the Fourier transform of the correlation function of the scattering potential of sample 1, with the help of Eq. (2.27), i.e.

$$\widetilde{C}_F^{(1)}(-\boldsymbol{K},\boldsymbol{K}) = \widetilde{f}_1^{\,*}(\boldsymbol{K})\widetilde{f}_1(\boldsymbol{K})\left\langle Q_1^*(\boldsymbol{K})Q_1(\boldsymbol{K})\right\rangle + \widetilde{f}_1^{\,*}(\boldsymbol{K})\widetilde{f}_2(\boldsymbol{K})\left\langle Q_1^*(\boldsymbol{K})\right\rangle$$

$$+\widetilde{f}_2^{\,*}(\boldsymbol{K})\widetilde{f}_1(\boldsymbol{K})\left\langle Q_1(\boldsymbol{K})\right\rangle + \widetilde{f}_2^{\,*}(\boldsymbol{K})\widetilde{f}_2(\boldsymbol{K}), \qquad (2.29)$$

where $Q_2(\boldsymbol{K}) = \exp(-i\boldsymbol{K}\cdot 0) = 1$ since the known particle is at origin. Without loss of generality we only consider the case where $\widetilde{f}_1(\boldsymbol{K})$ and $\widetilde{f}_2(\boldsymbol{K})$ are real (c.f. [35]). From Eqs. (2.28) and (2.29) we find that

$$\mathrm{Re}(\left\langle Q_1(\boldsymbol{K})\right\rangle) = \frac{\widetilde{C}_F^{(1)}(-\boldsymbol{K},\boldsymbol{K}) - \widetilde{C}_F^{(0)}(-\boldsymbol{K},\boldsymbol{K})}{2\widetilde{f}_1(\boldsymbol{K})\widetilde{f}_2(\boldsymbol{K})} - \frac{\widetilde{f}_2(\boldsymbol{K})}{2\widetilde{f}_1(\boldsymbol{K})}. \qquad (2.30)$$

We can also obtain the Fourier transform of the correlation function of the scattering potential of sample 2 from the scattering experiment, to be

$$\widetilde{C}_F^{(2)}(-\boldsymbol{K},\boldsymbol{K}) = \widetilde{f}_1^{\,*}(\boldsymbol{K})\widetilde{f}_1(\boldsymbol{K})\left\langle Q_1^*(\boldsymbol{K})Q_1(\boldsymbol{K})\right\rangle + \widetilde{f}_1^{\,*}(\boldsymbol{K})\widetilde{f}_2(\boldsymbol{K})\left\langle Q_1^*(\boldsymbol{K})\right\rangle \exp(-i\boldsymbol{K}\cdot\boldsymbol{r}_2)$$

$$+\widetilde{f}_2^{\,*}(\boldsymbol{K})\widetilde{f}_1(\boldsymbol{K})\left\langle Q_1(\boldsymbol{K})\right\rangle \exp(i\boldsymbol{K}\cdot\boldsymbol{r}_2) + \widetilde{f}_2^{\,*}(\boldsymbol{K})\widetilde{f}_2(\boldsymbol{K}), \qquad (2.31)$$

where we extract $\exp(i\boldsymbol{K}\cdot\boldsymbol{r}_2)$ from the angular brackets since the alien particle is of deterministic nature. Then, from Eq. (2.28), (2.30) and (2.31), one obtains

$$\mathrm{Im}(\left\langle Q_1(\boldsymbol{K})\right\rangle) = \mathrm{Re}(\left\langle Q_1(\boldsymbol{K})\right\rangle)\cot(\boldsymbol{K}\cdot\boldsymbol{r}_2)$$

$$-\frac{\widetilde{C}_F^{(2)}(-\boldsymbol{K},\boldsymbol{K})-\widetilde{C}_F^{(0)}(-\boldsymbol{K},\boldsymbol{K})}{2\widetilde{f}_1(\boldsymbol{K})\widetilde{f}_2(\boldsymbol{K})\sin(\boldsymbol{K}\cdot\boldsymbol{r}_2)}+\frac{\widetilde{f}_2(\boldsymbol{K})}{2\widetilde{f}_1(\boldsymbol{K})\sin(\boldsymbol{K}\cdot\boldsymbol{r}_2)}. \qquad (2.32)$$

Further the quantity $\langle Q_1(\boldsymbol{K})\rangle$ may be obtained from Eqs. (2.30) and (2.32) as

$$\langle Q_1(\boldsymbol{K})\rangle = \mathrm{Re}(\langle Q_1(\boldsymbol{K})\rangle)+i\,\mathrm{Im}(\langle Q_1(\boldsymbol{K})\rangle). \qquad (2.33)$$

Quantity $\langle Q(\boldsymbol{K})\rangle$ contains the information about the particulate medium in the absence of the alien particle. The three scattering experiments described above are designed to determine it in order to be employed below.

Now we assume that the alien particle is located within the original collection of normal particles at an unknown position $\boldsymbol{r}_0$. On performing one more scattering experiment, we may obtain the Fourier transform of the correlation function of the scattering potential of the mixed collection, as

$$\widetilde{C}_F^{(im)}(-\boldsymbol{K},\boldsymbol{K})=\widetilde{f}_1^{\,*}(\boldsymbol{K})\widetilde{f}_1(\boldsymbol{K})\langle Q_1^{*}(\boldsymbol{K})Q_1(\boldsymbol{K})\rangle+\widetilde{f}_1^{\,*}(\boldsymbol{K})\widetilde{f}_0(\boldsymbol{K})\langle Q_1^{*}(\boldsymbol{K})\rangle\exp(-i\boldsymbol{K}\cdot\boldsymbol{r}_0)$$

$$+\widetilde{f}_0^{\,*}(\boldsymbol{K})\widetilde{f}_1(\boldsymbol{K})\langle Q_1(\boldsymbol{K})\rangle\exp(i\boldsymbol{K}\cdot\boldsymbol{r}_0)+\widetilde{f}_0^{\,*}(\boldsymbol{K})\widetilde{f}_0(\boldsymbol{K}), \qquad (2.34)$$

where *im* denotes the impurity or the alien particle. From Eqs. (2.28), (2.30), (2.32) and (2.34) it follows that

$$\mathrm{Re}(\langle Q_1(\boldsymbol{K})\rangle)\cos(\boldsymbol{K}\cdot\boldsymbol{r}_0)-\mathrm{Im}(\langle Q_1(\boldsymbol{K})\rangle)\sin(\boldsymbol{K}\cdot\boldsymbol{r}_0)$$

$$=\frac{\widetilde{C}_F^{(im)}(-\boldsymbol{K},\boldsymbol{K})-\widetilde{C}_F^{(0)}(-\boldsymbol{K},\boldsymbol{K})}{2\widetilde{f}_1(\boldsymbol{K})\widetilde{f}_0(\boldsymbol{K})}-\frac{\widetilde{f}_0(\boldsymbol{K})}{2\widetilde{f}_1(\boldsymbol{K})}$$

$$\equiv C(\boldsymbol{K}). \tag{2.35}$$

To determine the position vector of the alien particle, it is crucial to have $\boldsymbol{K}\cdot\boldsymbol{r}_0 \ll 1$. On choosing the incident direction $\boldsymbol{s}_0 = (0,0,1)$ and the observation direction $\boldsymbol{s} = (s_x, 0, s_z)$, without loss of generality, we can measure the $x-$ component of the position vector $\boldsymbol{r}_0$, for which we have the constrains

$$|s_x| \ll 1, \qquad |1 - s_z| \ll 1, \qquad |1 - s_z| \ll |s_x|. \tag{2.36}$$

Inequalities (2.36) imply that $\boldsymbol{K}\cdot\boldsymbol{r}_0 \sim ks_x x$ (x_0 is the exact position and x is the approximate position). Retaining the first two terms of the Taylor expansion of the cosine function and the first term of the Taylor expansion of the sine function gives

$$\cos(\boldsymbol{K}\cdot\boldsymbol{r}_0) \sim 1 - \frac{1}{2}(\boldsymbol{K}\cdot\boldsymbol{r})^2, \qquad \sin(\boldsymbol{K}\cdot\boldsymbol{r}_0) \sim \boldsymbol{K}\cdot\boldsymbol{r}, \tag{2.37}$$

where the exact position vector $\boldsymbol{r}_0$ is replaced by the approximate position vector $\boldsymbol{r}$. On substituting form Eq. (2.37) into Eq. (2.35) we find that

$$x = \frac{-\mathrm{Im}(\langle Q_1(\boldsymbol{K})\rangle) + \sqrt{\mathrm{Im}^2(\langle Q_1(\boldsymbol{K})\rangle) - 2\,\mathrm{Re}(\langle Q_1(\boldsymbol{K})\rangle)[C(\boldsymbol{K}) - \mathrm{Re}(\langle Q_1(\boldsymbol{K})\rangle)]}}{ks_x\,\mathrm{Re}(\langle Q_1(\boldsymbol{K})\rangle)}, \tag{2.38}$$

where $C(\boldsymbol{K})$ is given by Eq. (2.35). Similar expression may be obtained for $y-$ component of the position vector $\boldsymbol{r}_0$, if we assume $\boldsymbol{s}_0 = (0,0,1)$ and $\boldsymbol{s} = (0, s_y, s_z)$ which satisfy the similar expression as Eq. (2.36). We note that for specific incident unit vector $\boldsymbol{s}_0 = (0,0,1)$, we may only determine $x-$ and $y-$components of the position vector $\boldsymbol{r}_0$,

however, for the $z-$component of $\boldsymbol{r}_0$, we might need the incident field propagating in another direction, say $\boldsymbol{s}_0 = (1,0,0)$. Although there may be some influence of the normal particles on the alien particle and vice versa, which might change their positions, such influence will be neglected in this section.

In a more general case, the impurity may consist of more than one particle. Under these circumstances, similar procedures give the average value of the position vectors of the *N* alien particles, which are concentrated in a small area, for instance

$$\bar{x} = \frac{-\mathrm{Im}(\langle Q_1(\boldsymbol{K})\rangle) + \sqrt{\mathrm{Im}^2(\langle Q_1(\boldsymbol{K})\rangle) - 2\,\mathrm{Re}(\langle Q_1(\boldsymbol{K})\rangle)[C^{(N)}(\boldsymbol{K}) - \mathrm{Re}(\langle Q_1(\boldsymbol{K})\rangle)]}}{ks_x\,\mathrm{Re}(\langle Q_1(\boldsymbol{K})\rangle)}, \quad (2.39)$$

where

$$C^{(N)}(\boldsymbol{K}) = \frac{\tilde{C}_F^{(im)}(-\boldsymbol{K},\boldsymbol{K}) - \tilde{C}_F^{(0)}(-\boldsymbol{K},\boldsymbol{K})}{2N\tilde{f}_1(\boldsymbol{K})\tilde{f}_0(\boldsymbol{K})} - \frac{N\tilde{f}_0(\boldsymbol{K})}{2\tilde{f}_1(\boldsymbol{K})}. \quad (2.40)$$

To justify the approximation in Eq. (2.37) we might have the requirements which are obtained from the expansion of cosine and sine function in the left hand side of Eq. (2.35),

$$\left|\frac{1}{24}(\boldsymbol{K}\cdot\boldsymbol{r}_0)^4 \cdot \mathrm{Re}(\langle Q_1(\boldsymbol{K})\rangle)\right| \ll \left|\boldsymbol{K}\cdot\boldsymbol{r}_0 \cdot \mathrm{Im}(\langle Q_1(\boldsymbol{K})\rangle)\right| \quad (2.41)$$

$$\left|\mathrm{Im}(\langle Q_1(\boldsymbol{K})\rangle)\cdot\frac{1}{6}(\boldsymbol{K}\cdot\boldsymbol{r}_0)^3\right| \ll \left|\frac{1}{2}(\boldsymbol{K}\cdot\boldsymbol{r}_0)^2 \cdot \mathrm{Re}(\langle Q_1(\boldsymbol{K})\rangle)\right|, \quad (2.42)$$

or

$$\left|\frac{\mathrm{Im}(\langle Q_1(\boldsymbol{K})\rangle)}{\mathrm{Re}(\langle Q_1(\boldsymbol{K})\rangle)}\right| \gg \frac{1}{24}\left|\boldsymbol{K}\cdot\boldsymbol{r}_0\right|^3 \tag{2.43}$$

$$\left|\frac{\mathrm{Im}(\langle Q_1(\boldsymbol{K})\rangle)}{\mathrm{Re}(\langle Q_1(\boldsymbol{K})\rangle)}\right| \ll 3\left|\boldsymbol{K}\cdot\boldsymbol{r}_0\right|^{-1}. \tag{2.44}$$

From the definition of $Q_1(\boldsymbol{K})$ Eqs. (2.43) and (2.44) are automatically satisfied under the assumptions expressed by inequalities Eq. (2.36) and if $\boldsymbol{K}\cdot\boldsymbol{r}_0 \ll 1$. From theoretical side it is desirable to make the value of s_x as small as possible, however, in practice, the best range is between $(10^{-4},10^{-3})$.

2.2.3 An example

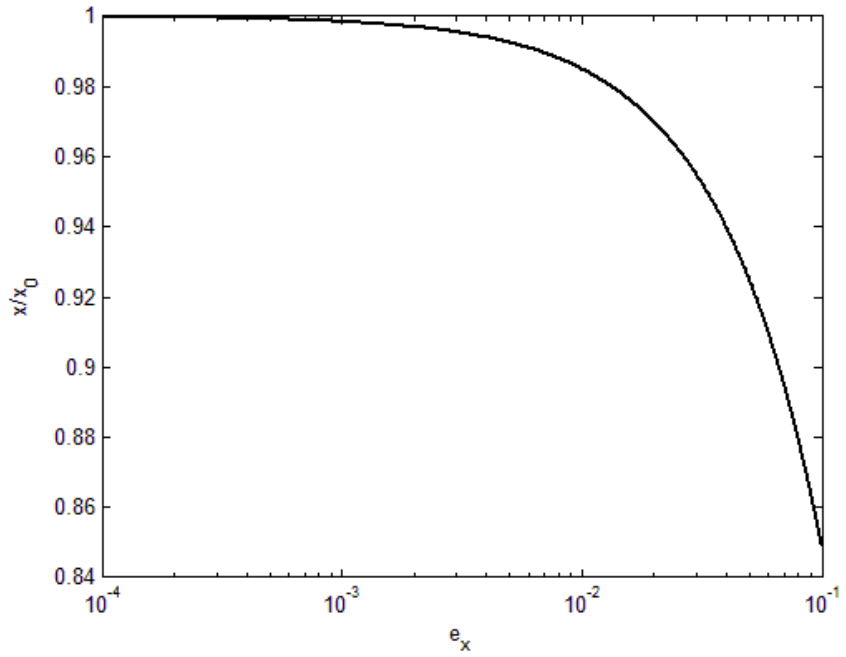

Fig. 2.2 Normalized x – component of the calculated position vector of the impurity with various s_x determined from 18 randomly distributed "good particles".

To illustrate the new technique we suppose that each particle has a scattering potential of a Gaussian form, i.e.

$$f_i(\boldsymbol{r}',\omega) = B\exp\left[-\frac{\boldsymbol{r}'^2}{2\sigma_i^2}\right] \qquad (i=0,1,2)\,, \tag{2.45}$$

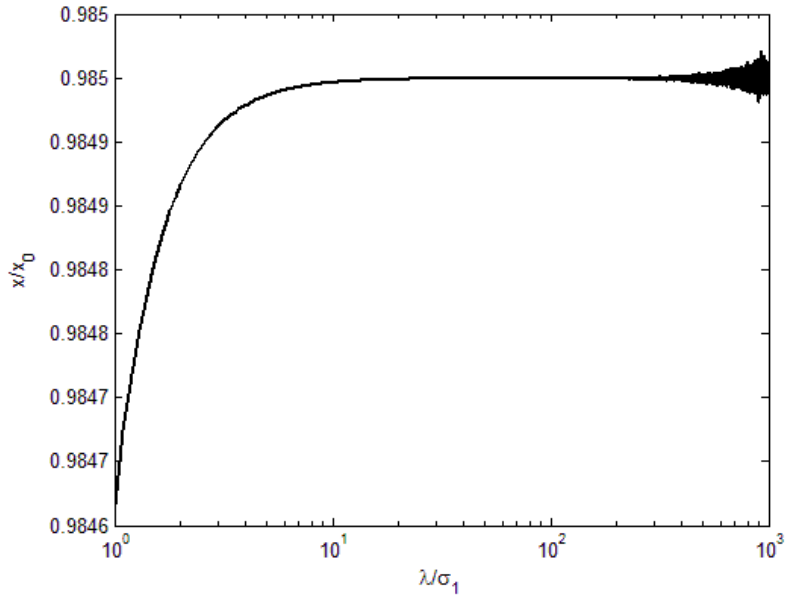

Fig. 2.3 Normalized x – component of the calculated position vector of the impurity with various wavelengths determined from 18 randomly distributed "good particles".

of which, the three-dimensional Fourier transformation can be found to be

$$\widetilde{f}_i(\boldsymbol{K},\omega) = B(2\pi)^{(3/2)}\sigma_i^3\exp\left[-\boldsymbol{K}^2\sigma_i^2/2\right] \qquad (i=0,1,2)\,. \tag{2.46}$$

Such a (soft) Gaussian profile of the scatterer potential is a mathematical model, which allows for analytic results. The use of hard-edge spheres might lead complications related to the discontinuity at the boundary [36, 37]. The parameters are $\lambda = 0.6328um$, $\sigma_1 = 0.09492um$ (the size of the normal particle), $\sigma_0 = \sigma_2 = 2\sigma_1$ (sizes of an alien particle

and a test particle), $B=1$, $s_x=0.01$ (otherwise chosen as a variable). From Fig. 2.2, we see that the optimal value range for s_x is $(10^{-4},10^{-3})$, making the measurement precise. Fig. 2.3 shows that the best wavelength of the incident plane wave is $(10,10^2)$ times larger compared with the size of the normal particle. The reliable results may be achieved

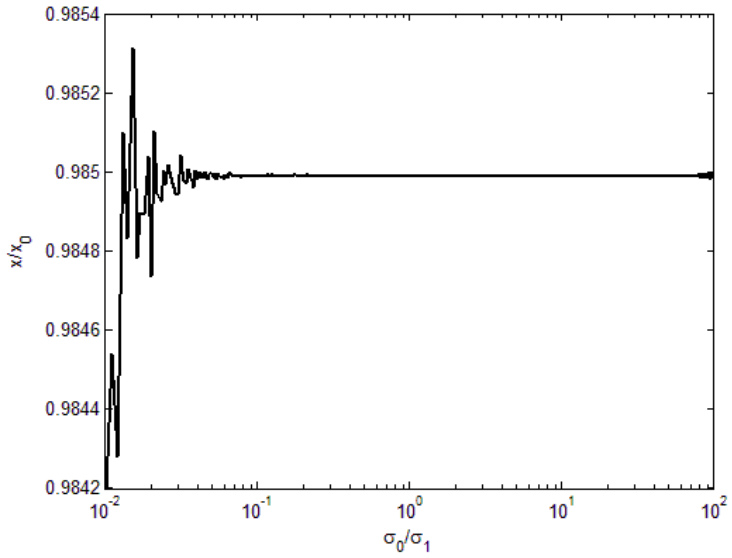

Fig. 2.4 Normalized x – component of the calculated position vector of the impurity with various size of the impurity determined from 18 randomly distributed "good particles".

if we measure the position of the alien particle with ratio $(10^{-1},10^2)$ compared to the size of the normal particles, as Fig. 2.4 illustrates. Our simulation (not included) showed that the above optimal ranges obtained from Figs. 2.2-2.4 are independent of the number of normal particles. In Fig. 2.5 we show the dependence of x/x_0 on a wavelength normalized by the size of the normal particle, λ/σ_1, for several values of N. The difference between the curves occurs only in the range (1,10).

2.2.4 Concluding remarks

In summary, using the previously developed method of finding the correlation function of the scattering potential of a stationary, random media from scattering experiments, we have developed the novel technique for tracing the position of an alien particle embedded in a random collection of normal particles. If there is more than one alien particle, the average position of impurities may also be obtained if those particles are concentrated within a small area compared to the size of the whole media. A method of determining the structure factor of a random collection of identical particles is also provided. Our findings are of importance for any applications for tracing an alien object within the random particulate medium, including medical diagnostics of malignant cells and remote sensing of embedded targets, to name a few.

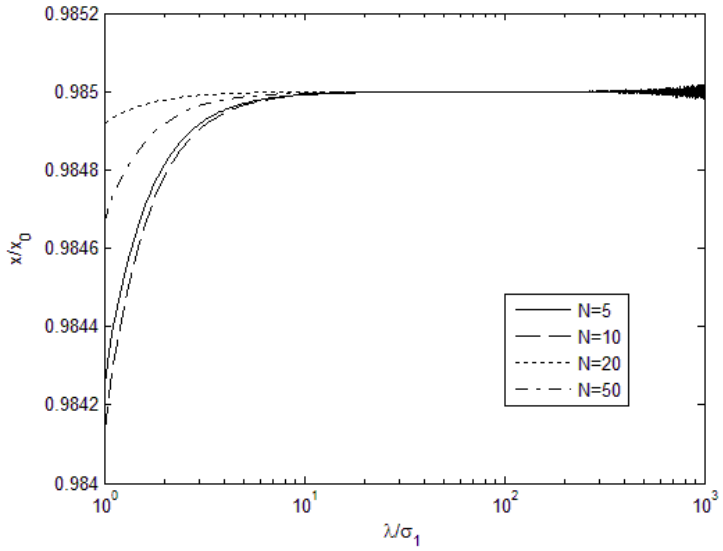

Fig. 2.5 Normalized x – component of the calculated position vector of the impurity with various wavelengths for different number of randomly distributed “good particles”.

2.3 Technique for Interaction of Optical Fields with Turbulent Medium Containing Particles

Very frequently it is of importance to predict how optical signals interact with media having turbulent nature and, at the same rate, contain randomly distributed particles. Such situations arise, for instance, in LIDAR (radar at optical frequencies) and Lasercom systems operating in atmosphere containing aerosols and water droplets, or in oceanic waters, full of plankton, sediments, air bubbles, etc. Moreover, bio-tissues, exhibiting fractal nature globally but contacting discrete structures (cells) can also be viewed as a candidate for our theory. The classic literature on this subject has always treated either propagation [38-39] or scattering aspects [40-43], separately being insufficient for the complete comprehension of the issue. Needless to mention that the radiative transfer approach [43], very popular among the experimentalists, provides only with approximate results and is perfect only for selected regimes, namely the ones where the interference effects may be neglected. The problem with merging rigorous propagation and scattering theories stems from the fact that different mathematical tools have to be used. For scattering, for instance, spherical harmonics are frequently are the elementary modes and angular (plane wave) decomposition modes is employed for propagation in turbulent media [44]. Very recently scattering matrix theory was developed [30] which makes it possible to treat scattering process on the basis of the angular spectrum representation of optical fields. Its combination with a recently introduced technique for propagation in turbulent media, which is also employing the angular spectrum decomposition, provides the unique tool for treating the problems of interest. In this section we are making an

attempt of merging two different theories, for scattering from particles and for propagation in continuous random medium, by noting that both can be based on the angular spectrum decomposition of wave-fields with any spectral and coherence properties.

2.3.1 Scattering theory in free space

Let us consider a monochromatic scalar field $U^{(i)}(\boldsymbol{r},\omega)$ oscillating at frequency ω and propagating into the positive half-space $z>0$ to point with position vector $\boldsymbol{r}$. In the form of the angular spectrum representation of plane waves, the incident field can be expressed as

$$U^{(i)}(\boldsymbol{r},\omega)=\int a^{(i)}(\boldsymbol{s},\omega)\exp(ik\boldsymbol{s}\cdot\boldsymbol{r})d^2s_\perp \tag{2.47}$$

where $\boldsymbol{s}=(s_x,s_y,s_z)$ is a unit vector, $\boldsymbol{s}_\perp=(s_x,s_y,0)$, $k=\omega/c$ is the wavenumber, $a^{(i)}(\boldsymbol{s},\omega)$ is the amplitude of an incident plane wave. Suppose now that the field is incident on a medium, which could be either continuous or a collection of particles occupying a finite domain D. The scattered field may also be expressed, in the form of the angular spectrum of plane waves, as

$$U^{(s)}(\boldsymbol{r},\omega)=\int a^{(s)}(\boldsymbol{s},\omega)\exp(ik\boldsymbol{s}\cdot\boldsymbol{r})d^2s_\perp \tag{2.48}$$

where $a^{(s)}(\boldsymbol{s},\omega)$ is the amplitude of the scattered field.

Within the validity of the first-order Born approximation the scattered field is defined in Eq. (1.22) with the scattering potential of the scattering medium $F(\boldsymbol{r}',\omega)$ defined in Eq. (1.12). For a collection of particles $F(\boldsymbol{r}',\omega)$ has the form

$$F(\boldsymbol{r}',\omega)=\sum_{n=1}^{L} f(\boldsymbol{r}'-\boldsymbol{r}_m,\omega) \tag{2.49}$$

where $f(\boldsymbol{r}',\omega)$ is the scattering potential for a specific particle. The Green's function describing light propagation in free space can also be expressed in terms of the plane waves, as a rewritten form from Eq. (1.38),

$$G(|\boldsymbol{r}-\boldsymbol{r}'|,\omega)=\frac{\exp(ik|\boldsymbol{r}-\boldsymbol{r}'|)}{|\boldsymbol{r}-\boldsymbol{r}'|}=\frac{ik}{2\pi}\int\frac{1}{s_z}\exp[ik\boldsymbol{s}\cdot(\boldsymbol{r}-\boldsymbol{r}')]d^2s_\perp \ . \tag{2.50}$$

On substituting from Eqs. (1.22), (2.47) and (2.50) into Eq. (2.48), we express the amplitude of the scattered field $a^{(s)}(\boldsymbol{s},\omega)$ through the amplitude of the incident field $a^{(i)}(\boldsymbol{s}';\omega)$

$$a^{(s)}(\boldsymbol{s},\omega)=\frac{ik}{2\pi s_z}\int S(\boldsymbol{s},\boldsymbol{s}',\omega)a^{(i)}(\boldsymbol{s}',\omega)d^2s'_\perp \ , \tag{2.51}$$

where $S(\boldsymbol{s},\boldsymbol{s}',\omega)$ is the scattering matrix, or S-matrix. Under the first-order Born approximation it may be expressed as follows [30]

$$S(\boldsymbol{s},\boldsymbol{s}',\omega)=F[k(\boldsymbol{s}-\boldsymbol{s}'),\omega] \ , \tag{2.52}$$

where $F[\boldsymbol{K},\omega]$ is the three-dimensional Fourier transform of the scattering potential.

2.3.2 Propagation in optical turbulence

The other counterpart of our development is the optical wave interaction with optical turbulence. We will now briefly review the angular spectrum approach for dealing with this issue [44]. Let us consider a monochromatic field $U^{(i)}(\boldsymbol{r},\omega)$ oscillating at frequency ω at a point with position vector $\boldsymbol{r}$ propagating in a random medium from the plane $z=0$ into a positive half space $z>0$. The space-dependent part of the field can be expressed in terms of its angular spectrum of plane waves [19]

$$U^{(i)}(\boldsymbol{r},\omega)=\int a^{(i)}(\boldsymbol{s},\omega)P_{\mathbf{s}}^{T}(\boldsymbol{r},\omega)\mathrm{d}^2 s_{\perp}, \tag{2.53}$$

where $P_{\mathbf{s}}^{T}(\boldsymbol{r},\omega)$ represents a plane wave distorted by the random medium at direction $\boldsymbol{s}$ at a position specified by vector $\boldsymbol{r}$ and $a(\boldsymbol{s},\omega)$ is the amplitude of the distorted plane wave in the angular spectrum, which may be related to the field $U_0(\boldsymbol{r}',\omega)$ in the source plane by

$$a^{(i)}(\boldsymbol{s},\omega)=\frac{1}{(2\pi)^2}\int U_0(\boldsymbol{\rho}',\omega)\exp(-ik\boldsymbol{s}\cdot\boldsymbol{\rho}')d^2\rho', \tag{2.54}$$

where $\boldsymbol{\rho}'=(x',y',0)$ is a point in the source plane. At this stage we will need to introduce the statistical description for the propagating field. The cross-spectral density function of the incident field is defined by the expression

$$W^{(i)}(\boldsymbol{r}_1,\boldsymbol{r}_2,\omega)=\left\langle U^{(i)*}(\boldsymbol{r}_1,\omega)U^{(i)}(\boldsymbol{r}_2,\omega)\right\rangle, \tag{2.55}$$

where the angular brackets stand for the ensemble average [23]. On substituting from Eq. (2.53) into Eq. (2.55), we find that the cross-spectral density function of the incident field propagating through the turbulence is given by the expression

$$W^{(i)}(\boldsymbol{r}_1,\boldsymbol{r}_2,\omega)=\int\left\langle a^{(i)*}(\boldsymbol{s}_1,\omega)a^{(i)}(\boldsymbol{s}_2,\omega)\right\rangle\left\langle P_{\mathbf{s}_1}^{T*}(\boldsymbol{r}_1,\omega)P_{\mathbf{s}_2}^{T}(\boldsymbol{r}_2,\omega)\right\rangle d^2s_{1\perp}d^2s_{2\perp}, \qquad (2.56)$$

where the second angular brackets denote ensemble average over the realizations of the turbulent medium. On substituting from Eq. (2.54) into the first bracket of Eq. (2.56) we find that

$$\left\langle a^{(i)*}(\boldsymbol{s}_1',\omega)a^{(i)}(\boldsymbol{s}_2',\omega)\right\rangle\equiv A^{(i)}(\boldsymbol{s}_1',\boldsymbol{s}_2',\omega)$$

$$=\frac{1}{(2\pi)^4}\int\int\left\langle U_0^*(\boldsymbol{\rho}_1',\omega)U_0(\boldsymbol{\rho}_2',\omega)\right\rangle \mathrm{e}^{ik(s_1'\cdot\boldsymbol{\rho}_1'-s_2'\cdot\boldsymbol{\rho}_2')}\,d^2\rho_1'd^2\rho_2'. \qquad (2.57)$$

Following the procedure of Ref. [44], the wide-sense statistically stationary plane wave $P_{\mathbf{s}}^{T}(\boldsymbol{r},\omega)$ propagating through a weakly scattering random medium can be represented by a Rytov series,

$$P_{\mathbf{s}}^{T}(\boldsymbol{r},\omega)=\exp(ik\boldsymbol{s}\cdot\boldsymbol{r})\exp[\psi_{\mathbf{s}}^{(1)}(\boldsymbol{r},\omega)+\psi_{\mathbf{s}}^{(2)}(\boldsymbol{r},\omega)+\ldots]. \qquad (2.58)$$

Here $\psi_{\mathbf{s}}^{(1)}(\mathbf{r},\omega)$ and $\psi_{\mathbf{s}}^{(2)}(\mathbf{r},\omega)$ are the complex phase perturbations of the first order and of the second order, respectively. On substituting from Eq. (2.58) into the second angular bracket of Eq. (2.56), we obtain via the method of cumulants, while keeping terms to the second order [39], the formula

$$\left\langle P_{\mathbf{s}_1}^{T*}(\boldsymbol{r}_1,\omega)P_{\mathbf{s}_2}^{T}(\boldsymbol{r}_2,\omega)\right\rangle=\exp[ik(\boldsymbol{s}_2\cdot\boldsymbol{r}_2-s_1\cdot\boldsymbol{r}_1)]$$

$$\times \exp\left[2E^{(1)}_{\mathbf{s}_1,\mathbf{s}_2}(\boldsymbol{r}_1,\boldsymbol{r}_2,\omega)+E^{(2)}_{\mathbf{s}_1,\mathbf{s}_2}(\boldsymbol{r}_1,\boldsymbol{r}_2,\omega)\right]. \tag{2.59}$$

The integrals in the exponential term, provided that the atmosphere is isotropic, can be expressed as,

$$E^{(1)}_{\mathbf{s}_1,\mathbf{s}_2}(\boldsymbol{r}_2 - \boldsymbol{r}_1,\omega) = -2\pi^2 k^2 \int_0^L \mathrm{d}z \int_0^\infty \kappa \mathrm{d}\kappa \Phi_n(z,\kappa) \tag{2.60}$$

$$E^{(2)}_{\mathbf{s}_1,\mathbf{s}_2}(\boldsymbol{r}_2 - \boldsymbol{r}_1,\omega) = 4\pi^2 k^2 \int_0^L \mathrm{d}z \int_0^\infty \kappa \mathrm{d}\kappa \Phi_n(z,\kappa)$$

$$\times J_0\left[\kappa\left|(\boldsymbol{r}_{2\perp}-\boldsymbol{r}_{1\perp})-(L-z)(\boldsymbol{s}_{2\perp}-\boldsymbol{s}_{1\perp})\right|\right], \tag{2.61}$$

where $\Phi_n(z,\kappa)$ is the power spectrum of turbulent fluctuations of refractive index, $\boldsymbol{\kappa}=(\kappa_x,\kappa_y,\kappa_z)$ is the spatial frequency vector and J_0 is the zero-order Bessel function of the first kind. For instance for atmospheric turbulence $\Phi_n(z,\kappa)$ is given in [39], for oceanic turbulence in [45], for bio-tissues in [46].

2.3.3 Transmission through turbulent medium containing randomly distributed particles

We now return to the case of interest when the incident field is being both scattered by particles and modulated by the turbulent medium. The form of the scattered field can now be obtained after considering the impact of each factor, the scatterers and the turbulence, on the same plane waves in the angular spectrum. Namely, on combining Eqs. (2.51) and (2.53) we find that the resulting field becomes

$$U^{(s)}(\boldsymbol{r},\omega)=\int a^{(s)}(\boldsymbol{s},\omega)P_{\mathbf{s}}^{T}(\boldsymbol{r},\omega)d^{2}s_{\perp}. \tag{2.62}$$

On substituting from Eq. (2.62) into (2.55), we find that the cross-spectral density function of the scattered field in turbulence can be expressed as

$$W^{(s)}(\boldsymbol{r}_1,\boldsymbol{r}_2,\omega)=\left\langle U^{(s)*}(\boldsymbol{r}_1,\omega)U^{(s)}(\boldsymbol{r}_2,\omega)\right\rangle$$

$$=\int\int\left\langle a^{(s)*}(\boldsymbol{s}_1,\omega)a^{(s)}(\boldsymbol{s}_2,\omega)\right\rangle\left\langle P_{\mathbf{s}_1}^{T*}(\boldsymbol{r}_1,\omega)P_{\mathbf{s}_2}^{T}(\boldsymbol{r}_2,\omega)\right\rangle d^{2}s_{1\perp}d^{2}s_{2\perp}, \tag{2.63}$$

Further, on substituting from Eq. (2.51) into the first angular bracket on the right side of the formula above, we obtain the correlation function of the amplitude of the scattered field as

$$\left\langle a^{(s)*}(\boldsymbol{s}_1,\omega)a^{(s)}(\boldsymbol{s}_2,\omega)\right\rangle=\left(\frac{k}{2\pi}\right)^{2}\frac{1}{s_{1z}s_{2z}}\int\int\left\langle S^{*}(\boldsymbol{s}_1,\boldsymbol{s}_1',\omega)S(\boldsymbol{s}_2,\boldsymbol{s}_2',\omega)\right\rangle$$

$$\times\left\langle a^{(i)*}(\boldsymbol{s}_1',\omega)a^{(i)}(\boldsymbol{s}_2',\omega)\right\rangle d^{2}s'_{1\perp}d^{2}s'_{2\perp}\ . \tag{2.64}$$

Here the correlation function of the scattering matrix is related to the six-dimensional Fourier transform of the correlation function of the scattering potential, i.e.

$$\left\langle S^{*}(\boldsymbol{s}_1,\boldsymbol{s}_1',\omega)S(\boldsymbol{s}_2,\boldsymbol{s}_2',\omega)\right\rangle=C_F\left[-k(\boldsymbol{s}_1-\boldsymbol{s}_1'),k(\boldsymbol{s}_2-\boldsymbol{s}_2'),\omega\right], \tag{2.65}$$

where $\boldsymbol{K}_i=k(\boldsymbol{s}_i-\boldsymbol{s}_i')$, $(i=1,2)$ and

$$C_F\left[\boldsymbol{K}_1,\boldsymbol{K}_2,\omega\right]=\int_D\int_D\left\langle F^{*}(\boldsymbol{r}_1',\omega)F(\boldsymbol{r}_2',\omega)\right\rangle\times\exp[-i(\boldsymbol{K}_1\cdot\boldsymbol{r}_1'+\boldsymbol{K}_2\cdot\boldsymbol{r}_2')]\mathrm{d}^3r_1'\,\mathrm{d}^3r_2'. \tag{2.66}$$

On substituting from Eqs. (2.59) and (2.64) into Eq. (2.63), we obtain the general expression for the cross-spectral density function of the field after transmission through turbulent and particulate random medium, viz.

$$W^{(s)}(\boldsymbol{r}_1,\boldsymbol{r}_2,\omega)=\left(\frac{k}{2\pi}\right)^2\iint\frac{1}{s_{1z}s_{2z}}\iint A^{(i)}(\boldsymbol{s}_1',\boldsymbol{s}_2',\omega)C_F\left[-\boldsymbol{K}_1,\boldsymbol{K}_2,\omega\right]d^2s'_{1\perp}d^2s'_{2\perp}$$

$$\times\exp[ik(\boldsymbol{s}_2\cdot\boldsymbol{r}_2-\boldsymbol{s}_1\cdot\boldsymbol{r}_1)]\exp\left[2E^{(1)}_{\mathbf{s}_1,\mathbf{s}_2}(\boldsymbol{r}_1,\boldsymbol{r}_2,\omega)+E^{(2)}_{\mathbf{s}_1,\mathbf{s}_2}(\boldsymbol{r}_1,\boldsymbol{r}_2,\omega)\right]d^2s_{1\perp}d^2s_{2\perp}. \tag{2.67}$$

In Eq. (2.67), $A^{(i)}$ is given by Eq. (2.57) and expresses the properties of the incident field, $C_F\left[\text{-}\boldsymbol{K}_1,\boldsymbol{K}_2,\omega\right]$ is given by Eq. (2.66) and characterizes the properties of the scattering medium. Finally $E^{(1)}_{\mathbf{s}_1,\mathbf{s}_2}(\boldsymbol{r}_1,\boldsymbol{r}_2,\omega)$, $E^{(2)}_{\mathbf{s}_1,\mathbf{s}_2}(\boldsymbol{r}_1,\boldsymbol{r}_2,\omega)$ are given by Eqs. (2.60), (2.61) and describe the effects of the atmospheric turbulence. Formula (2.67) is the main result of the section. It relates the cross-spectral density function of the scattered field with the correlation properties of the incident field (just being the spatial Fourier transform of the source cross-spectral density function), as well as with the statistics of turbulence and scattered collection.

2.3.4 Derivation and Example

We first show here on how to calculate Eqs. (2.60) and (2.61). We assume that the turbulence is modeled by the von Karman spectrum, which is given by [39]

$$\Phi_n(\kappa)=0.033C_n^2\frac{\exp\left[-\kappa^2/\kappa_m^2\right]}{(\kappa^2+\kappa_0^2)^{11/6}}, \tag{2.68}$$

where $C_n^2 = 10^{-14} m^{-2/3}$, $\kappa_m = 5.92/l_m$, with inner scale $l_m = 1mm$, and $\kappa_0 = 1/l_0$, with outer scale $l_0 = 10m$. If the power spectrum of atmospheric fluctuations does not depend on z, Eq. (2.60) can be reduced to the form

$$E^{(1)}_{\mathbf{s}_1,\mathbf{s}_2}(\boldsymbol{r}_2 - \boldsymbol{r}_1, \omega) = -2\pi^2 k^2 L \int_0^\infty \kappa \mathrm{d}\kappa \Phi_n(\kappa), \tag{2.69}$$

On substituting from Eq. (2.68) to Eq. (2.69), the integral could be calculated numerically and one get

$$E^{(1)}_{\mathbf{s}_1,\mathbf{s}_2}(\boldsymbol{r}_2 - \boldsymbol{r}_1, \omega) = -2\pi^2 \times 0.033 C_n^2 k^2 L \times 27.8495. \tag{2.70}$$

On the other hand, we are interested on the intensity of the propagating field. By taking $\mathbf{r}_1 = \mathbf{r}_2 = \mathbf{r}$, Eq. (2.61) is then shown to be

$$E^{(2)}_{\mathbf{s}_1,\mathbf{s}_2}(\boldsymbol{r}_2 - \boldsymbol{r}_1, \omega) = 4\pi^2 k^2 \int_0^\infty \kappa \mathrm{d}\kappa \Phi_n(\kappa) \int_0^L \mathrm{d}z J_0\left[\kappa(L-z)\left|\boldsymbol{s}_{2\perp} - \boldsymbol{s}_{1\perp}\right|\right], \tag{2.71}$$

where $0 \le z \le L$ in the integral. Using Eq. (3.11) of Ref. [44], i.e.,

$$\int_0^L dz J_0\left[\kappa z\left|\boldsymbol{s}_2 - \boldsymbol{s}_1\right|\right] = \frac{1}{\kappa\left|\boldsymbol{s}_2 - \boldsymbol{s}_1\right|} \int_0^{\kappa L|\boldsymbol{s}_2 - \boldsymbol{s}_1|} J_0(t) dt. \tag{2.72}$$

and Eq. (11.1.1) of Ref. [47],

$$\int_0^z J_0(t) dt = \sum_{k=0}^{\infty} 2 J_{2k+1}(z), \tag{2.73}$$

we could rewrite $E^{(2)}_{\mathbf{s}_1,\mathbf{s}_2}(\boldsymbol{r}_2 - \boldsymbol{r}_1, \omega)$ as

$$E^{(2)}_{\mathbf{s}_1,\mathbf{s}_2}(\boldsymbol{r}_2 - \boldsymbol{r}_1, \omega)$$

$$= 4\pi^2 \times 0.033 C_n^2 k^2 \times \frac{2}{\left|\boldsymbol{s}_{2\perp} - \boldsymbol{s}_{1\perp}\right|} \sum_{m=0}^{\infty} \left[\int_0^{\infty} \mathrm{d}\kappa \frac{\exp\left[-\kappa^2 / \kappa_m^2\right]}{(\kappa^2 + \kappa_0^2)^{11/6}} J_{2m+1}\left[\kappa L \left|\boldsymbol{s}_{2\perp} - \boldsymbol{s}_{1\perp}\right|\right] \right]. \tag{2.74}$$

Therefore, Eq. (2.61) can be written as a sum of a series of one-dimensional integrals in κ. In the example below, we show the intensity profile at the propagation distance $L = 1m$. For such a case, our calculations reveal that the first term in Eq. (2.74) is much larger than other terms, so we keep the first 10 terms to obtain the accurate result of Eq. (2.74).

We then assume that the incident beam is one plane wave with form $U_0(\boldsymbol{\rho}', \omega) = \exp(ik\boldsymbol{s}_0 \cdot \boldsymbol{\rho}')$, with the resulting amplitude of the plane wave as $a^{(i)}(\boldsymbol{s}, \omega) = \delta\left[k(\boldsymbol{s} - \boldsymbol{s}_0)\right]$. $A^{(i)}(\boldsymbol{s}_1', \boldsymbol{s}_2', \omega)$ is also calculated through Eq. (2.57). For scattering media, we consider a special case of gas-like disorder where identical particles are randomly positioned with Gaussian potential

$$f(\boldsymbol{r}', \omega) = \exp\left[-\frac{\boldsymbol{r}'^2}{2\sigma^2}\right], \tag{2.75}$$

and considered as statistically independent. In our simulation, the intensity profile is statistically averaged over 30 realizations. On substituting from Eq. (2.49) into Eq. (2.65), we have the correlation function of the scattering matrix of the form

$$\left\langle S^*(\boldsymbol{s}_1, \boldsymbol{s}_1', \omega) S(\boldsymbol{s}_2, \boldsymbol{s}_2', \omega) \right\rangle$$

$$= \tilde{f}^{*}\left[k(\boldsymbol{s}_1 - \boldsymbol{s}_1')\right]\tilde{f}\left[k(\boldsymbol{s}_2 - \boldsymbol{s}_2')\right]M\left[-k(\boldsymbol{s}_1 - \boldsymbol{s}_1'), k(\boldsymbol{s}_2 - \boldsymbol{s}_2'), \omega\right], \qquad (2.76)$$

where $\tilde{f}(\boldsymbol{K}, \omega) = (2\pi)^{3/2}\sigma^3 \exp\left[-\boldsymbol{K}^2\sigma^2 / 2\right]$ and

$$M(\boldsymbol{K}_1, \boldsymbol{K}_2, \omega) = \left\langle \sum_{m=1}^{L}\sum_{n=1}^{L} \exp\left[-\mathrm{i}(\boldsymbol{K}_2 \cdot \boldsymbol{r}_m + \boldsymbol{K}_1 \cdot \boldsymbol{r}_n)\right]\right\rangle. \qquad (2.77)$$

With all the above information, we can numerically calculate the integral Eq. (2.67). The parameters are chosen: $\lambda = 632.8nm$ and $\sigma = 0.1\lambda$. The plot below shows two cases: red solid curve, intensity of the incident beam scattered by a collection of particles within the surrounding of turbulence; black dashed curve, intensity of the incident beam scattered by a collection of particles without turbulence. The effect of the turbulence mitigates the disorder caused by the scattering particles of gas-like disorder.

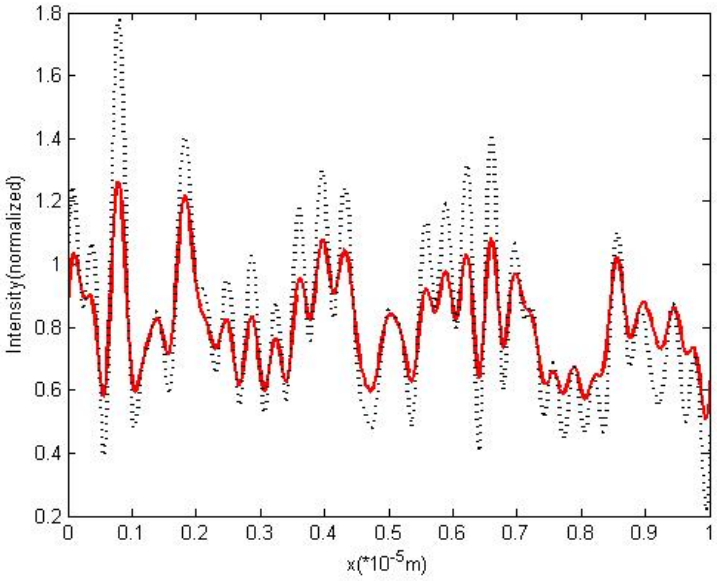

Fig.2.6 Normalized intensity of a plane wave propagating in the atmospheric turbulence with particles (solid curve); without particles (dotted curve) through section.

2.3.5 Concluding remarks

We have developed a new technique for treating passage of light fields in environments where both optical turbulence and particle scattering are present. The approach is based on the angular spectrum decomposition and is valid for a broad class of optical fields, which might have arbitrary spectral and coherence properties. We have restricted ourselves to weak scattering regime and weak turbulence regime. However, these limitations can readily be overcome on including more terms in the Born and in the Rytov series. This analysis may prove an invaluable theoretical tool for making predictions about performance of optical systems (imaging, communication, recognition and tracking) operating through complex media. The extension of the theory to electromagnetic domain and consideration of specific examples is left for a follow-up detailed publication.

Chapter 3

Electromagnetic Scattering Theory

3.1 Theory of Weak Scattering of Stochastic Electromagnetic Fields from Deterministic and Random Media

In classical optics domain scattering of electromagnetic fields from deterministic and random continuous, static scattering media is treated in Refs. [19-20,48] in great detail. Some other aspects of this research area are addressed in Refs. [49-53]. Theoretical and experimental studies relating to scattering from deterministic and random collections of particles were carried out in [25-26]. Some applications relating to determination of the structure of the medium from scattering experiments can be found in Ref. [54]. These investigations revealed that on scattering the statistical properties of light are influenced by both the correlation properties of the source and the structure and correlation properties of the medium. All these studies were confined to cases in which the incident field is either deterministic or scalar. Hence, it was not possible to account for changes in those characteristics of the scattered field, which are based on full electromagnetic description of stochastic fields, such as, for instance, the degree of polarization [19].

In this section we formulate the scattering theory that is valid for electromagnetic fields, of both deterministic and random nature, that scatter from deterministic or random

media. We use the assumption that the scatterer is weak, employing the first-order Born approximation, i.e. $U^{(s)} \ll U^{(i)}$. The new development allows for determining all the properties of the electromagnetic scattered field such as its spectral density, spectral degree of coherence and various polarimetric features, such as degree of polarization, ellipsometric properties, degree of cross-polarization, etc. Since it is often the case in scattering experiments, we predict evolution of the fields before and after scattering event, i.e. we incorporate their propagation from the source plane to the scattering medium and, after scattering, from the medium to the far-field. We carry the analysis in terms of the cross-spectral density matrices, from which one can determine all other second-order statistical properties of the field of interest. An example, in which spectral density, and the states of coherence and polarization of the scattered field, produced on scattering of uncorrelated partially polarized field from delta-correlated slab, is provided to illustrate the analytical results.

3.1.1 Propagation of the electric-field vector through the scattering medium

We begin by considering a monochromatic electric field oscillating at angular frequency ω and propagating from the source plane $z = 0$ into the half space $z > 0$ (see Fig. 3.1).

The transverse component of the electric field vector at a point specified by the position vector $\boldsymbol{\rho}'$ in the source plane has the form

$$\boldsymbol{E}_{\perp}^{(0)}(\boldsymbol{\rho}', \omega) = \left[E_x^{(0)}(\boldsymbol{\rho}', \omega), E_y^{(0)}(\boldsymbol{\rho}', \omega) \right]. \tag{3.1}$$

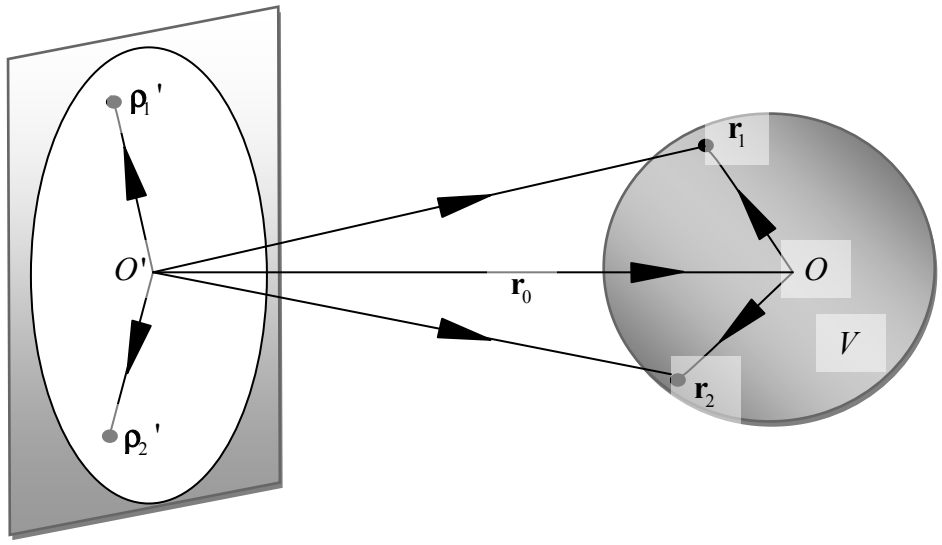

Fig. 3.1 Illustrating the notation related to propagation of the field from the source plane to the scatterer.

Following the Luneberg's formulas {see Eq. (1.37) also [56]} the three components of the electric field generated by the electric field in the source plane and propagated to a point specified by the position vector $\boldsymbol{r}_1$ in the half space $z > 0$ can be expressed as

$$E_x(\boldsymbol{r}_1,\omega) = -\frac{1}{2\pi}\int E_x^{(0)}(\boldsymbol{\rho}',\omega)\partial_{z_1} G(\boldsymbol{\rho}',\boldsymbol{r}_1,\omega)d^2\rho', \tag{3.2a}$$

$$E_y(\boldsymbol{r}_1,\omega) = -\frac{1}{2\pi}\int E_y^{(0)}(\boldsymbol{\rho}',\omega)\partial_{z_1} G(\boldsymbol{\rho}',\boldsymbol{r}_1,\omega)d^2\rho', \tag{3.2b}$$

$$E_z(\boldsymbol{r}_1,\omega) = \frac{1}{2\pi}\int\left[E_x^{(0)}(\boldsymbol{\rho}',\omega)\partial_{x_1} G(\boldsymbol{\rho}',\boldsymbol{r}_1,\omega) + E_y^{(0)}(\boldsymbol{\rho}',\omega)\partial_{y_1} G(\boldsymbol{\rho}',\boldsymbol{r}_1,\omega)\right]d^2\rho', \tag{3.2c}$$

where ∂ denotes partial derivative, x_1, y_1, z_1 are the Cartesian components of the position vector $\boldsymbol{r}_1$ and $G(\boldsymbol{\rho}',\boldsymbol{r}_1,\omega)$ is the outgoing free-space Green's function of the form

$$G(\boldsymbol{\rho}', \boldsymbol{r}, \omega) = \frac{\exp(ik\left|\boldsymbol{r} - \boldsymbol{\rho}'\right|)}{\left|\boldsymbol{r} - \boldsymbol{\rho}'\right|}\ , \tag{3.3}$$

where $k = \omega / c$ is the wave number and c is the speed of light in vacuum. From Eqs. (3.2), a linear transformation of the two-dimensional vector space containing the vector $\boldsymbol{E}_{\perp}^{(0)}(\boldsymbol{\rho}', \omega)$ onto the three-dimensional vector space containing the vector $\boldsymbol{E}(\boldsymbol{r}_1, \omega)$ can be conveniently written as

$$\boldsymbol{E}(\boldsymbol{r}_1, \omega) = \int \boldsymbol{E}_{\perp}^{(0)}(\boldsymbol{\rho}', \omega) \circ \mathbf{K}(\boldsymbol{\rho}', \boldsymbol{r}_1, \omega) \mathrm{d}^2\rho', \tag{3.4}$$

where the small circle $\circ$ denotes matrix multiplication, and

$$\boldsymbol{K}(\boldsymbol{\rho}', \boldsymbol{r}_1, \omega) = \frac{1}{2\pi}\begin{bmatrix} -\partial_{z_1} G(\boldsymbol{\rho}', \boldsymbol{r}_1, \omega) & 0 & \partial_{x_1} G(\boldsymbol{\rho}', \boldsymbol{r}_1, \omega) \\ 0 & -\partial_{z_1} G(\boldsymbol{\rho}', \boldsymbol{r}_1, \omega) & \partial_{y_1} G(\boldsymbol{\rho}', \boldsymbol{r}_1, \omega) \end{bmatrix}, \tag{3.5a}$$

$$= \frac{L(R_1, \omega)}{2\pi}\begin{bmatrix} -z_1 & 0 & x_1 - x' \\ 0 & -z_1 & y_1 - y' \end{bmatrix}. \tag{3.5b}$$

Here x', y' are the Cartesian components of the transverse vector $\boldsymbol{\rho}'$, and

$$L(R_1, \omega) = \frac{(ikR_1 - 1)\exp(ikR_1)}{R_1^{\,3}}, \tag{3.6}$$

with $R_1 = \left|\boldsymbol{r}_1 - \boldsymbol{\rho}'\right|$. More explicitly, Eq. (3.4) can be written as,

$\boldsymbol{E}(\boldsymbol{r}_1, \omega)$

$$= \frac{1}{2\pi}\int L(R_1, \omega)\begin{bmatrix} E_x^{(0)}(\boldsymbol{\rho}', \omega) & E_y^{(0)}(\boldsymbol{\rho}', \omega) \end{bmatrix} \circ \begin{bmatrix} -z_1 & 0 & x_1 - x' \\ 0 & -z_1 & y_1 - y' \end{bmatrix} d^2\rho\ . \tag{3.7}$$

When a monochromatic electromagnetic field is incident on a linear, isotropic, nonmagnetic medium occupying a finite domain V (see Fig. 3.2), the scattered field at a point specified by position vector $r\boldsymbol{s}$ ($\boldsymbol{s}^2 = 1$) may be expressed in the form [19],

$$\boldsymbol{E}^{(s)}(r\boldsymbol{s},\omega) = \boldsymbol{\nabla}\times\boldsymbol{\nabla}\times\boldsymbol{\Pi}_e(r\boldsymbol{s},\omega), \tag{3.8}$$

where $\boldsymbol{\Pi}_e$ is the electric Hertz potential defined by the formula

$$\boldsymbol{\Pi}_e(r\boldsymbol{s},\omega) = \int_V \boldsymbol{P}(\boldsymbol{r}_1,\omega)\frac{\exp(ik|r\boldsymbol{s}-\boldsymbol{r}_1|)}{|r\boldsymbol{s}-\boldsymbol{r}_1|}d^3r_1, \tag{3.9}$$

Here $\boldsymbol{P}(\boldsymbol{r}_1,\omega)$ is the polarization of the medium, which may be expressed as, within the accuracy of the first-order Born approximation, as

$$\boldsymbol{P}(\boldsymbol{r}_1,\omega) = \eta(\boldsymbol{r}_1)\boldsymbol{E}^{(i)}(\boldsymbol{r}_1,\omega) = \frac{1}{k^2}F(\boldsymbol{r}_1)\boldsymbol{E}^{(i)}(\boldsymbol{r}_1,\omega). \tag{3.10}$$

where η is the dielectric susceptibility and the scattering potential of the medium is defined in Eq. (1.12).

On substituting from Eqs. (3.9) and (3.10) into Eq. (3.8), we obtain the formula for the scattered field outside of the scattering medium

$$\boldsymbol{E}^{(s)}(r\boldsymbol{s},\omega) = \frac{1}{k^2}\boldsymbol{\nabla}\times\boldsymbol{\nabla}\times\int_V F(\boldsymbol{r}_1)\boldsymbol{E}^{(i)}(\boldsymbol{r}_1,\omega)\frac{\exp(ik|r\boldsymbol{s}-\boldsymbol{r}_1|)}{|r\boldsymbol{s}-\boldsymbol{r}_1|}d^3r_1. \tag{3.11}$$

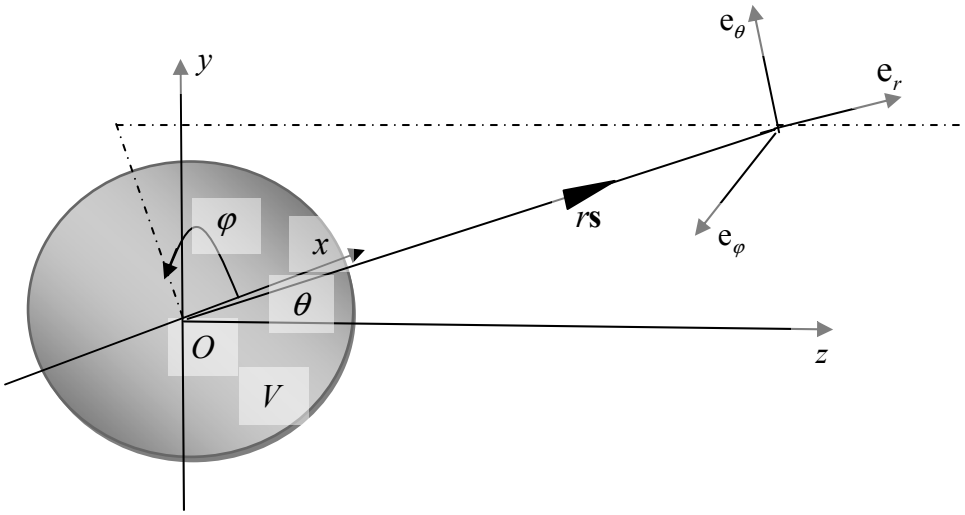

Fig. 3.2 Illustrating the spherical coordinate system and notation relating the scatterer and the scattered field in the far zone.

Eq. (3.11) is the general result for the scattered field within the accuracy of the first-order Born approximation, which is too complex to be employed in analytical calculations. It, however, simplifies significantly in the far zone of the scatterer. In this case Eq. (3.8) is reduced to the following formula

$$\boldsymbol{E}^{(s)}(r\boldsymbol{s},\omega) = -k^2 \frac{\exp(ikr)}{r}\{\boldsymbol{s}\times[\boldsymbol{s}\times\widetilde{\boldsymbol{P}}(k\boldsymbol{s},\omega)]\}, \tag{3.12}$$

where $\widetilde{\boldsymbol{P}}(k\boldsymbol{s},\omega)$ is the three-dimensional Fourier transform of $\boldsymbol{P}(\boldsymbol{r}_1)$, i.e.,

$$\widetilde{\boldsymbol{P}}(k\boldsymbol{s},\omega) = \int_V \boldsymbol{P}(\boldsymbol{r}_1)\,\mathrm{e}^{-ik\boldsymbol{s}\cdot\boldsymbol{r}_1}\,d^3r_1 = \frac{1}{k^2}\int_V F(\boldsymbol{r}_1)\boldsymbol{E}^{(i)}(\boldsymbol{r}_1)\,\mathrm{e}^{-ik\boldsymbol{s}\cdot\boldsymbol{r}_1}\,d^3r_1 . \tag{3.13}$$

On substituting from Eq. (3.13) into Eq. (3.12), after straightforward vector multiplication, we rewrite Eq. (3.12) as

$$\boldsymbol{E}^{(s)}(r\boldsymbol{s},\omega)=\frac{\exp(ikr)}{r}\int_V F(\boldsymbol{r}_1)[\boldsymbol{E}^{(i)}(\boldsymbol{r}_1)-(\boldsymbol{s}\cdot\boldsymbol{E}^{(i)}(\boldsymbol{r}_1))\boldsymbol{s}]\exp(-ik\boldsymbol{s}\cdot\boldsymbol{r}_1)d^3r_1 . \qquad (3.14)$$

which is the asymptotic expression of Eq. (3.11) in the far zone. More explicitly, Eq. (3.14) can be rewritten in matrix form

$$\boldsymbol{E}^{(s)}(r\boldsymbol{s},\omega)$$

$$=\frac{\exp(ikr)}{r}\int_V F(\boldsymbol{r}_1)\begin{bmatrix}E_x^{(i)}(\boldsymbol{r}_1,\omega)\\E_y^{(i)}(\boldsymbol{r}_1,\omega)\\E_z^{(i)}(\boldsymbol{r}_1,\omega)\end{bmatrix}^T\circ\begin{bmatrix}1-s_x^2 & -s_xs_y & -s_xs_z\\-s_ys_x & 1-s_y^2 & -s_ys_z\\-s_zs_x & -s_zs_y & 1-s_z^2\end{bmatrix}\exp(-ik\boldsymbol{s}\cdot\boldsymbol{r}_1)d^3r_1, \quad (3.15)$$

where $\boldsymbol{s}=(s_x,s_y,s_z)$.

It is evident from Eq. (3.12) that $\boldsymbol{s}\cdot\boldsymbol{E}^{(s)}(r\boldsymbol{s},\omega)=0$, i.e. that the scattered field in the far zone is orthogonal to $\boldsymbol{s}$, or, transverse. Therefore, it will be convenient to represent such a transverse field in terms of the spherical polar coordinate system where it only has two non-zero components. As illustrated in Fig. (3.2), the transformation between the Cartesian coordinate system and the spherical coordinate system can be expressed as

$$\begin{bmatrix}\mathrm{e}_r\\\mathrm{e}_\theta\\\mathrm{e}_\varphi\end{bmatrix}^T=\begin{bmatrix}\mathrm{e}_x\\\mathrm{e}_y\\\mathrm{e}_z\end{bmatrix}^T\circ\begin{bmatrix}\sin\theta\cos\varphi & \cos\theta\cos\varphi & -\sin\varphi\\\sin\theta\sin\varphi & \cos\theta\sin\varphi & \cos\varphi\\\cos\theta & -\sin\theta & 0\end{bmatrix}, \qquad (3.16)$$

or in the reverse form

$$\begin{bmatrix}\mathrm{e}_x\\\mathrm{e}_y\\\mathrm{e}_z\end{bmatrix}^T=\begin{bmatrix}\mathrm{e}_r\\\mathrm{e}_\theta\\\mathrm{e}_\varphi\end{bmatrix}^T\circ\begin{bmatrix}\sin\theta\cos\varphi & \sin\theta\sin\varphi & \cos\theta\\\cos\theta\cos\varphi & \cos\theta\sin\varphi & -\sin\theta\\-\sin\varphi & \cos\varphi & 0\end{bmatrix}, \qquad (3.17)$$

where $\mathrm{e}_x, \mathrm{e}_y, \mathrm{e}_z$, $\mathrm{e}_r, \mathrm{e}_\theta, \mathrm{e}_\varphi$ are the unit vectors. Thus, we may rewrite Eq. (3.15) as

$$\begin{bmatrix} E_r^{(s)}(\theta,\varphi) \\ E_\theta^{(s)}(\theta,\varphi) \\ E_\varphi^{(s)}(\theta,\varphi) \end{bmatrix}^T$$

$$= \frac{\exp(ikr)}{r} \int_V F(\boldsymbol{r}_1) \begin{bmatrix} E_x^{(i)}(\boldsymbol{r}_1,\omega) \\ E_y^{(i)}(\boldsymbol{r}_1,\omega) \\ E_z^{(i)}(\boldsymbol{r}_1,\omega) \end{bmatrix}^T \circ \begin{bmatrix} 0 & \cos\theta\cos\varphi & -\sin\varphi \\ 0 & \cos\theta\sin\varphi & \cos\varphi \\ 0 & -\sin\theta & 0 \end{bmatrix} \exp(-ik\boldsymbol{s}\cdot\boldsymbol{r}_1)\mathrm{d}^3 r_1 . \quad (3.18)$$

On passing to the next section we note that in order for a wave of wave number k, located at distance r from the scatterer to the observation point to be in the far field of scatterer with size a, the following restriction should be met (see Ref. [48], section 3.2)

$$kr \gg \max\left[1, \frac{1}{2}(ka)^2\right]. \quad (3.19)$$

Previously we set the origin in the source plane when we deal with the electric field in the half space $z > 0$ generated by the source plane. Then we set the origin in the scattering medium in order to derive the explicit form of the scattered field. In order to combine the two representations, we suppose the origin is located within the scattering medium and specified by the position vector $\boldsymbol{r}_0 = (x_0, y_0, z_0)$ from the perspective of the previous system. Then, Eq. (3.7) becomes (after replacing $\boldsymbol{r}_1$ by $\boldsymbol{r}_1 + \boldsymbol{r}_0$)

$$\boldsymbol{E}(\boldsymbol{r}_1,\omega)$$

$$= \frac{1}{2\pi} \int L(R_1,\omega) \begin{bmatrix} E_x^{(0)}(\boldsymbol{\rho}',\omega) & E_y^{(0)}(\boldsymbol{\rho}',\omega) \end{bmatrix} \circ \begin{bmatrix} -(z_1+z_0) & 0 & x_1+x_0-x' \\ 0 & -(z_1+z_0) & y_1+y_0-y' \end{bmatrix} \mathrm{d}^2\rho',$$

(3.20)

where now $R_1 = \left| \boldsymbol{r}_1 + \boldsymbol{r}_0 - \boldsymbol{\rho}' \right|$. On substituting from Eq. (3.20) into Eq. (3.18), we obtain for the scattered field in spherical polar coordinate system (keeping only θ, φ components) the formula

$$\begin{bmatrix} E_\theta^{(s)}(r\boldsymbol{s}) \\ E_\varphi^{(s)}(r\boldsymbol{s}) \end{bmatrix}^T = \frac{\exp(ikr)}{2\pi r}$$

$$\times \int_V \int F(\boldsymbol{r}_1) L(R_1, \omega) \left[E_x^{(0)}(\boldsymbol{\rho}', \omega) \quad E_y^{(0)}(\boldsymbol{\rho}', \omega) \right] \circ \boldsymbol{M}(\theta, \varphi, \boldsymbol{r}_1, \boldsymbol{\rho}') \exp(-ik\boldsymbol{s} \cdot \boldsymbol{r}_1) d^3 r_1 d^2 \rho' \ , \tag{3.21}$$

where $\boldsymbol{s} \cdot \boldsymbol{r}_1 = \sin\theta\cos\varphi x_1 + \sin\theta\sin\varphi y_1 + \cos\theta z_1$ and

$$\boldsymbol{M}(\theta, \varphi, \boldsymbol{r}_1, \boldsymbol{\rho}') = \begin{bmatrix} \cos\theta\cos\varphi(z_1 + z_0) + \sin\theta(x_1 + x_0 - x') & -\sin\varphi(z_1 + z_0) \\ \cos\theta\sin\varphi(z_1 + z_0) + \sin\theta(y_1 + y_0 - y') & \cos\varphi(z_1 + z_0) \end{bmatrix}. \tag{3.22}$$

3.1.2 Propagation of the 2×2 cross-spectral density matrix of the electromagnetic field

The transformation law for the cross-spectral density matrix of a stochastic, wide-sense statistically stationary electromagnetic field, which interacts with the scattering system of interest, can be determined from Eq. (3.21). Let the fluctuations of the electric field at the source plane be characterized by the 2×2 cross-spectral density matrix [20]

$$\boldsymbol{W}_\perp^{(0)}(\boldsymbol{\rho}'_1, \boldsymbol{\rho}'_2, \omega) = \left[\left\langle E_\alpha^{(0)*}(\boldsymbol{\rho}'_1, \omega) E_\beta^{(0)}(\boldsymbol{\rho}'_1, \omega) \right\rangle \right] \quad (\alpha = x, y; \beta = x, y) \, . \tag{3.23}$$

Then suppose that the correlation properties of the electric field at a pair of points in spherical polar coordinate system, specified by position vectors $r\boldsymbol{s}_1$ and $r\boldsymbol{s}_2$ $[\boldsymbol{s} = (\sin\theta\cos\varphi, \sin\theta\sin\varphi, \cos\theta)]$ are characterized by the 2×2 cross-spectral density matrix

$$\boldsymbol{W}(r\boldsymbol{s}_1, r\boldsymbol{s}_2, \omega) = \left[\left\langle E_\alpha^{(s)*}(r\boldsymbol{s}_1, \omega) E_\beta^{(s)}(r\boldsymbol{s}_2, \omega)\right\rangle\right] \quad (\alpha = \theta, \varphi; \beta = \theta, \varphi), \tag{3.24}$$

or, equivalently,

$$\boldsymbol{W}(r\boldsymbol{s}_1, r\boldsymbol{s}_2, \omega) = \left\langle \boldsymbol{E}^{(s)+}(r\boldsymbol{s}_1, \omega) \circ \boldsymbol{E}^{(s)}(r\boldsymbol{s}_2, \omega)\right\rangle, \tag{3.25}$$

where $\dagger$ denotes the Hermitian adjoint and $\boldsymbol{E}^{(s)}(r\boldsymbol{s}, \omega) = \left[E_\theta^{(s)}(r\boldsymbol{s}) \quad E_\varphi^{(s)}(r\boldsymbol{s})\right]$. Using Eq. (3.21), the matrix identity $(\boldsymbol{A}\circ\boldsymbol{B})^\dagger = \boldsymbol{B}^\dagger \circ \boldsymbol{A}^\dagger$, and after interchanging the order of averaging and integration, we find that

$$\boldsymbol{W}(r\boldsymbol{s}_1, r\boldsymbol{s}_2, \omega)$$

$$= \frac{1}{4\pi^2 r^2}\int_V\int_V\iint \left\langle F^*(\boldsymbol{r}_1)F(\boldsymbol{r}_2)\right\rangle L^*(R_1, \omega)L(R_2, \omega)\exp[ik(\boldsymbol{s}_1\cdot\boldsymbol{r}_1 - \boldsymbol{s}_2\cdot\boldsymbol{r}_2)]$$

$$\times\left\langle \boldsymbol{M}^T(\theta_1, \varphi_1, \boldsymbol{r}_1, \boldsymbol{\rho}_1')\circ \boldsymbol{E}_\perp^{(0)+}(\boldsymbol{\rho}_1', \omega)\circ \boldsymbol{E}_\perp^{(0)}(\boldsymbol{\rho}_2', \omega)\circ \boldsymbol{M}(\theta_2, \varphi_2, \boldsymbol{r}_2, \boldsymbol{\rho}_2')\right\rangle$$

$$\times d^2\rho_1' d^2\rho_2' d^3r_1 d^3r_2$$

$$= \frac{1}{4\pi^2 r^2}\int_V\int_V\iint \left\langle F^*(\boldsymbol{r}_1)F(\boldsymbol{r}_2)\right\rangle L^*(R_1, \omega)L(R_2, \omega)\exp[ik(\boldsymbol{s}_1\cdot\boldsymbol{r}_1 - \boldsymbol{s}_2\cdot\boldsymbol{r}_2)]$$

$$\times\boldsymbol{M}^T(\theta_1, \varphi_1, \boldsymbol{r}_1, \boldsymbol{\rho}_1')\circ \boldsymbol{W}_\perp^{(0)}(\boldsymbol{\rho}'_1, \boldsymbol{\rho}'_2, \omega)\circ \boldsymbol{M}(\theta_2, \varphi_2, \boldsymbol{r}_2, \boldsymbol{\rho}_2')$$

$$\times d^2\rho_1' d^2\rho_2' d^3r_1 d^3r_2, \tag{3.26}$$

or, more explicitly,

$$\begin{bmatrix} W_{\theta\theta} & W_{\theta\varphi} \\ W_{\varphi\theta} & W_{\varphi\varphi} \end{bmatrix}$$

$$= \frac{1}{4\pi^2 r^2}\int_V\int_V\iint\left\langle F^*(\boldsymbol{r}_1)F(\boldsymbol{r}_2)\right\rangle L^*(R_1,\omega)L(R_2,\omega)\exp[ik(\boldsymbol{s}_1\cdot\boldsymbol{r}_1-\boldsymbol{s}_2\cdot\boldsymbol{r}_2)]$$

$$\times\boldsymbol{M}^T(\theta_1,\varphi_1,\boldsymbol{r}_1,\boldsymbol{\rho}_1')\circ\begin{bmatrix} W_{xx}^{(0)} & W_{xy}^{(0)} \\ W_{yx}^{(0)} & W_{yy}^{(0)} \end{bmatrix}\circ\boldsymbol{M}(\theta_2,\varphi_2,\boldsymbol{r}_2,\boldsymbol{\rho}_2')d^2\rho_1' d^2\rho_2' d^3r_1 d^3r_2,$$

(3.27)

where $\boldsymbol{M}(\theta_1,\varphi_1,\boldsymbol{r}_1,\boldsymbol{\rho}_1')$ and $\boldsymbol{M}(\theta_2,\varphi_2,\boldsymbol{r}_2,\boldsymbol{\rho}_2')$ are given by Eq. (3.22) and $R_1=\left|\boldsymbol{r}_1+\boldsymbol{r}_0-\boldsymbol{\rho}_1'\right|$, $R_2=\left|\boldsymbol{r}_2+\boldsymbol{r}_0-\boldsymbol{\rho}_2'\right|$.

We note that in the case when the scattering medium is located close to the $z-$axis, i.e., about position $(0,0,z_0)$, with the use of Taylor expansion $\sqrt{1+\lambda}\sim 1+\frac{1}{2}\lambda\ (\lambda\to 0)$, Eq. (3.6) is reduced to

$$L(R_1,\omega)=\frac{ik}{(z_1+z_0)^2}\exp[ik(z_1+z_0)]\exp\{\frac{ik}{2(z_1+z_0)}[(x_1-x')^2+(y_1-y')^2]\}, \tag{3.28}$$

which considerably simplifies the subsequent analysis.

3.1.3 Example and concluding remarks

We will now restrict our attention to scattering of a field generated by an uncorrelated source, which in general is partially polarized, from a delta-correlated slab. Suppose that a field is generated in a two-dimensional domain D confined to the plane $z = 0$. Such a source may be characterized by the 2×2 cross-spectral density matrix of the form [57-58]

$$\boldsymbol{W}^{(0)}(\boldsymbol{\rho}_1', \boldsymbol{\rho}_2', \omega) = \boldsymbol{S}^{(0)}(\boldsymbol{\rho}_1', \omega)\delta^{(2)}(\boldsymbol{\rho}_2' - \boldsymbol{\rho}_1'), \tag{3.29}$$

where $\delta^{(2)}(\boldsymbol{\rho}_2' - \boldsymbol{\rho}_1')$ is a two-dimensional Dirac delta-function and

$$\boldsymbol{S}^{(0)}(\boldsymbol{\rho}', \omega) = [S_{ij}^{(0)}(\boldsymbol{\rho}', \omega)], \quad (i, j = x, y). \tag{3.30}$$

We also suppose that the fluctuations in the scattering volume are delta-correlated, i.e.

$$C_F(\boldsymbol{r}_1, \boldsymbol{r}_2, \omega) = \left\langle F^*(\boldsymbol{r}_1)F(\boldsymbol{r}_2)\right\rangle = A(\omega)\delta^{(3)}(\boldsymbol{r}_2 - \boldsymbol{r}_1), \tag{3.31}$$

$\delta^{(3)}(\boldsymbol{r}_2 - \boldsymbol{r}_1)$ being a three-dimensional Dirac delta function and $A(\omega)$ a function which is independent of position. On substituting from Eqs. (3.29), (3.30) and (3.31) into Eq. (3.27) we find that

$$[W_{\alpha\beta}(r\boldsymbol{s}_1, r\boldsymbol{s}_2, \omega)]$$

$$= \frac{1}{4\pi^2 r^2}\int_V\int A(\omega)\left|L(R_1, \omega)\right|^2 \exp[ik(\boldsymbol{s}_1 - \boldsymbol{s}_2)\cdot\boldsymbol{r}_1]$$

$$\times \boldsymbol{M}^T(\theta_1, \varphi_1, \boldsymbol{r}_1)\circ[S_{ij}^{(0)}(\boldsymbol{\rho}', \omega)]\circ\boldsymbol{M}(\theta_2, \varphi_2, \boldsymbol{r}_1)\mathrm{d}^2\rho'\,\mathrm{d}^3 r_1,$$

$$(\alpha, \beta = \theta, \varphi; i, j = x, y)\,. \quad (3.32)$$

We will now illustrate the preceding analysis by restricting ourselves to partially polarized incoherent electromagnetic Gaussian Schell-model beams, for which the elements of the correlation matrix are

$$S_{ij}^{(0)}(\boldsymbol{\rho}', \omega) = \sqrt{I_i I_j}\, B_{ij} \exp\{-\frac{\boldsymbol{\rho}'^2}{2\sigma^2}\}\,, \quad (i = x, y; j = x, y)\,. \qquad (3.33)$$

where, for simplicity, $I_x = I_y = 1$., i.e. the field in the source plane is unpolarized. It also follows from the properties of the cross-spectral density matrix that $B_{xy} = B_{yx} = B$ [20]. On substituting from Eqs. (3.28) and (3.33) into Eq. (3.32) after some straightforward calculations and decomposition of $\boldsymbol{M}(\theta, \varphi, \boldsymbol{r})$ matrix into two, we find that

$$[W_{\alpha\beta}(r\boldsymbol{s}_1, r\boldsymbol{s}_2, \omega)] = \frac{A(\omega)\sigma^2 k^2}{2\pi r^2} \begin{bmatrix} -\cos\theta_1 \cos\varphi_1 & -\cos\theta_1 \sin\varphi_1 & \sin\theta_1 \\ \sin\varphi_1 & -\cos\varphi_1 & 0 \end{bmatrix}$$

$$\circ \int_V \frac{\exp[ik(\boldsymbol{s}_1 - \boldsymbol{s}_2)\cdot \boldsymbol{r}_1]}{(z_1 + z_0)^4}$$

$$\times \begin{bmatrix} (z_1 + z_0)^2 & B(z_1 + z_0)^2 & -(z_1 + z_0)(x_1 + By_1) \\ B(z_1 + z_0)^2 & (z_1 + z_0)^2 & -(z_1 + z_0)(Bx_1 + y_1) \\ -(z_1 + z_0)(x_1 + By_1) & -(z_1 + z_0)(Bx_1 + y_1) & x_1^2 + y_1^2 + 2Bx_1 y_1 + 2\sigma^2 \end{bmatrix} \mathrm{d}^3 r_1$$

$$\circ \begin{bmatrix} -\cos\theta_2 \cos\varphi_2 & \sin\varphi_2 \\ -\cos\theta_2 \sin\varphi_2 & -\cos\varphi_2 \\ \sin\theta_2 & 0 \end{bmatrix} \quad (\alpha, \beta = \theta, \varphi)\,. \qquad (3.34)$$

For a specific case, we consider a delta-correlated hard-edge slab, with dimensions in Cartesian coordinate system $x_1 \in (-L_1, L_1)$, $y_1 \in (-L_2, L_2)$ and $z_1 \in (-L_3, L_3)$, which also satisfy that $L_1, L_2, L_3 \ll z_0$. We note that the assumption that the scattering medium has hard edges does not contradict the first-Born approximation as long as the refractive index within the slab differs only slightly from that of surrounding free space. We will calculate matrix $\left[S_{\alpha\beta}(r\boldsymbol{s},\omega)\right] = \left[W_{\alpha\beta}(r\boldsymbol{s}, r\boldsymbol{s},\omega)\right]$ on which the statistical properties of interest, such as the spectral density S and the spectral degree of polarization P, depend. Later we will turn to the spectral density matrix $\left[W_{\alpha\beta}(r\boldsymbol{s}_1, r\boldsymbol{s}_2,\omega)\right]$ at two different points on which the degree of coherence μ depends in the paraxial propagation regime, i.e. when inclination angle θ is small. Therefore, by assuming $\boldsymbol{s}_1 = \boldsymbol{s}_2 = \boldsymbol{s}$, we rewrite Eq. (3.34) as

$$[W_{\alpha\beta}(r\boldsymbol{s}, r\boldsymbol{s},\omega)]$$

$$= \frac{A(\omega)\sigma^2 k^2 V_0}{2\pi r^2 z_0^2} \begin{bmatrix} -\cos\theta\cos\varphi & -\cos\theta\sin\varphi & \sin\theta \\ \sin\varphi & -\cos\varphi & 0 \end{bmatrix}$$

$$\circ \begin{bmatrix} 1 & B & 0 \\ B & 1 & 0 \\ 0 & 0 & \dfrac{L_1^2}{3z_0^2} + \dfrac{L_2^2}{3z_0^2} + \dfrac{2\sigma^2}{z_0^2} \end{bmatrix} \circ \begin{bmatrix} -\cos\theta\cos\varphi & \sin\varphi \\ -\cos\theta\sin\varphi & -\cos\varphi \\ \sin\theta & 0 \end{bmatrix}$$

$$(\alpha, \beta = \theta, \varphi). \qquad (3.35)$$

For paraxial propagation (θ is small) the terms containing horizontal axis are negligible. Therefore, Eq. (3.22) becomes

$$\boldsymbol{M}(\theta,\varphi,\boldsymbol{r}_1)=\begin{bmatrix}\cos\theta\cos\varphi(z_1+z_0) & -\sin\varphi(z_1+z_0)\\ \cos\theta\sin\varphi(z_1+z_0) & \cos\varphi(z_1+z_0)\end{bmatrix}. \tag{3.36}$$

On substituting Eq. (3.36) into Eq. (3.35), we have, in a more explicit form, the 2×2 cross-spectral density matrix in spherical polar coordinate system,

$$[W_{\alpha\beta}(r\boldsymbol{s}_1,r\boldsymbol{s}_2,\omega)]=\frac{A(\omega)\sigma^2k^2}{2\pi r^2}\int_V\frac{\exp[ik(\boldsymbol{s}_1-\boldsymbol{s}_2)\cdot\boldsymbol{r}_1]}{(z_1+z_0)^2}\mathrm{d}^3r_1$$

$$\times\begin{bmatrix}\cos\theta_1\cos\varphi_1 & \cos\theta_1\sin\varphi_1\\ -\sin\varphi_1 & \cos\varphi_1\end{bmatrix}\circ\begin{bmatrix}1 & B\\ B & 1\end{bmatrix}\circ\begin{bmatrix}\cos\theta_2\cos\varphi_2 & -\sin\varphi_2\\ \cos\theta_2\sin\varphi_2 & \cos\varphi_2\end{bmatrix},$$

$$(\alpha,\beta=\theta,\varphi) \tag{3.37}$$

where $\boldsymbol{s}_1=(\sin\theta_1\cos\varphi_1,\sin\theta_1\sin\varphi_1,\cos\theta_1)$, $\boldsymbol{s}_2=(\sin\theta_2\cos\varphi_2,\sin\theta_2\sin\varphi_2,\cos\theta_2)$ are the unit vectors at two different directions. Under the hard-edge slab assumption, the integral in Eq. (3.37) becomes

$$\int_V\frac{\exp[ik(\boldsymbol{s}_1-\boldsymbol{s}_2)\cdot\boldsymbol{r}_1]}{(z_1+z_0)^2}d^3r_1=\frac{V_0}{z_0^2}\sin c(\frac{2s_xL_1}{\lambda})\sin c(\frac{2s_yL_2}{\lambda})\sin c(\frac{2s_zL_3}{\lambda}), \tag{3.38}$$

where $V_0=L_1L_2L_3$ being the volume of the slab, λ is the free-space wavelength associated with free-space wave number k and $s_i=(\boldsymbol{s}_1-\boldsymbol{s}_2)_i$ $(i=x,y,z)$, i.e., $s_x=\sin\theta_1\cos\varphi_1-\sin\theta_2\cos\varphi_2$, etc. On substituting from Eq. (3.38) into Eq. (3.37), the 2×2 cross-spectral density matrix of the scattered field in the far zone in paraxial

propagation, generated by a partially polarized incoherent electromagnetic source through a delta-correlated thin slab, in polar coordinate system, becomes

$$[W_{\alpha\beta}(r\mathbf{s}_1, r\mathbf{s}_2, \omega)]$$

$$= \frac{A(\omega)\sigma^2 k^2 V_0}{2\pi r^2 z_0^2} \sin c(\frac{2s_x L_1}{\lambda}) \sin c(\frac{2s_y L_2}{\lambda}) \sin c(\frac{2s_z L_3}{\lambda})$$

$$\times \begin{bmatrix} \cos\theta_1 \cos\varphi_1 & \cos\theta_1 \sin\varphi_1 \\ -\sin\varphi_1 & \cos\varphi_1 \end{bmatrix} \circ \begin{bmatrix} 1 & B \\ B & 1 \end{bmatrix} \circ \begin{bmatrix} \cos\theta_2 \cos\varphi_2 & -\sin\varphi_2 \\ \cos\theta_2 \sin\varphi_2 & \cos\varphi_2 \end{bmatrix}. \quad (3.39)$$

From the components of the cross-spectral density matrix the spectral density S, the degree of coherence μ and the spectral degree of polarization P are defined in Eq. (1.6), Eq. (1.7) and Eq. (1.8), respectively.

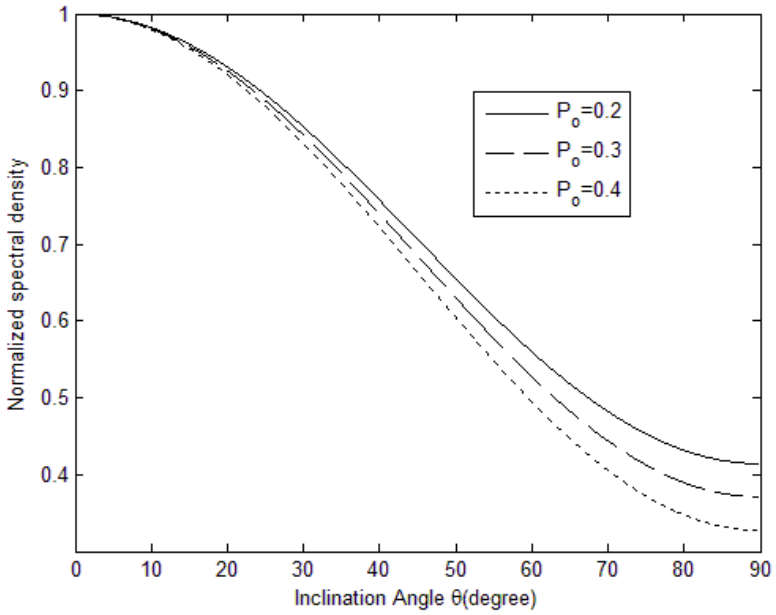

Fig. 3.3 Normalized spectral density of the scattered field in the far zone vs. the inclination angle, with $\varphi = \frac{\pi}{6}$.

We will now illustrate the results by a set of figures. The following parameters are used for the plots: $\omega = 10^{15} s^{-1}$, $\lambda = \frac{2\pi c}{\omega}$, $L_1 = L_2 = 5\times 10^3 \lambda$, $L_3 = 10^3 \lambda$, $z_0 = 10^5 \lambda$, $\sigma = 1mm$.

Fig. 3.3 shows the normalized spectral density defined by Eq. (1.6) of the field in the far zone generated by a partially polarized incoherent EMGSM source and scattered by a

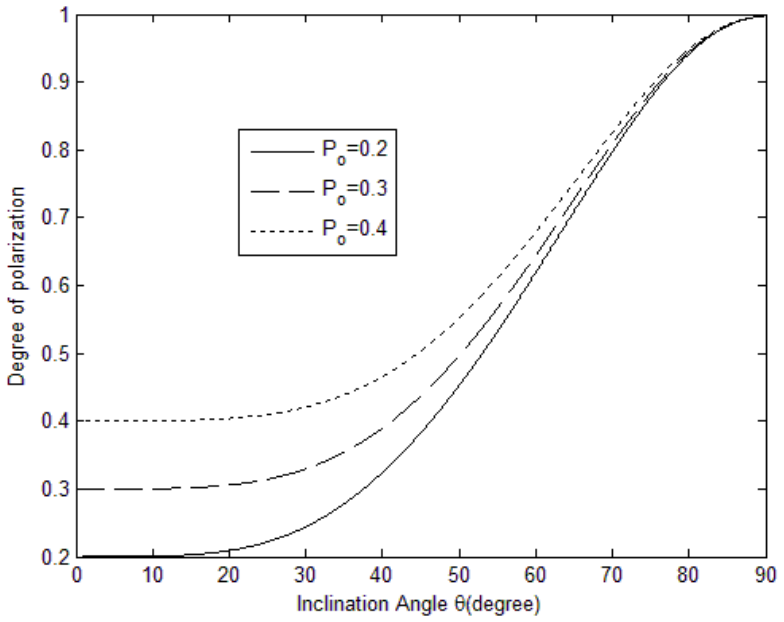

Fig. 3.4 The spectral degree of polarization of the scattered field in the far zone vs. the inclination angle, with $\varphi = 0$.

delta-correlated hard-edge scatterer for several values of the degree of polarization P_o of the field in the source plane. Fig 3.4 shows the degree of polarization, defined in Eq. (1.8), of the scattered field in the far zone. We see from Fig. 3.4 that the spectral degree of polarization of the scattered field in the paraxial region (the inclination angle is about zero) has its original value P_o. In fact, similar result can be found from Ref. [58], where propagation of a partially polarized incoherent electromagnetic source in the paraxial

approximation is considered without scattering. This may be verified by substituting a Gaussian Schell-model beam into Eqs. (9), (10) of Ref. [58].

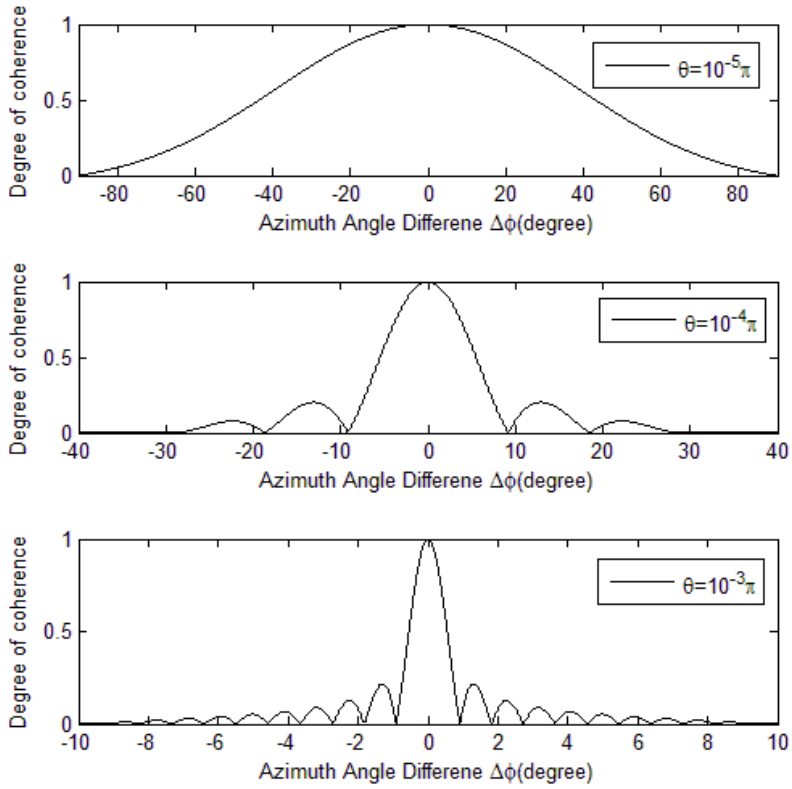

Fig. 3.5 The spectral degree of coherence of the scattered field in the far zone at two points vs. the azimuth separation angle $\Delta\varphi$.

In Fig. 3.5 we show the spectral degree of coherence, defined in Eq. (1.7), of the scattered field in the far zone with azimuthal separation angle $\Delta\varphi$. At the first glance, the value of degree of coherence is independent of the radial distance r, but it is not the case. Since for larger radial distance, two points with fixed azimuth angle difference will separate from each other larger, i.e. the distance between two points with fixed azimuth angle difference is proportional to the radial distance r. For coherence area ΔA is

proportional to r^2 which obeys the van Cittert-Zernike theorem in the far zone. Fig. 3.5 clearly shows the fact that for small inclination angles, the degree of coherence curve is wider, since the distance between two points is smaller.

3.2 Momentum of Light Scattered from Collections of Particles

In applications involving optical trapping of particles, such as optical tweezers which recently gained popularity [59-60], it is crucial to determine and control the momentum flow of the electromagnetic field. The momentum flow at any spatial position and time instant can be found from the Maxwell stress tensor. The basic theory on this subject relating to monochromatic fields can be found in classic text [61], and its extension to partially coherent fields belongs to Ref. [62] in space-time domain and to Ref. [63] in space-frequency domain, including the corresponding momentum conservation laws.

In optical tweezers it is crucial not only to control the momentum flow of the field incident on the particles but also to predict its behavior upon scattering. The purpose of this work is to evaluate the angular distribution of the momentum flow of an electromagnetic field scattered by a deterministic or random media, which may be a single scatterer or a collection, and to elucidate how the momentum flow of the scattered light wave relates to the individual and collective properties of the scatterers. To illustrate our theoretical analysis, we consider a pair of numerical examples in which a polychromatic electromagnetic plane wave is scattered from a collection of identical particles having deterministic potentials and either deterministic or random locations.

3.2.1 Momentum flow of an electromagnetic field on weak scattering.

We begin by considering a polychromatic electromagnetic vector-field $\boldsymbol{E}^{(i)}(\boldsymbol{r},\omega)=\left[E_x^{(i)}(\boldsymbol{r},\omega),E_y^{(i)}(\boldsymbol{r},\omega),E_z^{(i)}(\boldsymbol{r},\omega)\right]$ at a point with position-vector $\boldsymbol{r}$, at angular frequency ω, which is incident onto a medium with volume V where only the polarization, $\boldsymbol{P}(\boldsymbol{r},\omega)$, is induced, i.e. only the electric properties of the medium modulate the field in a nontrivial fashion. It is the case for most substances. Specialized to polychromatic fields, the scattered electric and magnetic fields outside the scattering volume V may be expressed, respectively, as (Ref. [19], Sec. 13.6)

$$\boldsymbol{E}^{(s)}(\boldsymbol{r},\omega)=\boldsymbol{\nabla}\times\boldsymbol{\nabla}\times\boldsymbol{\Pi}_e(\boldsymbol{r},\omega), \tag{3.40}$$

$$\boldsymbol{B}^{(s)}(\boldsymbol{r},\omega)=-ik\boldsymbol{\nabla}\times\boldsymbol{\Pi}_e(\boldsymbol{r},\omega), \tag{3.41}$$

where $\boldsymbol{\Pi}_e(\boldsymbol{r},\omega)$ is defined by Eq. (3.9) (we repeat here for the convenience of readers)

$$\boldsymbol{\Pi}_e(\boldsymbol{r},\omega)=\int_V \boldsymbol{P}(\boldsymbol{r}',\omega)G(\boldsymbol{r}-\boldsymbol{r}')d^3r', \tag{3.42}$$

where $\boldsymbol{r}'$ is a point within volume V and

$$G(\boldsymbol{R})=G(R)=\frac{\exp(ikR)}{R}, \tag{3.43}$$

is the free-space Green's function for the Helmholtz equation. Further, if the response of the medium is linear and the scattering is sufficiently weak, the constitutive relation may be expressed, within the accuracy of the first-order Born approximation, as [20]

$$\begin{aligned}\boldsymbol{P}(\boldsymbol{r}',\omega) &= \eta(\boldsymbol{r}',\omega)\boldsymbol{E}^{(i)}(\boldsymbol{r}',\omega) \\ &= \frac{1}{k^2}F(\boldsymbol{r}',\omega)\boldsymbol{E}^{(i)}(\boldsymbol{r}',\omega)\end{aligned}, \tag{3.44}$$

where $\eta(\boldsymbol{r}',\omega)$ is the dielectric susceptibility and $F(\boldsymbol{r}',\omega)$ is the scattering potential of the medium being defined by Eq. (1.12).

It is often of interest in scattering experiments to examine the behavior of the scattered field in the far zone. By denoting $\boldsymbol{r} = r\boldsymbol{s}$, $\boldsymbol{s}$ being the unit vector, we can approximate the free-space Green's function by the form

$$\frac{\exp(ik|\boldsymbol{r}-\boldsymbol{r}'|)}{|\boldsymbol{r}-\boldsymbol{r}'|} = \frac{\exp(ikr)}{r}\exp(-ik\mathbf{s}\cdot r'). \tag{3.45}$$

On substituting from Eqs. (3.42), (3.44) and (3.45) into Eq. (3.40) we find that the scattered electric field in the far zone becomes [see Eq. (3.16)]

$$\boldsymbol{E}^{(s)}(\boldsymbol{r},\omega) = \frac{\exp(ikr)}{r}\int_V F(\boldsymbol{r}',\omega)\boldsymbol{E}^{(i)}(\boldsymbol{r}',\omega)\circ\hat{\boldsymbol{S}}_1(\boldsymbol{s})\exp(-ik\boldsymbol{s}\cdot\boldsymbol{r}')d^3r', \tag{3.46}$$

where circle stands for matrix multiplication (not to be confused with dot product and cross-product) and tensor $\hat{\boldsymbol{S}}_1(\boldsymbol{s})$ in the explicit form is

$$\hat{\boldsymbol{S}}_1(\boldsymbol{s}) = \begin{pmatrix} 1-s_x^2 & -s_xs_y & -s_xs_z \\ -s_ys_x & 1-s_y^2 & -s_ys_z \\ -s_zs_x & -s_zs_y & 1-s_z^2 \end{pmatrix}. \tag{3.47}$$

Similar procedure leads to the expression of the scattered magnetic field in the far zone:

$$\boldsymbol{B}^{(s)}(\boldsymbol{r},\omega)=\frac{\exp(ikr)}{r}\int_V F(\boldsymbol{r}',\omega)\boldsymbol{E}^{(i)}(\boldsymbol{r}',\omega)\circ\widehat{\boldsymbol{S}}_2(\boldsymbol{s})\exp(-ik\boldsymbol{s}\cdot\boldsymbol{r}')d^3r', \tag{3.48}$$

with

$$\widehat{\boldsymbol{S}}_2(\boldsymbol{s})=\begin{pmatrix}0 & s_z & -s_y\\ -s_z & 0 & s_x\\ s_y & -s_x & 0\end{pmatrix}. \tag{3.49}$$

We note that Eqs. (3.46) and (3.48) are the same transformation laws in form, except they involve different transformation matrices, Eqs. (3.47) and (3.49), respectively. In particular, $\widehat{\boldsymbol{S}}_1$ is a symmetric matrix while $\widehat{\boldsymbol{S}}_2$ is anti-symmetric one. Further, since $\boldsymbol{s}\cdot\boldsymbol{E}^{(s)}=0$, $\boldsymbol{s}\cdot\boldsymbol{B}^{(s)}=0$, and $\boldsymbol{B}^{(s)}=\boldsymbol{s}\times\boldsymbol{E}^{(s)}$, the scattered electromagnetic field is the outgoing spherical wave which propagates in the direction of the unit vector $\boldsymbol{s}$, i.e. in the outward radial direction from the scatterer. The incident field and the transformation matrices are all expressed in the Cartesian coordinate system, hence the resulting scattered fields are also in the same system. Then the total field including the incident filed and the scattered field may be expressed

$$\boldsymbol{E}(\boldsymbol{r},\omega)=\boldsymbol{E}^{(i)}(\boldsymbol{r},\omega)+\boldsymbol{E}^{(s)}(\boldsymbol{r},\omega), \tag{3.50}$$

$$\boldsymbol{B}(\boldsymbol{r},\omega)=\boldsymbol{B}^{(i)}(\boldsymbol{r},\omega)+\boldsymbol{B}^{(s)}(\boldsymbol{r},\omega). \tag{3.51}$$

The fields considered are out of the dielectric materials to avoid the Abraham-Minkowski controversy [64]. The Maxwell stress tensor $\widehat{\boldsymbol{T}}(\boldsymbol{r},\omega)$ of a monochromatic field in the space-frequency domain was shown to be given by the formula [63]

$$\hat{\boldsymbol{T}}(\boldsymbol{r},\omega)=\frac{1}{4\pi}\left\{\boldsymbol{E}^{\dagger}(\boldsymbol{r},\omega)\circ\boldsymbol{E}(\boldsymbol{r},\omega)-\frac{1}{2}Tr\left[\boldsymbol{E}^{\dagger}(\boldsymbol{r},\omega)\circ\boldsymbol{E}(\boldsymbol{r},\omega)\right]\hat{\boldsymbol{I}}\right\}$$

$$+\frac{1}{4\pi}\left\{\boldsymbol{B}^{\dagger}(\boldsymbol{r},\omega)\circ\boldsymbol{B}(\boldsymbol{r},\omega)-\frac{1}{2}Tr\left[\boldsymbol{B}^{\dagger}(\boldsymbol{r},\omega)\circ\boldsymbol{B}(\boldsymbol{r},\omega)\right]\hat{\boldsymbol{I}}\right\}, \qquad (3.52)$$

where $\hat{\boldsymbol{I}}$ is a unit 3×3 matrix and Tr stands for the trace of a matrix. Then the momentum flow $\boldsymbol{Q}(r\boldsymbol{s})$ is defined, as a function of normal direction $\boldsymbol{s}$, as

$$\boldsymbol{Q}(r\boldsymbol{s})=\boldsymbol{s}\cdot\hat{\boldsymbol{T}}(\boldsymbol{r},\omega)\,. \qquad (3.53)$$

The total change in momentum within the volume V containing the scattering media can be identified as the sum of the change in mechanical momentum of the scattering media and the change in the momentum of enclosed electromagnetic fields. According to the momentum conservation law the total change in momentum is equal to the net momentum flow introduced by the total field, through the surface enclosing volume V, which may be predicted by Eq. (3.53).

3.2.2 Momentum flow of a scattered polychromatic plane wave

Let us now confine our analysis to the case of an incident polychromatic plane wave propagating along the $z-$axis, i.e. having wave vector $\boldsymbol{s}_0=[0,0,1]$

$$E_{\gamma}^{(i)}(\boldsymbol{r}',\omega)=a_{\gamma}(\omega)\exp(ik\boldsymbol{s}_0\cdot\boldsymbol{r}') \quad (\gamma=x,y)\,, \qquad (3.54)$$

where $a_{\gamma}(\omega)$ is the amplitude of the electric field and only the two transverse components are nontrivial. The magnetic counterpart of the incident field

$\boldsymbol{B}^{(i)}(\boldsymbol{r}',\omega)=\boldsymbol{s}_0\times\boldsymbol{E}^{(i)}(\boldsymbol{r}',\omega)$ (Ref. [19], Sec. 1.4) may be expressed, for the planar wave-front, as

$$\boldsymbol{B}^{(i)}(\boldsymbol{r}',\omega)=\boldsymbol{E}^{(i)}(\boldsymbol{r}',\omega)\circ\widehat{\boldsymbol{S}}_2(\boldsymbol{s}_0)\,, \tag{3.55}$$

where $\boldsymbol{B}^{(i)}(\boldsymbol{r}',\omega)=\left[B_x^{(i)}(\boldsymbol{r}',\omega),B_y^{(i)}(\boldsymbol{r}',\omega),B_z^{(i)}(\boldsymbol{r}',\omega)\right]$ and

$$\widehat{\boldsymbol{S}}_2(\boldsymbol{s}_0)=\begin{pmatrix}0&1&0\\-1&0&0\\0&0&0\end{pmatrix}. \tag{3.56}$$

where the $\widehat{\boldsymbol{S}}_2$ matrix is introduced in Eq. (3.49). In a general case when either the incident field is stochastic, wide-sense statistically stationary and/or scattering medium acts on the incident field in a random but static manner the resulting scattered electromagnetic field is also wide-sense statistically stationary [23]. To characterize the second-order correlation properties of fluctuating fields we use the cross-spectral density tensors at coinciding spatial arguments for its electric and magnetic counterparts as follows [23]

$$\boldsymbol{W}^{E}(\boldsymbol{r},\boldsymbol{r},\omega)=\left\langle\boldsymbol{E}^{\dagger}(\boldsymbol{r},\omega)\circ\boldsymbol{E}(\boldsymbol{r},\omega)\right\rangle, \tag{3.57}$$

$$\boldsymbol{W}^{B}(\boldsymbol{r},\boldsymbol{r},\omega)=\left\langle\boldsymbol{B}^{\dagger}(\boldsymbol{r},\omega)\circ\boldsymbol{B}(\boldsymbol{r},\omega)\right\rangle, \tag{3.58}$$

dagger standing for Hermitian adjoint, and angular brackets denoting the ensemble average in the sense of classic coherence theory in the space-frequency domain.

On substituting from Eq. (3.54) into Eq. (3.57) we find that at coinciding spatial arguments the electric cross-spectral density matrix of the incident polychromatic plane wave has the form

$$\boldsymbol{W}^{(ii),E}(\boldsymbol{r},\boldsymbol{r},\omega)=S^{(i)}(\omega)\widehat{\boldsymbol{C}}\,, \tag{3.59}$$

where $\left\langle a_\gamma^*(\omega)a_\chi(\omega)\right\rangle = A_\gamma A_\chi B_{\gamma\chi}S^{(i)}(\omega)$, star standing for complex conjugate, and tensor

$$\widehat{\boldsymbol{C}}=\begin{pmatrix} A_x^2 & A_xA_yB & 0\\ A_yA_xB & A_y^2 & 0\\ 0 & 0 & 0\end{pmatrix}, \tag{3.60}$$

characterizes the correlation properties between the mutually orthogonal components of the field. In a similar way we find that the correlation tensor of the incident magnetic fields has the form

$$\boldsymbol{W}^{(ii),B}(\boldsymbol{r},\boldsymbol{r},\omega)=-S^{(i)}(\omega)\widehat{\boldsymbol{S}}_2(\boldsymbol{s}_0)\circ\widehat{\boldsymbol{C}}\circ\widehat{\boldsymbol{S}}_2(\boldsymbol{s}_0)\,, \tag{3.61}$$

where the negative sign results from the anti-symmetry of tensor $\widehat{\boldsymbol{S}}_2(\boldsymbol{s}_0)$.

The correlation tensors of the scattered electric and magnetic fields can also be determined on substituting from Eq. (3.47) into Eq. (3.57) and from Eq. (3.49) into Eq. (3.58), using Eq. (3.59) respectively,

$$\boldsymbol{W}^{(ss),E}(\boldsymbol{r},\boldsymbol{r},\omega)=\frac{1}{r^2}\widetilde{C}_F(-\boldsymbol{K},\boldsymbol{K},\omega)\widehat{\boldsymbol{S}}_1(\boldsymbol{s})\circ\boldsymbol{W}^{(ii),E}(\boldsymbol{r},\boldsymbol{r},\omega)\circ\widehat{\boldsymbol{S}}_1(\boldsymbol{s})$$

$$=\frac{1}{r^2}S^{(i)}(\omega)\widetilde{C}_F(-\boldsymbol{K},\boldsymbol{K},\omega)\widehat{\boldsymbol{S}}_1(\boldsymbol{s})\circ\widehat{\boldsymbol{C}}\circ\widehat{\boldsymbol{S}}_1(\boldsymbol{s})\,, \tag{3.62}$$

$$\boldsymbol{W}^{(ss),B}(\boldsymbol{r},\boldsymbol{r},\omega)=-\frac{1}{r^2}\widetilde{C}_F(-\boldsymbol{K},\boldsymbol{K},\omega)\widehat{\boldsymbol{S}}_2(\boldsymbol{s})\circ\boldsymbol{W}^{(ii),E}(\boldsymbol{r},\boldsymbol{r},\omega)\circ\widehat{\boldsymbol{S}}_2(\boldsymbol{s})$$

$$=-\frac{1}{r^2}S^{(i)}(\omega)\widetilde{C}_F(-\boldsymbol{K},\boldsymbol{K},\omega)\widehat{\boldsymbol{S}}_2(\boldsymbol{s})\circ\widehat{\boldsymbol{C}}\circ\widehat{\boldsymbol{S}}_2(\boldsymbol{s}), \tag{3.63}$$

where $\boldsymbol{K}=k(\boldsymbol{s}-\boldsymbol{s}_0)$ resembles the momentum transfer vector in quantum mechanics and

$$\widetilde{C}_F(-\boldsymbol{K},\boldsymbol{K},\omega)=\int_V\int_V\left\langle F^*(\boldsymbol{r}_1',\omega)F(\boldsymbol{r}_2',\omega)\right\rangle_m\exp[-i\boldsymbol{K}\cdot(\boldsymbol{r}_2'-\boldsymbol{r}_1')]d^3r_1'\,d^3r_2', \tag{3.64}$$

is the six-dimensional Fourier transform of the correlation function of the scattering potential of the medium.

The total electric field produced on scattering is the sum of the incident electric field and the scattered electric field and, hence, the cross-spectral density tensor of the total field includes a cross-term appearing from their interference. The same is true for the magnetic fields. Thus we have by substituting Eqs. (3.50) and (3.51) into Eqs. (3.57) and (3.58), respectively,

$$\boldsymbol{W}^{E}(\boldsymbol{r},\boldsymbol{r},\omega)=\boldsymbol{W}^{(ii),E}(\boldsymbol{r},\boldsymbol{r},\omega)+\boldsymbol{W}^{(ss),E}(\boldsymbol{r},\boldsymbol{r},\omega)+\boldsymbol{W}^{(is),E}(\boldsymbol{r},\boldsymbol{r},\omega), \tag{3.65}$$

$$\boldsymbol{W}^{B}(\boldsymbol{r},\boldsymbol{r},\omega)=\boldsymbol{W}^{(ii),B}(\boldsymbol{r},\boldsymbol{r},\omega)+\boldsymbol{W}^{(ss),B}(\boldsymbol{r},\boldsymbol{r},\omega)+\boldsymbol{W}^{(is),B}(\boldsymbol{r},\boldsymbol{r},\omega). \tag{3.66}$$

where the mixed terms are given by the formulas

$$\boldsymbol{W}^{(is),E}(\boldsymbol{r},\boldsymbol{r},\omega)=\left\langle\boldsymbol{E}^{(s)+}(\boldsymbol{r},\omega)\circ\boldsymbol{E}^{(i)}(\boldsymbol{r},\omega)+\boldsymbol{E}^{(i)+}(\boldsymbol{r},\omega)\circ\boldsymbol{E}^{(s)}(\boldsymbol{r},\omega)\right\rangle, \tag{3.67}$$

$$\boldsymbol{W}^{(is),B}(\boldsymbol{r},\boldsymbol{r},\omega)=\left\langle\boldsymbol{B}^{(s)+}(\boldsymbol{r},\omega)\circ\boldsymbol{B}^{(i)}(\boldsymbol{r},\omega)+\boldsymbol{B}^{(i)+}(\boldsymbol{r},\omega)\circ\boldsymbol{B}^{(s)}(\boldsymbol{r},\omega)\right\rangle. \tag{3.68}$$

We will now turn our attention to calculation of the momentum flow of the scattered field. For electromagnetic stochastic fields the ensemble averaged version of the stress tensor can then be generalized from Eq. (3.53) as [63]

$$\left\langle \hat{\boldsymbol{T}}(\boldsymbol{r},\omega)\right\rangle = \frac{1}{4\pi}\left\{\boldsymbol{W}^{E}(\boldsymbol{r},\boldsymbol{r},\omega) - \frac{1}{2}Tr\left[\boldsymbol{W}^{E}(\boldsymbol{r},\boldsymbol{r},\omega)\right]\hat{\boldsymbol{I}}\right\}$$

$$+\frac{1}{4\pi}\left\{\boldsymbol{W}^{B}(\boldsymbol{r},\boldsymbol{r},\omega) - \frac{1}{2}Tr\left[\boldsymbol{W}^{B}(\boldsymbol{r},\boldsymbol{r},\omega)\right]\hat{\boldsymbol{I}}\right\}. \tag{3.69}$$

On substituting from Eqs. (3.65) and (3.66) into Eq. (3.69), we find that in the situation involving scattering the total stress tensor has the following general form:

$$\left\langle \hat{\boldsymbol{T}}(\boldsymbol{r},\omega)\right\rangle = \left\langle \hat{\boldsymbol{T}}^{(i)}(\boldsymbol{r},\omega)\right\rangle + \left\langle \hat{\boldsymbol{T}}^{(s)}(\boldsymbol{r},\omega)\right\rangle + \left\langle \hat{\boldsymbol{T}}^{(is)}(\boldsymbol{r},\omega)\right\rangle. \tag{3.70}$$

Here the Maxwell stress tensors of the incident and scattered fields as well as of the mixed term are, respectively:

$$\left\langle \hat{\boldsymbol{T}}^{(i)}\right\rangle = \frac{1}{4\pi}\left\{\left(\boldsymbol{W}^{(ii),E} + \boldsymbol{W}^{(ii),B}\right) - \frac{1}{2}Tr\left(\boldsymbol{W}^{(ii),E} + \boldsymbol{W}^{(ii),B}\right)\hat{\boldsymbol{I}}\right\}, \tag{3.71}$$

$$\left\langle \hat{\boldsymbol{T}}^{(s)}\right\rangle = \frac{1}{4\pi}\left\{\left(\boldsymbol{W}^{(ss),E} + \boldsymbol{W}^{(ss),B}\right) - \frac{1}{2}Tr\left(\boldsymbol{W}^{(ss),E} + \boldsymbol{W}^{(ss),B}\right)\hat{\boldsymbol{I}}\right\}, \tag{3.72}$$

$$\left\langle \hat{\boldsymbol{T}}^{(is)}\right\rangle = \frac{1}{4\pi}\left\{\left(\boldsymbol{W}^{(is),E} + \boldsymbol{W}^{(is),B}\right) - \frac{1}{2}Tr\left(\boldsymbol{W}^{(is),E} + \boldsymbol{W}^{(is),B}\right)\hat{\boldsymbol{I}}\right\}, \tag{3.73}$$

where the arguments of the tensors are suppressed for brevity. In the present work we assume that the interference between the incident and the scattered fields is weak and can

be neglected, i.e. $\left\langle \hat{\boldsymbol{T}}^{(is)} \right\rangle \approx 0$, which is usually the case. We make such an assumption since a random scattering medium may change the incident field, making the statistical properties of the scattered field completely uncorrelated with the original incident field. Therefore in a majority of recently published papers about scattering, the researchers only consider the correlation properties between the scattered fields themselves (see, for example, Ref.[20], Chap.6; Ref.[14]; Ref. [32]). Then the explicit expression for $\left\langle \hat{\boldsymbol{T}}^{(i)} \right\rangle$ may be obtained by substituting from Eqs. (3.59) and (3.61) into Eq. (3.71) as

$$\left\langle \hat{\boldsymbol{T}}^{(i)}(\boldsymbol{r},\omega) \right\rangle = -\frac{1}{4\pi} S^{(i)}(\omega) \begin{pmatrix} 0 & 0 & 0 \\ 0 & 0 & 0 \\ 0 & 0 & A_x^2 + A_y^2 \end{pmatrix}. \tag{3.74}$$

We note that for the momentum flow of the incident plane wave propagating into a plane perpendicular to radial unit vector $\mathbf{s}$, only the $z-$component is nontrivial since [see Eq. (3.53)]

$$\boldsymbol{Q}^{(i)}(r\boldsymbol{s}) = \boldsymbol{s} \cdot \left\langle \hat{\boldsymbol{T}}^{(i)}(\boldsymbol{r},\omega) \right\rangle = -\frac{1}{4\pi} S^{(i)}(\omega) \begin{pmatrix} 0 & 0 & \left(A_x^2 + A_y^2\right) s_z \end{pmatrix}. \tag{3.75}$$

On the other hand, for the scattered field the Maxwell stress tensor is a function of radial direction $\boldsymbol{s}$, which can be readily asserted on substituting from Eqs. (3.62) and (3.63) into Eq. (3.72), to obtain the expression for the momentum flow $\boldsymbol{Q}^{(s)}(r\boldsymbol{s})$ of the scattered field as

$$\boldsymbol{Q}^{(s)}(r\boldsymbol{s}) \equiv \boldsymbol{s} \cdot \left\langle \hat{\boldsymbol{T}}^{(s)}(\boldsymbol{r},\omega) \right\rangle$$

$$= -\frac{1}{4\pi r^2} S^{(i)}(\omega)\widetilde{C}_F(-\boldsymbol{K}, \boldsymbol{K}, \omega)\left(Tr\widehat{\boldsymbol{C}} - \boldsymbol{s}\circ\widehat{\boldsymbol{C}}\circ\boldsymbol{s}^T\right)\boldsymbol{s}, \tag{3.76}$$

where $\boldsymbol{s} = \left(s_x, s_y, s_z\right)$. Eq. (3.76) is the main result of the paper. It can be used to determine the angular distribution of the momentum flow of the scattered field in the far zone as it propagates into a plane perpendicular to radial unit vector $\boldsymbol{s}$. We note that only the field component along the radial direction is nontrivial and is independent of the incident direction. Eq. (3.76) implies that the momentum flow $\boldsymbol{Q}^{(s)}(r\boldsymbol{s})$ of the scattered field depends on the correlation function of the potential of the scattering medium and on the correlation properties of the incident field. Thus, there is no net momentum flow for an incident electromagnetic plane wave, even though the angular distribution of the stress tensor is nontrivial. However, as for the momentum flow introduced by the scattered field, its angular distribution does not only depend on the degree of polarization of the incident plane waves, but also upon the distribution of the scattering materials and the correlation properties of the media. Therefore, the net scattered momentum flow is nontrivial, being influenced by physical and statistical properties of the scattering medium.

3.2.3 Numerical examples

We will now employ the theoretical development of Sections 3.2.1 and 3.2.2 for solving an important class of problems relating to angular momentum distribution of light scattered from deterministic and random particulate media. For simplicity we will confine ourselves only to collections of identical particles. The scattering potential of the collection can be expressed as sum

$$F(\boldsymbol{r}',\omega)=\sum_{m=1}^{M} f(\boldsymbol{r}'-\boldsymbol{r}_m,\omega)\,, \tag{3.77}$$

where $\boldsymbol{r}_m$ is the center of a particle labeled with m . Further, the Fourier transform of the correlation function of the medium then takes form [20]

$$\widetilde{C}_F(-\boldsymbol{K},\boldsymbol{K},\omega)=\left|\widetilde{f}(\boldsymbol{K},\omega)\right|^2 M(\boldsymbol{K},\omega)\,, \tag{3.78}$$

where $\widetilde{f}(\boldsymbol{K},\omega)$ is the Fourier transform of scattering potential of a single particle $f(\boldsymbol{r}',\omega)$, and $M(\boldsymbol{K},\omega)=\left\langle\left|\sum_{m=1}^{M}\exp(-i\boldsymbol{K}\cdot\boldsymbol{r}_m)\right|^2\right\rangle$ is the structure factor containing the correlation information of the entire particle system. We assume the scattering potential of the particle is of Gaussian distribution, i.e., $f(\boldsymbol{r}',\omega)=\exp\left[-\frac{\boldsymbol{r}'^2}{2\sigma^2}\right]$. With $s_x=\sin\theta\cos\varphi$, $s_y=\sin\theta\sin\varphi$ and $s_z=\cos\theta$ (see Fig. 3.2), we calculate the distribution of the momentum flow of the scattered fields at the scattering plane $\varphi=0$. The parameters of the incident plane wave are chosen to be: $\lambda=0.6328\mu m$, $A_x=A_y=1$, $B=0.2$.

In Fig. 3.6 we consider the models of particle collections distributed along the x-axis that we use for numerical calculations. In particular, in Fig. 3.6(a) we show the simplest case of a pair of symmetrically located particles, with centers at $(d/2,0,0)$ and $(-d/2,0,0)$, respectively. In Figs. 3.7 and 3.8 we present the momentum flow of the field scattered from collection of Fig. 3.6(a). It becomes clear from these two figures that the separation between the two particles influences the number and position of the peaks

of the momentum flow, while the size of the particles changes the peak value and retains the position of each peak. To understand the peak positions which are determined by the interference between particles, we first derive, from Eq. (3.76), the condition for the valley points (i.e., where $\left|\boldsymbol{Q}^{(s)}(r\boldsymbol{s})\right| = 0$):

$$d_{sp}\sin\theta = (n+\frac{1}{2})\lambda\,,\quad (n=0,1,2...)\,, \tag{3.79}$$

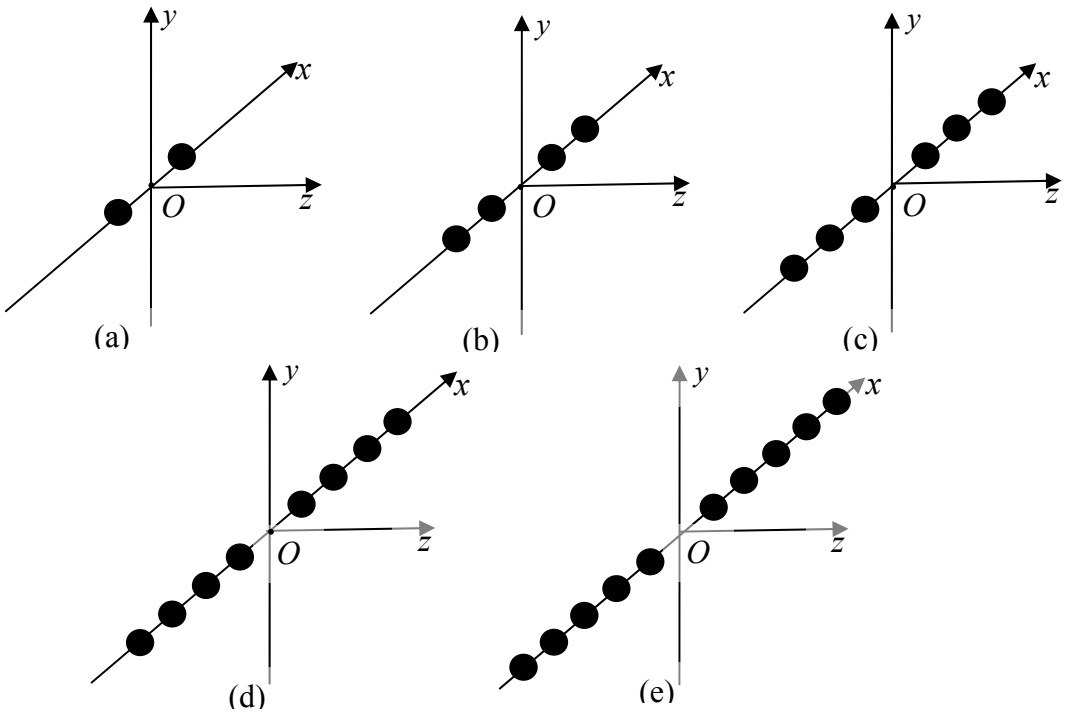

Fig. 3.6 The coordinates of particles (a) (d/2,0,0), (-d/2,0,0); (b) (d/2,0,0), (-d/2,0,0), (d,0,0), (-d,0,0); (c) (d/2,0,0), (-d/2,0,0), (d,0,0), (-d,0,0), (3d/2,0,0), (-3d/2,0,0); (d) (d/2,0,0), (-d/2,0,0), (d,0,0), (-d,0,0), (3d/2,0,0), (-3d/2,0,0), (2d,0,0), (-2d,0,0); (e) (d/2,0,0), (-d/2,0,0), (d,0,0), (-d,0,0), (3d/2,0,0), (-3d/2,0,0), (2d,0,0), (-2d,0,0), (5d/2,0,0), (-5d/2,0,0).

where d_{sp} is the spacing distance between two particles. This equation matches the positions of valley points in Figs. 3.7 and 3.8 accurately. Therefore for the case where the peak points are about the center of the two neighboring valley points (for example, $kd = 8\pi$ and $kd = 16\pi$), the peak points' positions may be approximately estimated by the equation

$$d_{sp} \sin\theta = n\lambda, \quad (n = 0, 1, 2...). \tag{3.80}$$

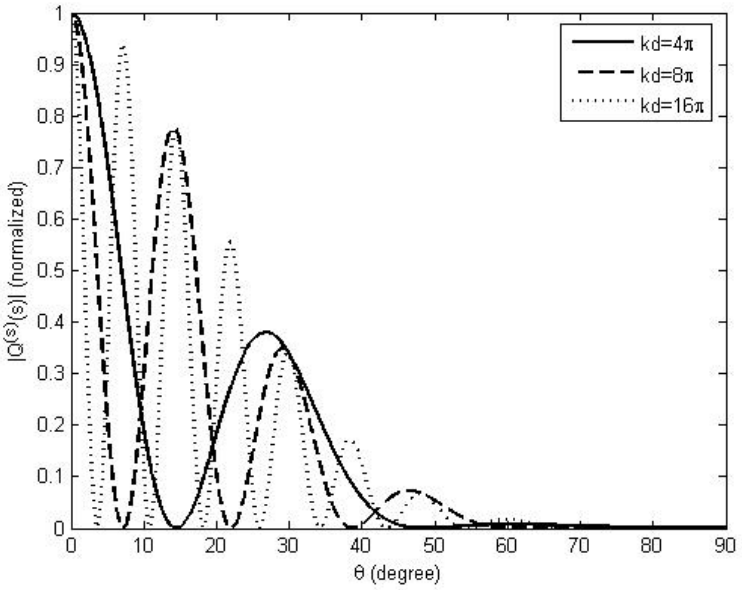

Fig. 3.7 (Normalized) distribution of momentum flow of the far field scattered from a pair of symmetrically distributed particles (Fig. 3.6(a)) for various seperation d as a function of angle θ, with $\sigma = 0.3\lambda$.

The reason that Eq. (3.79) is accurate for valley points while Eq. (3.80) is only approximately correct for the peak points may be explained as follows. In our case we consider the correlation between two scattered fields and, more importantly, we calculate the momentum flow (not just the spectral density). So the quantity [Eq. (3.76) with Eq.

(3.78)] is not only affected by the interference between the two waves as included in $M(\boldsymbol{K},\omega)$, but also the properties of the scattering medium, included in $\left|\tilde{f}(\boldsymbol{K},\omega)\right|^2$, and the properties of the incident field, included in $\left(Tr\hat{\boldsymbol{C}}-\boldsymbol{s}\circ\hat{\boldsymbol{C}}\circ\boldsymbol{s}^T\right)$. The peak points for the interference pattern are moved due to this reason, while the valley points where the spectral density is zero are unchanged since they retain the value zero despite of the product of other terms.

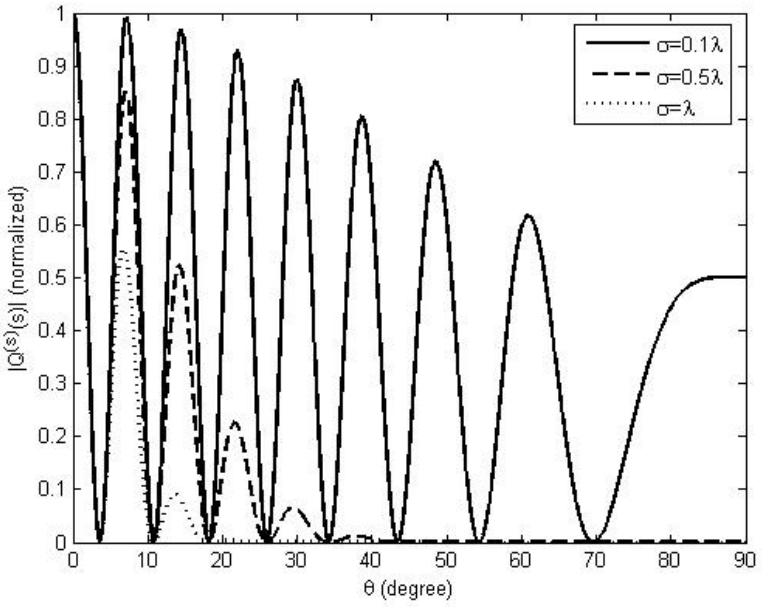

Fig. 3.8 (Normalized) distribution of momentum flow of the far field scattered from a pair of symmetrically distributed particles (Fig. 3.6(a)) for various particel size σ as a function of angle θ, with $kd=16\pi$.

For particles distributed according to Figs. 3.6(b) – 3.6(e), the scattered angular distribution of momentum flow is given in Fig. 3.9. It is interesting to note that there is one maximum peak value around 14° indepenent of the number of particles symmetrically

distributed along the x- axis, with the second peak appearing around 30°. This case with more than two particles is a more interesting problem since the interference of the scattered wave would not only come from the two adjacent particles but also from other particles. In our case the interference from multiple particles may be suitably divided into separate interference between two particles. Then for the set-ups in Fig. 3.6, the possible spacing distance between any two particles would be $d/2$, d, $3d/2$, $2d$, $5d/2$, $3d$, $7d/2$, $4d$, $9d/2$, $5d$. For spacing values $d_{sp} = \frac{l}{2}d$ ($l = 1, 2, ...10$) in Eq. (3.80), the possible peak positions would be (with $kd = 16\pi$)

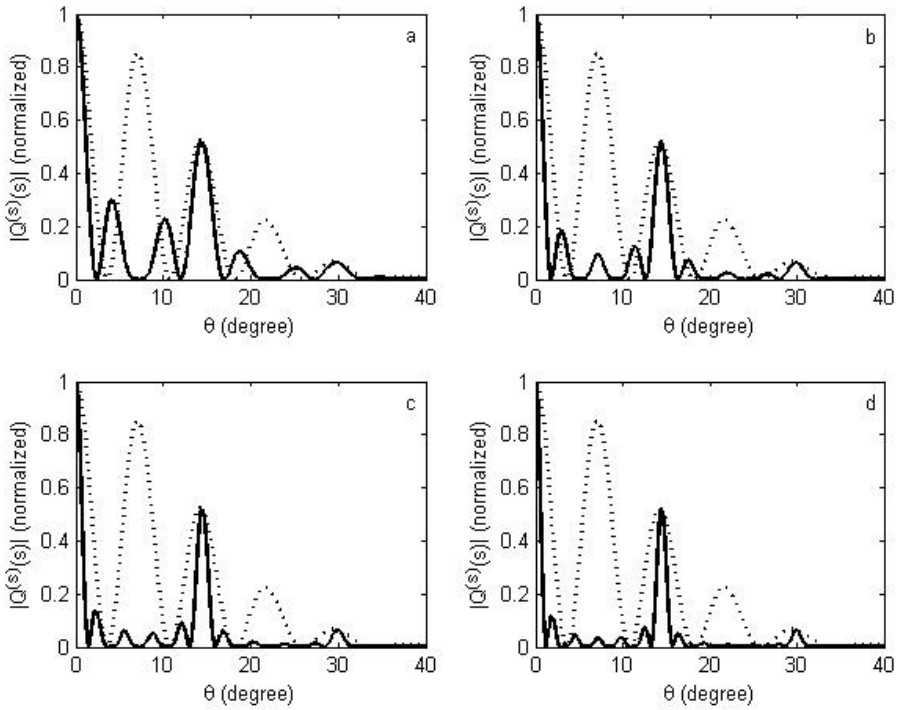

Fig. 3.9 (Normalized) distribution of momentum flow of the far field scattered from collections of particles shown in Fig. 3.6(a) (dotted curve) and (a) in Fig. 3.6(b) (solid curve); (b) in Fig. 3.6(c) (solid curve); (c) in Fig. 3.6(d) (solid curve); (d) in Fig. 3.6(e) (solid curve) with $kd = 16\pi$ and $\sigma = 0.5\lambda$.

$$\sin\theta = \frac{n}{4l},\ (n = 0,1,2...). \tag{3.81}$$

Therefore for all the possible spacing choices, they share the common the peak position at $\sin\theta_{mm} = 1/4$ with $\theta_{mm} = 14.4775$ degree (mm means major maximum), which explains the first major maximum. For other major maximum, similar explanation applies. And the governing equation for the nth major maximum is $(d/2)\sin\theta = n\lambda$.

Spacing distance d_{sp}	Counting numbers	Peak positions $\sin\theta$ (up to first major maximum)
$d/2$	8	$1/4$
d	7	$1/8, 1/4$
$3d/2$	6	$1/12, 1/6, 1/4$
$2d$	4	$1/16, 1/8, 3/16, 1/4$
$5d/2$	4	$1/20, 1/10, 3/20, 1/5, 1/4$
$3d$	5	$1/24, 1/12, 1/8, 1/6, 5/24, 1/4$
$7d/2$	4	$1/28, 1/14, 3/28, 1/7, 5/28, 3/14, 1/4$
$4d$	3	$1/32, 1/16, 3/32, 1/8, 5/32, 3/16, 7/32, 1/4$
$9d/2$	2	$1/36, 1/18, 1/12, 1/9, 5/36, 3/18, 7/36, 2/9, 1/4$
$5d$	1	$1/40, 1/20, 3/40, 1/10, 1/8, 3/20, 7/40, 1/5, 9/40, 1/4$

Table 3.1 List of all the possible spacing distances with counting numbers and peak positions for the set-up in Fig. 3.6(e).

From Fig. 3.9, the fact that the number of minor peaks is equal to half of the number of particles can also be explained by the interference between waves scattered from the particles. It can be assumed the minor peaks are associated with different orders of maxima between two particles with distance equal to $(M+1)d/2$. The reason for this assumption may be explained as follows. Let us consider the most complicated case in Fig. 3.6(e), where $M = 5$. We may obtain the all the possible spacing distances between

any two particles and count the numbers that the spacing distance appears. One may see from Table 3.1 that the peak positions for the spacing distances $d/2$, d, $3d/2$ are overlapped by the peak positions for the spacing $3d$. And the counting number for spacing $3d$ is greater than other spacing possibilities except $d/2$, d and $3d/2$, whose peak positions have been overlapped. Therefore the minor peak positions may be dominated by the different orders of maximum of distance $3d$, although the exact minor peak positions may be slightly different due to the existence of interference of other choices of spacing distances. Furthermore, $3d=(M+1)d/2$, where $M=5$ is the number of particles at one side of origin. Other cases with different number of particles may be similarly analyzed.

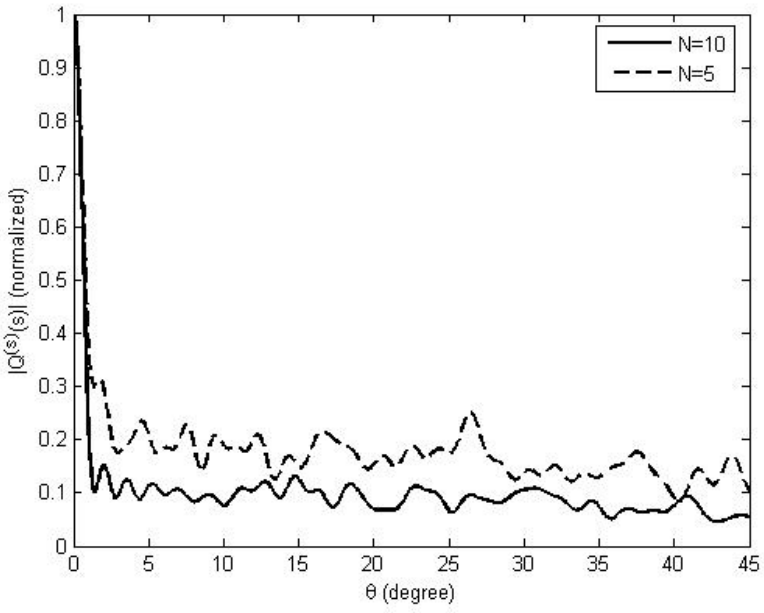

Fig. 3.10 (Normalized) distribution of momentum flow of the far field scattered from collections of particles randomly distributed with $\sigma=0.1\lambda$.

In Fig. 3.10 we consider a special case of a gas-like disorder [65] where identical particles with Gaussian potentials randomly positioned along the x-axis. In this case the particles are considered as statistically independent. Then structure factor becomes $M(\boldsymbol{K},\omega) = N = \frac{1}{N} M(0,\omega)$ for all $\boldsymbol{K}$ except $\boldsymbol{K} = 0$. Fig. 3.10 shows the angular distribution of momentum flow of the scattered far field from $N = 5$ and $N = 10$ particles, respectively. The range of x-axis within which all the particles are randomly distributed is 40λ , i.e., $-20\lambda \sim 20\lambda$. Therefore, the average spacing between neighboring particles for 10 particles is 4λ and for 5 particles is 8λ, respectively. In each case the momentum flow is the statistical average over 30 realizations. The absolute value of momentum flow $\left|\boldsymbol{Q}^{(s)}(r\boldsymbol{s})\right|$ decreases abruptly to a value on the order of 1/N over the several degrees from the forward scattering direction and then levels off with a small negative slope due to the additional terms in Eq. (3.76). The fluctuations in the tail of $\left|\boldsymbol{Q}^{(s)}(r\boldsymbol{s})\right|$ are caused by the limited number of particles in the ensemble: for sufficiently large values of N the momentum flow drops to zero over the first several degrees.

3.2.4 Concluding remarks

In summary, we have derived the expression for the angular distribution of the momentum flow of the field produced on scattering of a plane wave from random media, which can be a single particle or collection as well as of deterministic or random nature. We have found that both polarization properties of the incident electromagnetic plane wave and the scattering potentials of the scattering material influence the distribution of

the momentum flow of the scattered field. From the examples considered, the size of particles, the separation between them, and the nature of the collection (deterministic or random centers' locations) significantly influence the angular distribution of the momentum flow throughout the far zone of the scatterer.

3.3 Polarization of Random Light Beams Scattered from Bio-tissues

Some years ago the power spectra of the microscopic refractive index variation were obtained for typical biological tissues [66]. Several proposed mathematical models of the experimentally fitted spectrum have later provided a powerful tool for analytic investigations of the statistical properties of random light on interaction with (propagation through or scattering from) tissues [66-67]. For example, based on such models it is possible to show that for most biological tissues the spectrum of the backscattered light is blue-shifted with respect to the spectrum of the incident light [68], although the red shift is generally observed on forward scattering [69].

To our knowledge all previous studies about random light scattering from tissues were confined to scalar treatment, and, hence, could not account for polarimetric changes. It is known, however, that random light passing in some weekly-fluctuating media, such as atmosphere and ocean may lead to significant polarimetric modulation [70-71]. Based on the recently introduced electromagnetic (EM) scattering theory of random light [14], we derive the expression for the cross-spectral density (CSD) matrix of the field scattered from bio-tissues with given power spectrum and determine the changes in the degree of polarization (DOP) in the far zone of the tissue slice.

3.3.1 Refractive-index fluctuation under Markov approximation

Let us consider a thin tissue slice containing refractive index inhomogeneties with a continuum of scales between inner and outer scales, the variations in which are typically small [66]. We can

express the refractive index of a tissue layer being a random function of position as a sum of its mean and a spatially varying part, $n(\boldsymbol{r}') = \langle n(\boldsymbol{r}') \rangle + \delta n(\boldsymbol{r}')$, where $\boldsymbol{r}'$ denotes a location within the tissue and $\langle n(\boldsymbol{r}') \rangle \simeq \langle n \rangle$. Then the scattering potential of the tissue slice takes the form

$$F(\boldsymbol{r}', \omega) = k^2 \left[n^2(\boldsymbol{r}') - 1 \right] / 4\pi$$

$$= k^2 \left[\langle n \rangle^2 - 1 + 2 \langle n \rangle \delta n(\boldsymbol{r}') + \delta n^2(\boldsymbol{r}') \right] / 4\pi , \qquad (3.82)$$

Further, the spatial correlation function of the scattering potential becomes

$$C_F(\boldsymbol{r}_1', \boldsymbol{r}_2', \omega) = \left\langle F^*(\boldsymbol{r}_1', \omega) F(\boldsymbol{r}_2', \omega) \right\rangle$$

$$= k^4 [(\langle n \rangle^2 - 1)^2 + 2(\langle n \rangle^2 - 1) \langle \delta n^2 \rangle + 4 \langle n \rangle^2 \langle \delta n(\boldsymbol{r}_1') \delta n(\boldsymbol{r}_2') \rangle] / 16\pi^2 , \qquad (3.83)$$

where higher-order terms have been neglected and $\langle \delta n^2 \rangle$ is the variance of the tissue refractive index fluctuation. Eq. (3.83) implies that the correlation function contains constant terms and a term including the correlation function $\langle \delta n(\boldsymbol{r}_1') \delta n(\boldsymbol{r}_2') \rangle$, which gives rise to optical phase distortion and, hence, is of our major concern [66,68]. If the refractive index fluctuations are statistically homogeneous we may employ Markov approximation under which [39]

$$\langle \delta n(\boldsymbol{r}_1') \delta n(\boldsymbol{r}_2') \rangle = 2\pi \delta(z) \int \Phi_n(\boldsymbol{K}) \exp[i \boldsymbol{K}_\perp \cdot (\boldsymbol{\rho}_1' - \boldsymbol{\rho}_2')] d^2\kappa , \qquad (3.84)$$

where $\boldsymbol{r}_1' = (\boldsymbol{\rho}_1', z_1')$, $\boldsymbol{r}_2' = (\boldsymbol{\rho}_2', z_2')$, $z = z_1' - z_2'$ and $\Phi_n(\boldsymbol{K})$ is the three-dimensional spatial power spectrum of the refractive-index fluctuations, and $\boldsymbol{K} = (\boldsymbol{K}_\perp, 0) = (\kappa_x, \kappa_y, 0)$. The

six-dimensional spatial Fourier transform of the correlation function $C_F(\boldsymbol{r}_1', \boldsymbol{r}_2', \omega)$ of the scattering potential can then be readily evaluated as:

$$\tilde{C}_F(\boldsymbol{K}_1, \boldsymbol{K}_2, \omega) = \int_D \int_D \exp[-i(\boldsymbol{K}_1 \cdot \boldsymbol{r}_1' + \boldsymbol{K}_2 \cdot \boldsymbol{r}_2')] C_F(\boldsymbol{r}_1', \boldsymbol{r}_2', \omega) d^3\boldsymbol{r}_1' d^3\boldsymbol{r}_2'$$

$$= 8\pi^3 k^4 \langle n \rangle^2 L \Phi_n \left(\frac{\boldsymbol{K}_{1\perp} - \boldsymbol{K}_{2\perp}}{2} \right) \delta^{(2)}(\boldsymbol{K}_{1\perp} + \boldsymbol{K}_{2\perp}) \sin c \left[\frac{(\kappa_{1z} + \kappa_{2z})L}{2} \right], \quad (3.85)$$

where L is the thickness of the tissue layer. To arrive to results in Eq. (3.85) a Fourier transform identity for the delta-function was employed.

3.3.2 Scattered field statistics from thin bio-tissue in the far zone

Suppose now that a monochromatic EM field $E^{(i)}(\boldsymbol{r}', \omega)$ radiated from the source plane and incident onto the tissue is scattered into the field $E^{(s)}(r\boldsymbol{s}, \omega)$. The scattered field in the far zone can be expressed as [14] (see Fig. 3.11)

$$\boldsymbol{E}_{sp}^{(s)}(r\boldsymbol{s}, \omega) = \frac{\mathrm{e}^{ikr}}{r} \int_D F(\boldsymbol{r}', \omega) \boldsymbol{E}^{(i)}(\boldsymbol{r}', \omega) \circ \boldsymbol{S}(\theta, \phi) \exp(-ik\boldsymbol{s} \cdot \boldsymbol{r}') d^3\boldsymbol{r}', \quad (3.86)$$

where $\boldsymbol{E}_{sp}^{(s)} = [E_r^{(s)}, E_\theta^{(s)}, E_\phi^{(s)}]$ and $\boldsymbol{E}^{(i)} = [E_x^{(i)}, E_y^{(i)}, E_z^{(i)}]$ are vector-fields in spherical polar and in Cartesian coordinates, respectively, $\boldsymbol{s} = [\sin\theta\cos\phi, \sin\theta\sin\phi, \cos\theta]$ is the unit vector pointing from the origin within the tissue to the observed point and

$$\boldsymbol{S}(\theta, \phi) = \begin{pmatrix} 0 & \cos\theta\cos\phi & -\sin\phi \\ 0 & \cos\theta\sin\phi & \cos\phi \\ 0 & -\sin\theta & 0 \end{pmatrix}. \quad (3.87)$$

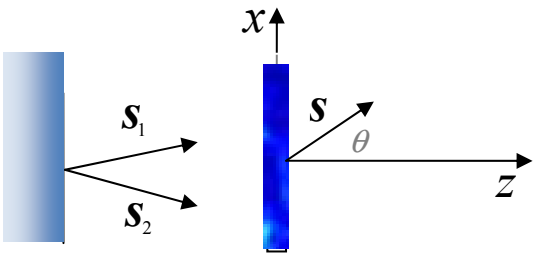

Fig. 3.11 Notations relating to scattering from tissues.

The CSD matrix of the scattered electric field at a point specified by position vector $r\boldsymbol{s}$ in the spherical polar coordinates is then readily found to be [14]

$$\boldsymbol{W}_{sp}^{(s)}(r\boldsymbol{s}, r\boldsymbol{s}, \omega)$$

$$= \left\langle \boldsymbol{E}_{sp}^{(s)+}(r\boldsymbol{s}, \omega) \circ \boldsymbol{E}_{sp}^{(s)}(r\boldsymbol{s}, \omega) \right\rangle$$

$$= \frac{1}{r^2} \boldsymbol{S}^{\dagger}(\theta, \phi) \circ \int_D \int_D \boldsymbol{W}^{(i)}(\boldsymbol{r}_1', \boldsymbol{r}_2', \omega) C_F(\boldsymbol{r}_1', \boldsymbol{r}_2', \omega) \exp[ik\boldsymbol{s} \cdot (\boldsymbol{r}_1' - \boldsymbol{r}_2')] d^3\boldsymbol{r}_1' d^3\boldsymbol{r}_2' \circ \boldsymbol{S}(\theta, \phi), \quad (3.88)$$

where $\boldsymbol{W}^{(i)}(\boldsymbol{r}_1', \boldsymbol{r}_2', \omega) = \left\langle \boldsymbol{E}^{(i)+}(\boldsymbol{r}_1', \omega) \circ \boldsymbol{E}^{(i)}(\boldsymbol{r}_2', \omega) \right\rangle$ is the CSD matrix of the incident beam within the tissue slice, which can be conveniently represented by a spectrum of plane waves. Since we assume that the origin of the coordinate system is located within the tissue slice, the plane waves which should start from the origin at the source plane in the regular representation may be rewritten through the transformation of the coordinates. Assuming that the center of the source plane is at $(0, 0, -z_0)$ with respect to the origin within the tissue, we find that

$$\boldsymbol{W}^{(i)}(\boldsymbol{r}_1', \boldsymbol{r}_2', \omega)$$

$$= \iint \boldsymbol{A}(\boldsymbol{s}_{1\perp}, \boldsymbol{s}_{2\perp}, \omega) \exp[ik(s_{2z} - s_{1z})z_0] \exp[ik(\boldsymbol{s}_2 \cdot \boldsymbol{r}_2' - \boldsymbol{s}_1 \cdot \boldsymbol{r}_1')] ds_{1\perp}^2 ds_{2\perp}^2 , \quad (3.89)$$

where $\boldsymbol{A}(\boldsymbol{s}_{1\perp}, \boldsymbol{s}_{2\perp}, \omega)$ is the angular correlation function between two plane-wave modes and $z_0 \gg \lambda$, implying that only modes with $|\boldsymbol{s}_{1\perp}| \le 1$ or $|\boldsymbol{s}_{2\perp}| \le 1$ contribute to the spectrum, i.e. the evanescent waves are neglected. On substituting from Eq. (3.89) into Eq. (3.88), the CSD matrix of the scattered field can be expressed as

$$\boldsymbol{W}_{sp}^{(s)}(r\boldsymbol{s}, r\boldsymbol{s}, \omega) = \frac{1}{r^2} \boldsymbol{S}^{+}(\theta, \phi) \circ \iint \boldsymbol{A}(\boldsymbol{s}_{1\perp}, \boldsymbol{s}_{2\perp}, \omega)$$

$$\times \tilde{C}_F[-k(\boldsymbol{s} - \boldsymbol{s}_1), k(\boldsymbol{s} - \boldsymbol{s}_2), \omega] \exp[ik(s_{2z} - s_{1z})z_0] ds_{1\perp}^2 ds_{2\perp}^2 \circ \boldsymbol{S}(\theta, \phi) . \quad (3.90)$$

In Eq. (3.90) $\boldsymbol{s}$ is a unit vector pointing to the observed point while $\boldsymbol{s}_1$ and $\boldsymbol{s}_2$ indicate the directions of plane waves from the incident beam angular spectrum. Let us now substitute from Eq. (3.85) into Eq. (3.90) with $\boldsymbol{K}_1 = -k(\boldsymbol{s} - \boldsymbol{s}_1)$, $\boldsymbol{K}_2 = k(\boldsymbol{s} - \boldsymbol{s}_2)$ to obtain

$$\boldsymbol{W}_{sp}^{(s)}(r\boldsymbol{s}, r\boldsymbol{s}, \omega)$$

$$= \frac{8\pi^3 k^2 L \langle n \rangle^2}{r^2} \boldsymbol{S}^{+}(\theta, \phi) \circ \int \boldsymbol{A}(\boldsymbol{s}_{1\perp}, \omega) \Phi_n[-k(\boldsymbol{s}_{\perp} - \boldsymbol{s}_{1\perp})] ds_{1\perp}^2 \circ \boldsymbol{S}(\theta, \phi) , \quad (3.91)$$

where $s_x = \sin\theta\cos\phi$, $s_y = \sin\theta\sin\phi$, $s_z = \cos\theta$ and formula $\delta^{(2)}(\boldsymbol{K}_{1\perp} + \boldsymbol{K}_{2\perp}) = \delta^{(2)}(\boldsymbol{s}_{1\perp} - \boldsymbol{s}_{2\perp}) / k^2$ is employed. Equation (3.91) is the main result of this section, which shows the relation between correlation properties of the illumination, the tissue refractive index variation and the scattered field statistics in the far zone. Since the elements of the first column of the **S** matrix are all zero, only four elements of matrix

$\boldsymbol{W}^{(s)}$ have non-trivial values. Such transverse field can be used for defining the spectral DOP in two-dimensional formalism [see Eq. (1.8)]:

$$P(\boldsymbol{r},\omega)=\sqrt{1-\frac{4Det\mathbf{W}_{\theta\phi}(\boldsymbol{r},\boldsymbol{r},\omega)}{[Tr\mathbf{W}_{\theta\phi}(\boldsymbol{r},\boldsymbol{r},\omega)]^2}}\ . \tag{3.92}$$

where $\mathbf{W}_{\theta\phi}=[\mathbf{W}_{ij}],(i,j=\theta,\phi)$ is the 2×2 matrix.

3.3.3 Example and concluding remarks

We will now consider the model power spectrum of bio-tissue index fluctuations [66]:

$$\Phi_n(K)=4\pi\left\langle\delta n^2\right\rangle L_o^2(m-1)(1+K^2L_o^2)^{-m}\ , \tag{3.93}$$

where $K=\left|\boldsymbol{K}_\perp\right|$. For different tissues, the spectrum has different values of slope m and outer scale L_0. For example, for liver parenchyma (mouse), $m=1.41(\pm0.06)$ and $L_o=8\mu m$; for intestinal epithelium (mouse), $m=1.33(\pm0.03)$ and $L_o=10\mu m$; for upper dermis (human), $m=1.43(\pm0.04)$ and $L_o=4\mu m$; for deep dermis (mouse), $m=1.28(\pm0.02)$ and $L_o=5\mu m$. The thickness of the slice should not exceed the outer scale L_0 [69]. As model for illumination field we will use an EM Gaussian Schell-model beam:

$$W_{\alpha\beta}^{(0)}(\boldsymbol{\rho}_1,\boldsymbol{\rho}_2,\omega)=A_\alpha A_\beta B_{\alpha\beta}\exp\left[-\frac{\boldsymbol{\rho}_1^2+\boldsymbol{\rho}_2^2}{4\sigma_I^2}\right]\exp\left[-\frac{(\boldsymbol{\rho}_2-\boldsymbol{\rho}_1)^2}{2\delta_{\alpha\beta}^2}\right], \tag{3.94}$$

whose angular correlation function has form

$A_{\alpha\beta}(\boldsymbol{s}_{1\perp}, \boldsymbol{s}_{2\perp})$

$$= \frac{A_\alpha A_\beta B_{\alpha\beta} k^4 \sigma_I^4}{\pi^2 (1 + 4\sigma_I^2 / \delta_{\alpha\beta}^2)} \exp\left[-\frac{k^2 (\boldsymbol{s}_{1\perp}^2 + \boldsymbol{s}_{2\perp}^2)}{4/\delta_{\alpha\beta}^2 + 1/\sigma_I^2} \right] \exp\left[-\frac{2\sigma_I^4 k^2 (\boldsymbol{s}_{1\perp} - \boldsymbol{s}_{2\perp})^2}{4\sigma_I^2 + \delta_{\alpha\beta}^2} \right], \qquad (3.95)$$

with $\alpha, \beta = x, y$. Eq. (3.94) is valid when the origin is in the source plane and the transformation of coordinates does not influence the form of the angular correlation function in Eq. (3.95). Unless specified in captions, the following parameters were used: $k = 10^7 m^{-1}$, $A_x = 1$, $A_y = 1$, $B_{xx} = B_{yy} = 1$, $B_{xy} = B_{yx} = 0.2$, $\sigma = 10^{-3} m$, $\phi = 0$, $\delta_{xx} = 10^{-5} m$, $\delta_{yy} = 2 \times 10^{-5} m$, and $\delta_{xy} = \delta_{yx} = 2.5 \times 10^{-5} m$.

Figure 3.12 shows that for different types of bio-tissues, the DOP of its scattered far field is considerably influenced by the characteristics of tissue, which may provide a useful tool for sensing and recognition and in distinguishing a pathological tissue from a normal one.

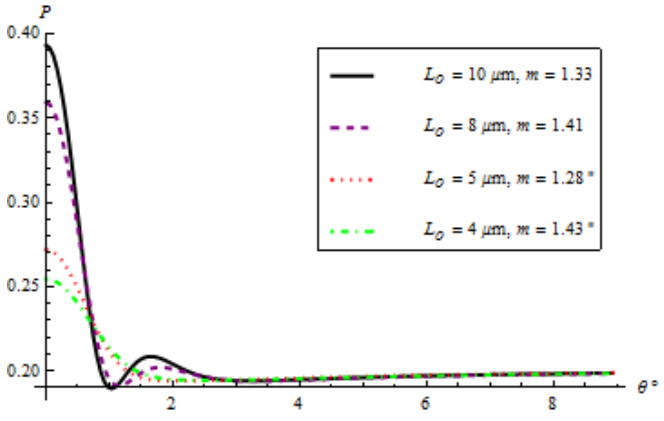

Fig. 3.12 Scattered DOP for different bio-tissues.

For the tissues considered in this paper, their correlation lengths are ranged from $10^{-6}m$ to $10^{-5}m$ [66]. Fig. 3.13 shows the DOP of scattered light if incident beam has correlation coefficients $\delta_{xx}=10^{l}m,\ \ \delta_{yy}=2\times10^{l}m,\ \ \delta_{xy}=\delta_{yx}=2.5\times10^{l}m$. It becomes evident that only when the correlation widths of the incident beam are close to the tissue correlation length, significant changes in the angular DOP profile can be observed. The detail of DOP variation in the case $l=-5$ in Fig. 3.13 can also be found as the thick line in Fig. 3.12.

For uncorrelated incident beam $B_{xy}=B_{yx}=0$, and hence, its DOP reduces to $P_o=\left|A_x^2-A_y^2\right|/(A_x^2+A_y^2)$. In Fig. 3.14 we calculate the change in DOP of scattered light for several selected values of the DOP of incident uncorrelated beam. The polarization of the scattered field is seen to be modulated at most for an unpolarized incident beam.

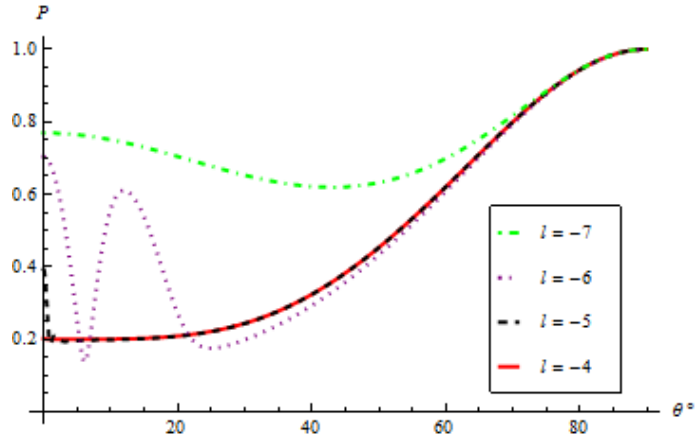

Fig. 3.13 DOP of light scattered from intestinal epithelium (mouse).

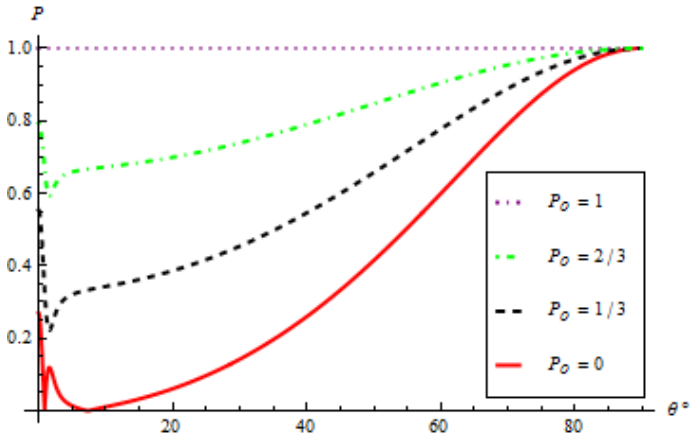

Fig. 3.14 DOP of the field with different $P_0(A_x, A_y)$ and $B_{xy} = B_{yx} = 0$ scattered from intestinal epithelium (mouse).

Thus we have derived the expression for the DOP of an EM random light beam scattered from a thin slice of bio-tissue with prescribed power spectrum [see Eqs. (3.91) and (3.92)]. We found that the DOP reflects both the statistical properties of incident radiation and those of tissue, i.e. m and L_0. Our results can be of particular interest for tissue sensing [69].

Chapter 4

Summary

We have presented the advances to the theories of scalar and electromagnetic scattering of random optical fields from deterministic and random media which are based on rigorous theoretical foundations: the Maxwell's equations and the classical statistical optics. The major contributions by the author to the optical community included in this thesis are outlined below:

- The concept of the pair-structure matrix of a scattering collection is introduced for complete characterization of the correlation properties of between particles of one type and across different types. The elements of this matrix are shown to considerably affect the statistics of scattered light.
- A method based on light scattering for tracing an alien particle embedded in a particulate, random medium is developed.
- A novel theoretical approach to description of optical fields on interaction with a continuous turbulent medium containing discrete scatterers is suggested.
- The classic scalar weak scattering theory is generalized to the electromagnetic domain. Based on this theory it is demonstrated for the first time how the predictions about the distribution of the spectral, coherence and polarization states of random light beams scattered from weakly fluctuating media can be made.

- The angular distribution of the momentum flow of a field produced on scattering of a plane wave from random media is evaluated and shown to be intimately related to the properties of the scatterer.
- The electromagnetic scattering theory is applied to the scattering from a thin bio-tissue slice. The polarization properties of scattered radiation are shown to be closely related to the distribution of the refractive index in the slice and the states of coherence and polarization of the illumination.

References

1. Z. Tong and O. Korotkova, “Electromagnetic nonuniformly correlated beams”, J. Opt. Soc. Am. A 29, 2154-2158 (2012).

2. Z. Tong and O. Korotkova, “Far-field analysis of spectral shifts in Gaussian Schell-model beams propagating through media with arbitrary refractive properties”, J. Opt. 12, 095708 (2010).

3. Z. Tong, O. Korotkova, Y. Cai, H. T. Eyyuboglu and Y. Baykal, “Correlation properties of random electromagnetic beams in laser resonators”, Appl. Phys. B 97, 849-857 (2009).

4. S. Sahin, Z. Tong and O. Korotkova, “Sensing of semi-rough targets embedded in atmospheric turbulence by means of stochastic electromagnetic beams”, Opt. Commun. 283, 4512-4518 (2010).

5. Z. Tong and O. Korotkova, “Stochastic electromagnetic beams in positive- and negative-phase materials”, Opt. Lett. 35, 175-177 (2010).

6. Z. Tong and O. Korotkova, “Spectral shifts and switches in random fields upon interaction with negative-phase materials”, Phys. Rev. A 82, 013829 (2010).

7. Z. Tong and O. Korotkova, “Nonuniformly correlated light beams in uniformly correlated media”, Opt. Lett. 37, 3240-3242 (2012).

8. Z. Mei, Z. Tong and O. Korotkova, “Electromagnetic non-uniformly correlated beams in turbulent atmosphere”, Opt. Express 20, 26458-26463 (2012).

9. Z. Tong, “Degree of coherence in curvilinear coordinates and its application to scattering”, J. Opt. Soc. Am. A 29, 1421-1426 (2012).

10. Z. Tong and O. Korotkova, “Technique for interaction of optical fields with turbulent medium containing particles”, Opt. Lett. 36, 3157-3159 (2011).

11. Z. Tong and O. Korotkova, “Momentum of light scattered from collections of particles”, Phys. Rev. A 84, 043835 (2011).

12. Z. Tong and O. Korotkova, “Method for tracing the position of an alien object embedded in a random particulate medium”, J. Opt. Soc. Am. A 28, 1595-1599 (2011).

13. Z. Tong and O. Korotkova, “Pair-structure matrix of random collection of particles: Implications for light scattering”, Opt. Commun. 284, 5598-5600 (2011).

14. Z. Tong and O. Korotkova, “Theory of weak scattering of stochastic electromagnetic fields from deterministic and random media”, Phys. Rev. A 82, 033836 (2010).

15. Z. Tong and O. Korotkova, “Contribution of evanescent incident waves to the scattered far field”, Phys. Rev. A 85, 043802 (2012).

16. Z. Tong and O. Korotkova, “Electromagnetic scattering from biological tissue”, Photonics Asia 85531I-85531I-5 (2012).

17. Z. Tong and O. Korotkova, “Beyond the classical Rayleigh limit with twisted light”, Opt. Lett. 37, 2595-2597 (2012).

18. Z. Tong, Y. Cai and O. Korotkova, “Ghost imaging with electromagnetic stochastic beams”, Opt. Commun. 283, 3838-3845 (2010).

19. M. Born and E. Wolf, *Principles of Optics* (Cambridge U. Press, 1999).

20. E. Wolf, *Introduction to the Theory of Coherence and Polarization of Light* (Cambridge U. Press, 2007).

21. E. Wolf, “Statistical similarity as a unifying concept of the theories of coherence and polarization of light”, Opt. Commun. 283, 4427-4429 (2010).

22. E. Wolf, “Unified theory of coherence and polarization of random electromagnetic beams”, Phys. Lett. A 312, 263-267 (2003).

23. L. Mandel and E. Wolf, *Optical Coherence and Quantum Optics* (Cambridge U. Press, 1995).

24. M. L. Mishchenko, L. D. Travis, and A. A. Lacis, *Multiple Scattering of Light By Particles* (Cambridge U. Press, 2006).

25. X. Du and D. Zhao, “Scattering of light by a system of anisotropic particles”, Opt. Lett. 35, 1518-1520 (2010).

26. A. Dogariu and E. Wolf, “Spectral changes produced by static scattering on a system of particles”, Opt. Lett. 23, 1340-1342 (1998).

27. S. Sahin and O. Korotkova, “Scattering of scalar light fields from collections of particles”, Phys. Rev. A 78, 063815 (2008).

28. S. Sahin and O. Korotkova, “Effect of the pair-structure factor of a particulate medium on scalar wave scattering in the first Born approximation”, Opt. Lett. 34, 1762-1764 (2009).

29. T. Wang and D. Zhao, “Determination of pair-structure factor of scattering potential of a collection of particles”, Opt. Lett. 35, 318-320 (2010).

30. O. Korotkova and E. Wolf, "Scattering matrix theory for stochastic scalar fields", Phys. Rev. E 75, 056609 (2007).

31. X. Du and D. Zhao, "Scattering of light by Gaussian-correlated quasi-homogeneous anisotropic media", Opt. Lett. 35, 384-386 (2010).

32. T. Wang and D. Zhao, "Scattering theory of stochastic electromagnetic light waves", Opt. Lett. 35, 2412-2414 (2010).

33. M. Lahiri, E. Wolf, D. Fischer and T. Shirai, "Determination of correlation functions of scattering potentials of stochastic media from scattering experiments", Phys. Rev. Lett. 102, 123901 (2009).

34. D. Zhao, O. Korotkova and E. Wolf, "Application of correlation-induced spectral changes to inverse scattering", Opt. Lett. 32, 3483-3485 (2007).

35. For example, the Fourier transform of the scattering potential of Gaussian type is a resulting real function. See Eq. (2.55). For other scattering potentials with exponential term of $i\mathbf{K}\cdot\mathbf{r}$, such term will reduce to unity due to our requirement Eq. (2.47).

36. T. D. Visser and E. Wolf, "Potential scattering with field discontinuities at the boundaries", Phys. Rev. E 59, 2355-2360 (1999).

37. T. van Dijk, D. G. Fischer, T. D. Visser and E. Wolf, "Effects of spatial coherence on the angular distribution of radiant intensity generated by scattering on a sphere", Phys. Rev. Lett. 104, 173902 (2010).

38. V. I. Tatarskii, *Wave Propagation in a Turbulent Medium* (Dover and McGraw-Hill, New York, 1967).

39. L. C. Andrews, R. L. Phillips, *Laser Beam Propagation through Random Media* (SPIE, Bellingham, 1998).

40. C. F. Bohren, D. R. *Huffman, Absorption and Scattering of Light by Small Particles* (Wiley, New York, 1983).

41. M. I. Mishchenko, L. D. Travis, A. A. Lacis, *Scattering, Absorption, and Emission of Light by Small Particles* (Cambridge U. Press, Cambridge, 2002).

42. A. Isimaru, *Electromagnetic Wave Propagation, Radiation, and Scattering* (Prentice Hall, Englewood Cloffs, NJ, 1991).

43. S. Chandrasekhar, *Radiative Transfer* (Dover, New York, 1960).

44. G. Gbur and O. Korotkova, "Angular spectrum representation for the propagation of arbitrary coherent and partially coherent beams through atmospheric turbulence", J. Opt. Soc. Am. A 24, 745 (2007).

45. V. V. Nikishov, V. I. Nikishov, “Spectrum of turbulent fluctuations of the sea-water refraction index”, Int. J. Fluid Mech. Res. 27, 82 (2000).

46. W. Gao, “Changes of polarization of light beams on propagation through tissue”, Opt. Commun. 260, 749 (2006).

47. M. Abramowitz and I. A. Stegun, *Handbook of Mathematical Functions* (Dover, 1965).

48. M. I. Mishchenko, L. D. Travis, and A. A. Lacis, *Multiple Scattering of Light By Particles* (Cambridge, U. Press, 2006).

49. J. Janson, T. Janson and E. Wolf, “Spatial coherence discrimination in scattering”, Opt. Lett. **6**, 1060 (1988).

50. E. Wolf, J. T. Foley, and F. Gori, “Frequency shifts of spectral lines produced by scattering from spatially random media”, J. Opt. Soc. Am. A **6**, 1142 (1990).

51. D. G. Fischer and E. Wolf, "Inverse problems with quasi-homogeneous random media”, J. Opt. Soc. Am. A **11**, 1128 (1994).

52. T. D. Visser, D. G. Fischer, and E. Wolf, “Scattering of light from quasi-homogeneous sources by quasi-homogeneous media”, J. Opt. Soc. Am. A, **23**, 1631 (2006).

53. T. Wang, D. M. Zhao, “Condition for the invariance of the spectral degree of coherence of a completely coherent light wave on weak scattering”, Opt. Lett. **35**, 847-849 (2010).

54. E. Baleine and A. Dogariu, “Variable coherence tomography”, Opt. Lett. **29**, 1233 (2004).

55. E. Baleine and A. Dogariu, “Variable coherence scattering microscopy”, Phys. Rev. Lett. **95**, 193904 (2005).

56. R. K. Luneburg, *Mathematical Theory of Optics* (University of California Press, Berkeley, California, 1964).

57. M. A. Alonso, O. Korotkova and E. Wolf, “Propagation of the electric correlation matrix and the van Cittert-Zernike theorem for random electromagnetic fields", J. Mod. Opt. **53**, 969-978 (2006).

58. T. Shirai, “Some consequences of the van Cittert-Zernike theorem for partially polarized stochastic electromagnetic fields”, Opt. Lett. **34**, 3761-3763 (2009).

59. A. Ashkin, J. M. Sdiedzic, J. E. Bjorkholm and S. Chu, “Observation of a single-beam gradient force optical trap for dielectric particles”, Opt. Lett. **11**, 288 (1986).

60. K. C. Neuman and S. M. Block, "Optical trapping", Rev. Sci. Instr. **75**, 2787 (2004).

61. J. D. Jackson, *Classical Electrodynamics*, 2nd ed. (Wiley, New York, 1975).

62. P. Roman and E. Wolf, "Correlation theory of stationary electromagnetic fields—part II: conservation laws", Nuovo Cimento 17, 477 (1960).

63. S. M. Kim and G. Gbur, "Momentum conservation in partially coherent wave fields", Phy. Rev. A **79**, 033844 (2009).

64. R. N. C. Pfeifer, T. A. Nieminen, N. R. Heckenberg and H. Rubinsztein-Dunlop, "Colloquium: Momentum of an electromagnetic wave in dielectric media", Rev. Mod. Phys. **79**, 1197 (2007).

65. J. M. Ziman, *Models of Disorder* (Cambridge U. Press, 1979).

66. J. Schmitt and G. Kumar, "Turbulent nature of refractive-index variations in biological tissue", Opt. Lett. **21**, 1310 (1996).

67. C. J. R. Sheppard, "Fractal model of light scattering in biological tissues and cells", Opt. Lett. **32**, 142 (2007).

68. W. Gao, "Spectral changes of the light produced by scattering from tissue", Opt. Lett. **35**, 862 (2010).

69. R. Zhu, S. Sridharan, K. Tangella, A. Balla, and G. Popescu, "Correlation-induced spectral changes in tissues", Opt. Lett. **36**, 4209 (2011).

70. E. Shchepakina and O. Korotkova, "Second-order statistics of stochastic electromagnetic beams propagating through non-Kolmogorov turbulence", Opt. Express **18**, 10650 (2010).

71. O. Korotkova and N. Farwell, "Effect of oceanic turbulence on polarization of stochastic beams", Opt. Commun. **284**, 1740 (2011).